

Proteomic Comparison of Biomaterial Implants for Regeneration of  
Peripheral Nerve Tissue

by

Kathy K. Miu  
S.B. Engineering Sciences  
Harvard University

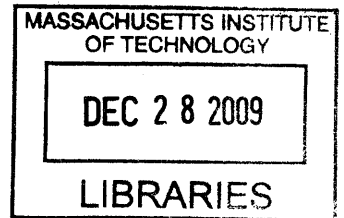
SUBMITTED TO THE DEPARTMENT OF MECHANICAL ENGINEERING IN  
PARTIAL FULFILLMENT OF THE REQUIREMENTS FOR THE DEGREE OF

MASTER OF SCIENCE IN MECHANICAL ENGINEERING  
AT THE  
MASSACHUSETTS INSTITUTE OF TECHNOLOGY

SEPTEMBER 2009

© 2009 Kathy K. Miu. All rights reserved.

The author hereby grants MIT permission to reproduce  
and distribute publicly paper and electronic  
copies of this thesis document in whole or in part  
in any medium now known or hereafter created.



ARCHIVES

Signature of Author: \_\_\_\_\_

Department of Mechanical Engineering  
August 24, 2009

Certified by: \_\_\_\_\_

Ioannis V. Yannas  
Professor of Mechanical and Biological Engineering  
Thesis Supervisor

Accepted by: \_\_\_\_\_

David E. Hardt  
Chairman, Department Committee on Graduate Students

# Proteomic Comparison of Biomaterial Implants for Regeneration of Peripheral Nerve Tissue

by

**Kathy K. Miu**

**Submitted to the Department of Mechanical Engineering  
on August 24, 2009 in Partial Fulfillment of the  
Requirements for the Degree of  
Master of Science in Mechanical Engineering**

## Abstract

Tissue regenerates resulting from the healing of transected peripheral nerve differ in morphological and electrophysiological properties based on the biomaterial implant used to bridge the interneural wound gap. At gap lengths  $\geq 10$  mm, impermeable silicone tubes promote little to no nerve regenerate unlike its porous, degradable collagen alternative. This study assayed rat sciatic nerve wounds treated with silicone and collagen tubes at a 14-day time point for concentration differences in transforming growth factor beta 1, 2, 3 (TGF  $\beta 1$ ,  $\beta 2$ , and  $\beta 3$ ) and alpha smooth muscle actin ( $\alpha$  SMA) to measure disparities in proteins associated with wound healing that may determine nonregenerative from regenerative outcomes.

Transected nerves treated with silicone or collagen tubes were compared on a “whole wound” basis to determine differences in protein expression over the entire tissue and on a “per segment” basis to determine local differences in protein expression over  $\sim 2$ -4 mm regions of tissue. Immunofluorescent comparisons of wounds were performed on cross sections taken along the length of the nerve. In each cross section, a region of interest (ROI) was defined from the periphery of the regenerate tissue to  $\sim 65$   $\mu\text{m}$  radially inwards where presence of a contractile capsule was reported by earlier investigators and also observed in this study.

A 200% increase in whole wound TGF  $\beta 3$  levels in the collagen compared to the silicone treatment group was determined by immunoblot ( $p=0.0026$ ). A 30-50% increase in whole wound TGF  $\beta 1$  levels was found in the silicone compared to the collagen treatment group, which was statistically significant by only one of the two assays used (enzyme-linked immunosorbent assay;  $p=0.0021$ ). There was no significant difference in TGF  $\beta 2$  levels between treatment groups. Whole wound expression of  $\alpha$  SMA was 440% greater in the silicone treatment group than in the collagen treatment group by immunoblot measurement. Immunofluorescent measurement indicated that  $\alpha$  SMA expression in the ROI was 160% greater in silicone than in collagen treated wounds, with significant differences in the nerve stumps (proximal,  $p=.0243$ ; distal,  $p=.0021$ ).

Proteomic comparisons suggest that collagen tubes are more effective at promoting nerve regenerate than silicone tubes due to heightened levels of TGF  $\beta 3$ , less  $\alpha$  SMA expression, and possibly decreased levels of TGF  $\beta 1$  at early stages of wound healing. Trends in protein differences observed in nerve wounds treated with regenerative versus nonregenerative devices are consistent with differences observed in wounds in the early fetal versus adult healing stages. Results from this study support early fetal regeneration as a model for induced regeneration in the peripheral nerve.

Thesis Supervisor: Ioannis Yannas

Title: Professor of Mechanical and Biological Engineering

## Acknowledgements

I would like to first thank my research advisor, Professor I.V. Yannas, for the guidance and encouragement that he has given me throughout this process. With his support I grew as a student and researcher. I feel that I have developed the breadth of my skill set in ways I had not anticipated, and for that I am extremely grateful to my lab. Specifically, I would like to thank: Eric Soller for shaping the experimental design of this project and participating in many of the rat surgeries and sacrifices; Matthew Wong for demonstrating segmentation of the OCT-embedded tissues; Amit Roy for explaining biological assays and for optimizing tissue digestion; Dimitrios Tzeranis for teaching me how to run gels, image immunoblots, and being a knowledgeable resource for immunofluorescence; and Lily Xu for helping me to image slides.

There are several affiliates of this project to whom I owe gratitude. Special recognition goes to Professor Myron Spector, his laboratory, and Alice Alexander for their cooperation at the Boston VA Medical Center. At this facility, Dr. Hu-Ping Hsu operated on the animal subjects used in this study. Alice Alexander, Alix Weaver, and Karen Shu were of immense help in demonstrating techniques useful for immunostaining, and Lily Jeng acquainted me with linear intercept analysis for characterizing my collagen tubes. In addition, many thanks are due to the laboratories of Professor Peter Dedon (MIT) and Dr. George Murphy (Brigham & Women's Hospital) for permitting me use of the Alpha Innotech FluorChem 8900 imager and microtome-cryostat, respectively.

Lastly, I thank my friends and family for their support while I have been at MIT. It was due to their kind words and outstanding company that I experienced great joys while here. I would especially like to recognize my roommate, Jessica Chang, for her encouragement, technical advice, and late night laboratory equipment access!

## Table of Contents

Abstract.....	2
Acknowledgements.....	3
List of Tables and Figures.....	6
Chapter 1: Introduction.....	9
Chapter 2: Background.....	12
<b>2.1 Peripheral Nerve Wounds.....</b>	<b>12</b>
2.1.1 <i>Anatomical and Functional Context</i> .....	12
2.1.2 <i>Animal Model</i> .....	13
<b>2.2 Wound Healing Response .....</b>	<b>14</b>
2.2.1 <i>Spontaneous Peripheral Nerve Healing</i> .....	14
2.2.2 <i>Induced Regeneration using Tubulation</i> .....	15
2.2.3 <i>Theories of Peripheral Nerve Wound Healing</i> .....	17
<b>2.3 Early Fetal Repair as a Model for Regeneration .....</b>	<b>19</b>
2.3.1 <i>Spontaneous Late Fetal and Adult Wound Repair</i> .....	19
2.3.2 <i>Early Fetal Wound Healing</i> .....	20
2.3.3 <i>Proteins Investigated in this Study</i> .....	21
2.3.4 <i>Transcriptional Comparison of Collagen versus Silicone Devices</i> .....	25
Chapter 3: Materials and Methods.....	27
<b>3.1 Implant Preparation .....</b>	<b>27</b>
3.1.1 <i>Silicone Nerve Tube Preparation</i> .....	27
3.1.2 <i>Collagen Nerve Tube Preparation</i> .....	28
<b>3.2 Implant Characterization.....</b>	<b>29</b>
3.2.1 <i>Determining Collagen Device Porosity</i> .....	32
3.2.2 <i>Results</i> .....	34
<b>3.3 Peripheral Nerve Regenerate Procurement and Storage.....</b>	<b>36</b>
3.3.1 <i>Experimental Samples</i> .....	36
3.3.2 <i>Surgeries and Device Implantation</i> .....	38
3.3.3 <i>Post-Operative Care</i> .....	39
3.3.4 <i>14-Day Post-Operative Sacrifice</i> .....	39
3.3.5 <i>Tissue Processing for ELISA and Immunoblotting</i> .....	39
3.3.6 <i>Tissue Processing for Immunofluorescence</i> .....	41
<b>3.5 Enzyme-linked Immunosorbent Assay (ELISA) .....</b>	<b>43</b>
3.5.1 <i>Concept</i> .....	43
3.5.2 <i>Discussion of Assay Choice</i> .....	44
3.5.3 <i>ELISA Method</i> .....	45
3.5.4 <i>ELISA Data Analysis</i> .....	46
<b>3.6 Immunoblot Assay .....</b>	<b>47</b>
3.6.1 <i>Concept</i> .....	47
3.6.2 <i>Assessment of Antibody Specificity</i> .....	48
3.6.3 <i>Antibody Choice</i> .....	50
3.6.4 <i>Immunoblot Method</i> .....	52
3.6.5 <i>Immunoblot Data Analysis</i> .....	53
<b>3.7 Direct Immunofluorescence Assay .....</b>	<b>54</b>
3.7.1 <i>Concept</i> .....	54

3.7.2 Discussion of Assay Choice .....	55
3.7.3 Immunofluorescence Method .....	56
3.7.4 Immunofluorescence Data Analysis .....	57
3.7.5 Correction Factor Results .....	60
Chapter 4: Results and Error Analysis .....	62
4.1 TGF $\beta$ 1 Expression .....	63
4.2 TGF $\beta$ 2 Expression .....	66
4.3 TGF $\beta$ 3 Expression .....	68
4.4 $\alpha$ SMA Expression .....	70
Chapter 5: Discussion .....	75
5.1 TGF $\beta$ 1 Expression .....	75
5.2 TGF $\beta$ 2 Expression .....	76
5.3 TGF $\beta$ 3 Expression .....	77
5.4 $\alpha$ SMA Expression .....	78
Chapter 6: Summary .....	80
References .....	81
Appendix A: Protocols .....	86
A.1 5% Collagen Tube Fabrication Protocol .....	86
A.2 Dehydrothermal Treatment (DHT) of Implant Devices .....	90
A.3 Sterile Procedure and Implant Assembly for Surgery Preparation .....	92
A.4 Surgical Protocol .....	93
A.5 Post-Operative Care and Supervision Protocol .....	95
A.6 Animal Sacrifice .....	96
A.7 Optimal Cutting Temperature (OCT) Embedded Tissue Processing Protocol .....	97
A.8 Formalin-Fixed Paraffin-Embedded (FFPE) Tissue Processing Protocol .....	98
A.9 JB-4 Embedding, Staining, and Imaging for Pore Analysis .....	100
A.10 Linear Intercept Method for Pore Size Analysis .....	102
A.11 Tissue Digestion for ELISA and Immunoblotting Quantification .....	113
A.12 TGF $\beta$ 1 Enzyme-Linked Immunosorbent Assay (ELISA) .....	114
A.13 Calculating ELISA Mass Protein per Mass Tissue Statistic .....	116
A.14 Dot Blot Technique for Antibody Cross-Reactivity Assessment .....	117
A.15 Immunoblot Detection of Protein in Tissue Samples .....	119
A.16 Semiquantification of Immunoblot Bands .....	123
A.17 Direct Immunofluorescence Measurement of Protein in Formalin Fixed, Paraffin- Embedded Tissue .....	124
A.18 Determining Immunoblot Correction Factor for $\alpha$ SMA Using Immunofluorescence Data .....	126
A.19 Quantifying $\alpha$ SMA Fluorescence Intensity Using Concentric Shell Sampling Specified by Radial Distance from Edge .....	128

## List of Tables and Figures

Figure 1. Cross-sectional anatomy of the peripheral nerve illustrating the connective tissue layers and unmyelinated (left inset) and unmyelinated (right inset) axons (Lee and Wolfe, 2000). .....	13
Figure 2. Anatomy of the rodent hind limb indicating the location of sciatic nerve in relation to other anatomical structures (Chamberlain, 1998). .....	13
Table 1. Clinical comparison of rat sciatic nerve wounds treated with unfilled silicone or unfilled collagen tube devices, 10 mm gap (Chamberlain, 1998a; Chamberlain <i>et al.</i> , 1998b, 2000) .....	16
Table 2. Significant effects of treatment device (collagen or silicone tube) on TGF $\beta$ 1, TGF $\beta$ 2, TGF $\beta$ 3, and $\alpha$ SMA mRNA expression levels in whole peripheral nerve wounds (Wong 2008). .....	26
Table 3. 48 hour 120C DHT crosslinked collagen tubes (groups A, B, and C) used in pore size characterization .....	31
Figure 3. SEM images of collagen tubes from group A (a,d), group B (b,e), and group C (c,f). (a-c) Lateral, inner surface view of nerve tubes. (d-f) Lateral, outer surface view of nerve tubes. ....	34
Figure 4. Cross sectional images of collagen tubes from groups A (a, d), B (b, e), and C (c, f). Aniline blue stained JB-4 embedded sections (a-c) and corresponding SEM images (d-f).....	35
Table 4. Average pore size for 48 hour 120°C DHT crosslinked collagen tubes used in 2008 and 2009 proteomic studies .....	36
Figure 5. Pore diameter (mean $\pm$ SEM) for 48 hour DHT crosslinked collagen tubes used in 2008 and 2009 proteomic studies .....	36
Table 5. Sample sizes for treatment groups studied with ELISA, immunoblotting, and immunofluorescence .....	38
Figure 6. Use of implanted tube to bridge 10 mm gap between proximal and distal ends of sciatic nerve wound (adapted from Chamberlain, 1998). .....	38
Figure 7. Segmentation of nerve samples into five ~3 mm segments with the requirement that segment 1 contain the proximal nerve stump and that segment 5 contain the distal nerve stump (adapted from Wong, 2008). .....	40
Figure 8. Segmentation of samples into five 3.5-4 mm pieces for paraffin embedding. Locations are in reference to proximal end of implant. ....	42
Table 6. Proteins used as positive and negative controls to assess TGF $\beta$ antibody specificity... ..	49
Table 7. Primary antibody candidates for use in TGF $\beta$ immunoblots .....	50
Figure 9. Dot blot results for antibody binding to TGF $\beta$ 1, TGF $\beta$ 2, TGF $\beta$ 3, and BSA (negative control) protein spots. ....	51
Table 8. Evaluation of antibody binding to protein spots in dot blot test. The number of pluses indicate relative amount of intensity, while a minus indicates no intensity from a spot. ....	51
Table 9. Evaluation of antibody binding to the PVDF membrane. The number of pluses indicate relative amount of intensity, while a minus indicates no intensity from a spot. ....	51
Table 10. Primary and secondary antibodies used for immunoblot detection .....	53
Figure 10. Excitation and emission spectra of Cy3 fluorophore (Invitrogen). Maximal excitation of Cy3 occurs at 550 nm, with peak emission at 570 nm. Cy3 visualization can be visualized with traditional TRITC filter sets (nearly identical emission and excitation spectra). ....	55
Figure 11. One 10x captured image of collagen treated wound cross section stained for $\alpha$ SMA (red). Multiple 10x images are stitched together to create image of entire nerve cross section.	

White lines delineate borders between regions of the image. The background (region 1) is negative space on the slide containing no tissue. Scar and blood vessel formation (region 2) on the outside surface of the collagen tube stains highly for  $\alpha$  SMA. The collagen tube (region 3) is still intact at 2 weeks and harbors some contractile cells expressing  $\alpha$  SMA. The regenerate (region 4) has some  $\alpha$  SMA expression, with intense staining from blood vessels (arrow)..... 58

Table 11. Percent contributions of  $\alpha$  SMA expression from sources internal and external to regenerate tissue..... 60

Table 12. Percent contributions of cellular content from sources internal and external to regenerate tissue..... 61

Figure 12. 14-day whole wound TGF  $\beta$ 1 expression (mean  $\pm$  SEM) as determined by ELISA. Expression was normalized by mass of the whole explanted tissue..... 63

Figure 13. 14-day whole wound TGF  $\beta$ 1 expression (mean  $\pm$  SEM) as determined by average immunoblot intensity per unit area. Expression was normalized by cellular content. .... 63

Figure 14. 14-day TGF  $\beta$ 1 expression (mean  $\pm$  SEM) on per segment basis as determined by ELISA. Expression was normalized by mass of the explanted tissue segment..... 64

Figure 15. 14-day TGF  $\beta$ 1 expression (mean  $\pm$  SEM) on per segment basis as determined by average immunoblot intensity per unit area. Expression was normalized by cellular content. ... 65

Figure 16. 14 day whole wound TGF  $\beta$ 2 expression (mean  $\pm$  SEM) as determined by average immunoblot intensity per unit area. Expression was normalized by cellular content. .... 66

Figure 17. 14-day TGF  $\beta$ 2 expression (mean  $\pm$  SEM) on per segment basis as determined by average immunoblot intensity per unit area. Expression was normalized by cellular content. ... 67

Figure 18. 14-day whole wound TGF  $\beta$ 3 expression (mean  $\pm$  SEM) as determined by average immunoblot intensity per unit area. Expression is normalized for cellular content. .... 68

Figure 19. 14-day TGF  $\beta$ 3 expression (mean  $\pm$  SEM) on per segment basis as determined by average immunoblot intensity per unit area. Expression was normalized by cellular content. ... 69

Figure 20. 14-day whole wound  $\alpha$  SMA expression (mean  $\pm$  SEM) as determined by average immunoblot intensity per unit area. Expression has been adjusted to reflect  $\alpha$  SMA expression inside the regenerate only with normalization by cellular content. .... 70

Figure 21. 14-day  $\alpha$  SMA expression (mean  $\pm$  SEM) on per segment basis as determined by average immunoblot intensity per unit area. Expression has been adjusted to reflect  $\alpha$  SMA expression inside the regenerate only with normalization by cellular content. .... 71

Figure 22.  $\alpha$  SMA expression in 14-day (a) silicone and (b) collagen treated peripheral nerve wounds. Cross sections were taken 2.5 mm from the proximal end of the tube, and intensity measurements were taken from the edge of the regenerate to  $\sim$ 65  $\mu$ m radially into the center of the cross section to capture  $\alpha$  SMA expression from circumferential contractile cell layers observed in silicone treated wounds by previous investigators. .... 72

Figure 23. 14-day  $\alpha$  SMA expression (mean  $\pm$  SEM) for 5 locations sampled in nerve using immunofluorescence intensity as a metric. Intensity data for cross sections were summed over a concentric shell extending from the periphery to  $\sim$ 65  $\mu$ m toward the center of the regenerate and averaged across treatment groups. .... 73

Table 13. Polynomial order 2 best fit curve to describe peripheral  $\alpha$  SMA expression across the entire nerve..... 74

Figure 24. Teflon and aluminum mold schematic ..... 88

Figure 25. Teflon and aluminum mold (side view) with inserted mandrels..... 88

Figure 26. Collagen nerve tube produced from Teflon and aluminum mold ..... 89

Table 14. Tissue processor settings for paraffin embedding ..... 99





## Chapter 1: Introduction

Peripheral nerve regeneration is currently an important focus in biomedical and bioengineering research because of serious complications, e.g. paralysis or loss of sensation, which occur as a result of trauma to the nerve. Each year, about 200,000 patients in the United States undergo surgical operations to treat peripheral nervous system (PNS) injuries (Madison *et al.*, 1992). The work of the MIT Fibers and Polymers Laboratory involves studying and modifying the wound healing mechanism *in vivo* in order to prevent or lessen the clinical consequences arising from these injuries. Severe PNS wounds spontaneously heal by closure and scar formation instead of regeneration of functional tissue. When the damaged peripheral nerve fails to regenerate or reconnect, stumps called neuromas form at both ends of the nerve, resulting in a wound gap in between (Dellon, 1990). The gap disconnecting the proximal and distal ends of the nerve trunk disrupts signal transmission to or from the central nervous system and leads to loss of motor and sensory function.

Implantation of nerve tube devices to induce tissue regeneration between the ends of severed peripheral nerve has been successful in the rat animal model over gap lengths on the order of several millimeters (Yannas, 2001). To improve clinical outcomes, it is imperative to optimize for the biomaterial device used as the implanted conduit for axonal growth across the gap. Electrophysiological and morphological studies have demonstrated that collagen tubes induce a better quality regenerate than the traditional silicone device (Chamberlain, 1998; Spilker, 2000; Kemp *et al.*, 2008). The regenerate formed from collagen treated wounds more closely resembles and functions as nerve trunk. However, understanding of this outcome needs to be further approached from a biochemical and biomechanical perspective.

This study was a protein level investigation of peripheral nerve regeneration induced by collagen nerve tubes versus silicone tubes and is meant to complement the thesis work done by Wong to probe whether differences in transcriptional activity could explain the clinical disparity between the two biomaterial devices (2008). The experiments in the current study involved the evaluation of rat sciatic nerves undergoing early stage wound healing with the aid of a collagen or silicone treatment device. The ends of the transected nerve were separated apart by a 10 mm gap. The nerve and regenerate were explanted two weeks post-operatively from the date of transection and tube implantation. The involvement of various proteins present during wound healing was determined through quantitative and qualitative biological assays such as enzyme-linked immunosorbent assay (ELISA), immunoblotting, and immunofluorescence.

The hypothesis of this study was largely based on the paradigm that the change in spontaneous adult wound healing to induced regenerative healing can be compared to the reverse of the transition that is observed in early to late fetal wound repair. Unlike wounds in the late fetal stage which close by contraction and scar formation, early fetal injuries are able to heal spontaneously through regeneration and therefore serve as the desired clinical model for inducing regeneration in adults (Yannas, 2005). To this end, much research emphasis was placed on the members of the transforming growth factor beta (TGF  $\beta$ ) protein family which are thought to be antagonists or protagonists of regeneration due to their relative up or down regulation in early to late fetal wound healing environments (Shah et al, 1995; Soo et al, 2003). TGF  $\beta$ 1, TGF  $\beta$ 2, and TGF  $\beta$ 3 are the three members of this family present in mammals, and despite their homology, are hypothesized to play different roles in wound healing. This conjecture was tested by measurement of each protein in peripheral nerve wounds undergoing regenerative versus nonregenerative repair based on the use of a collagen or silicone treatment

device. In addition, measurement of alpha smooth muscle actin ( $\alpha$  SMA), a cytoskeletal component of differentiated fibroblasts, was chosen to assess how the concentration of a protein that has been associated with wound contraction might vary might alter in the healing milieu inside a regenerative versus nonregenerative device. The roles of these proteins in wound healing are described at greater length in Section 2.3.

## Chapter 2: Background

### 2.1 Peripheral Nerve Wounds

#### 2.1.1 Anatomical and Functional Context

The peripheral nervous system is comprised of the sensory, motor, and mixed nerves that branch from the central nervous system to the periphery of the body. Inside the nerve are various cell types, circulatory and lymphatic vessels, and connective tissue layers (Afifi and Bergman, 1997). Neurons, the primary unit of the nerve, and their supporting cells, known as Schwann cells, are found in the innermost connective tissue layer called the endoneurium. Neurons are structurally composed of dendrites, a 5-100  $\mu\text{m}$  diameter soma (cell body), and a long, thin axon that extends from the soma to a distal target in the periphery of the body. Signals are sent as action potentials (electrical spikes) down the axon, which can be covered in insulating layers known as the myelin sheath that helps signal conduction. In a normal nerve, the action potentials arrive at the axon terminal which synapses with another neuron in the central nervous system to deliver sensory information or at a neuromuscular junction to induce movement.

Within the nerve, axons are clustered in groups called fascicles, one or more of which are ensheathed by the perineurium, another connective tissue layer (Afifi and Bergman, 1997). The perineurium provides some tensile strength and elasticity to the nerve and acts as a diffusion barrier between neurons and blood vessels. The epineurium is the outermost layer of loose connective tissue containing blood and lymphatic vessels. It serves functionally as a structure to dissipate mechanical stresses put on the nerve during incidents of trauma.

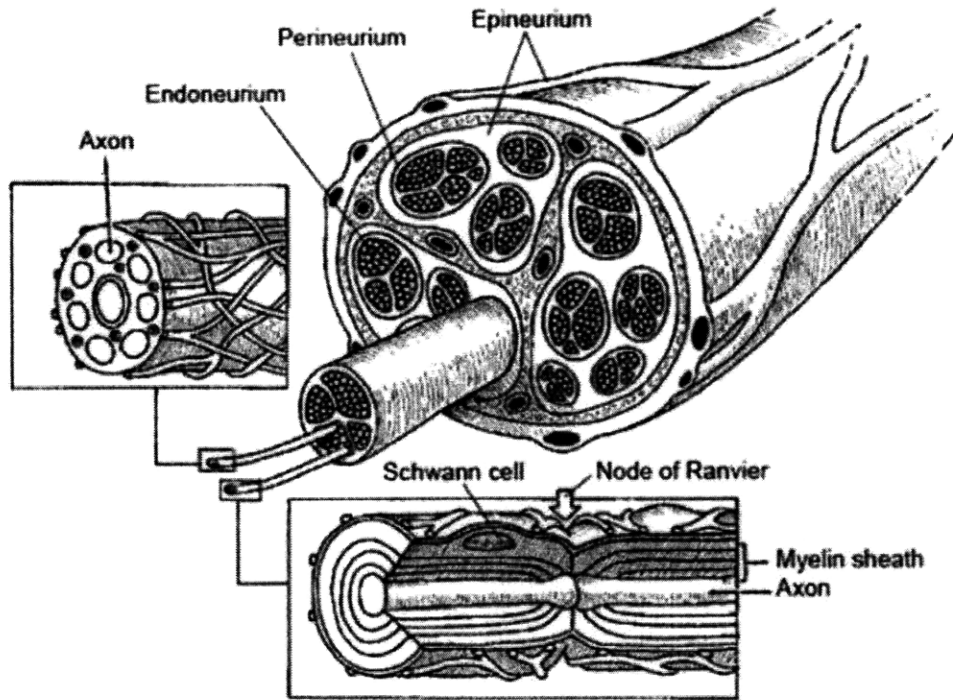


Figure 1. Cross-sectional anatomy of the peripheral nerve illustrating the connective tissue layers and unmyelinated (left inset) and myelinated (right inset) axons (Lee and Wolfe, 2000).

### 2.1.2 Animal Model

This wound healing study investigated differential protein expression in two treatments of rat sciatic nerve transection. The rat sciatic nerve has been a commonly used model to study PNS wound healing (Lundborg *et al.*, 1982; Archibald *et al.*, 1991; Chamberlain, 1996, 1998a; Chamberlain *et al.*, 1998b, 2000; Spilker, 2000; Harley, 2002; Wong, 2008). The sciatic nerve begins from the lumbar

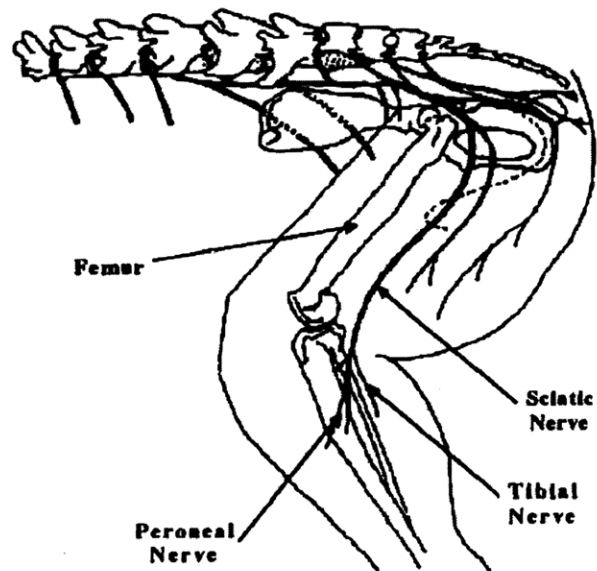


Figure 2. Anatomy of the rodent hind limb indicating the location of sciatic nerve in relation to other anatomical structures (Chamberlain, 1998).

region of the spinal cord and runs down through the buttocks into the lower limb. In the thigh,

the sciatic nerve branches into the tibial and common peroneal nerves, which innervate the lower leg and foot.

## **2.2 Wound Healing Response**

### *2.2.1 Spontaneous Peripheral Nerve Healing*

After peripheral nerve has been completely transected, the wounded neurons undergo some degenerative processes and then make attempts at regeneration (Lee and Wolfe, 2000). The entire soma swells in response to injury (Afifi and Bergman, 1997). The cell nucleus shifts from the center of the cell body to periphery and organelles proliferate and enlarge in size. There is a change in metabolic priority to produce new materials for axonal repair and growth: messenger RNA; lipids; cytoskeletal proteins, e.g. actin, tubulin, and neurofilament protein; growth associated proteins; and neuronotropic factors. The axon and myelin sheath undergo degeneration. Macrophages invade the wound to phagocytose any fragments. An axon sprout grows from the proximal stump and is mediated by growth cones to penetrate through the extracellular matrix (ECM).

Full recovery can take from three months to half a year. If regeneration fails, the cell atrophies and is replaced by glia. If the neuronal cell bodies are able to survive the injury, the ideal wound healing outcome is reanastomosis, which involves the reconnection of axons to their appropriate distal target. If the proximal and distal ends of the nerve fail to meet, caps at each end of the trunk called neuromas form (Dellon, 1990).

### 2.2.2 Induced Regeneration using Tubulation

Regeneration of severed peripheral nerve has been induced with some success using implantation of a tube device to bridge the wound gap between the disconnected nerve ends. The ideal implant for nerve regeneration would consider the following factors: support and possibly stimulation of axonal growth; resorption via the metabolic pathways of the host, with the appropriate resorption kinetics to accommodate the time needed for axonal growth across the gap; and nontoxic, nonantigenic, and noncarcinogenic properties as to not harm the host or trigger an unreasonable immune response (Archibald *et al.*, 1991). The use of tubulation as a conduit for axonal growth through an interneural wound gap has existed for over 100 years, though the devices have ranged in compositions from autografted naturally occurring tissues, nondegradable synthetic materials, and degradable natural and synthetic materials (Fields *et al.*, 1989). Silicone tubing was one of the original devices chosen for nerve repair and is used as a benchmark to compare devices of other materials (Lundborg *et al.*, 1982; Fu and Gordon, 1997). Studies probing the regenerative ability of tubes composed of various biomaterials involve the creation of a well-defined defect on an animal of study (Yannas, 2001). Full transection of the peripheral nerve is performed on an animal model and the implanted device is sutured to the nerve to bridge a gap of known length. The animal is allowed to recover from the surgical procedure and the repair response of the peripheral nerve takes its course. After a prescribed number of days, weeks, or months, depending on the timescale of study, the resulting wound chamber, whose bounds are defined by the tubulation, now encompasses the transected nerve trunks and any newly formed tissue and exudate present within the gap. The wound is explanted at time points of interest and clinical assessments are made.

Investigators such as Chamberlain and Kemp *et al.* have compared the clinical outcomes of treating peripheral nerve wounds with silicone tubes and collagen tubes (Chamberlain, 1998a; Chamberlain *et al.*, 1998b, 2000; Kemp *et al.* 2008). It was found that collagen tubes promote superior nerve trunk regenerate than does the silicone standard at several gap lengths and different time scales. Using a 10 mm gap model, collagen tube treated nerves displayed improved clinical performance including farther axon growth, greater myelination, and enhanced vasculature in measurements performed one to two months post-operatively, and in the longer term, larger axon size and count, better conduction properties, and improved sensorimotor recuperation. Table 1 is a brief listing of previously observed contrasts between 10 mm gap rat sciatic nerve wounds treated with silicone and collagen devices found by Chamberlain *et al.* in 60 week post-operative measurements (1998a, 1998b, 2000).

Measurement	Observations on Silicone versus Collagen Device Performance on 10 mm gap Rat Sciatic Nerve Wounds, 60 Week Post-Operative
Total tissue cable area	About six times the area in collagen treated ( $0.58 \pm 0.07$ ) than in silicone treated (0.09)
Mean diameter of regenerate, center of gap	Twice as large in collagen treated (~1.3 mm) than silicone (~.55 mm)
Myelinated axons per nerve	About 50-60 times as many in collagen treated (~11,000) than silicone (~200)
Thickness of fibrous tissue capsule at regenerate periphery, center of gap	About ten times thicker in silicone treated than in collagen treated

**Table 1. Clinical comparison of rat sciatic nerve wounds treated with unfilled silicone or unfilled collagen tube devices, 10 mm gap (Chamberlain, 1998a; Chamberlain *et al.*, 1998b, 2000)**

Tubulation studies of various gap lengths and time scales have found interesting morphological and physiological disparities in the regenerate that resulted from bridging the nerve wound with a collagen or silicone device. Archibald *et al.* have even shown the collagen device performing up to the level of an autograft (2004), as did Chamberlain *et al.* (1998).



### 2.2.3 Theories of Peripheral Nerve Wound Healing

Given the disparity in device performance in the treatment of severed peripheral nerve, it is important to gain understanding of the mechanism underlying wound healing to produce the most efficacious devices. It has been observed that within hours of nerve transection and device implantation, the implanted tube becomes filled with endoneurial fluid and axons begin withdrawing from the distal stump. Within a week, a cable consisting of blood clot forms. Depending on the implant characteristics, the amount of contractile capsule that forms on the perimeter of the nerve trunk and of microtubule synthesis by Schwann cells in the first few weeks appears to determine whether a neuroma is formed and whether microtubules bridging the gap enable axon elongation (Yannas, Zhang *et al.*, 2007).

Several theories have emerged in an attempt to explain the phenomena which occur *in vivo* during spontaneous nerve healing based on observations seen in experimental wound chambers. These theories are the neurotrophic theory, contact guidance theory, pressure cuff theory, and basement membrane microtubule theory. While each theory is supported by empirical data, the mechanism underlying peripheral nerve wound healing is probably a complex combination of these biochemical and biomechanical explanations.

#### 2.2.3.1 Neurotrophic Theory

Neurotrophic theory attributes axon elongation and migration of supporting cells across the interneural wound gap to the release of growth factors by the distal end of the wound (Yannas, Zhang *et al.*, 2007). The diffusion of growth factors across the gap towards the proximal nerve trunk hypothetically acts as a guiding neurotrophic influence for proper reanastomosis. In support of this theory, an inserted distal stump in a chamber containing a

proximal nerve stump allows for regenerative success over greater distances than an open ended chamber (no distal stump) or ligated distal stump (Lundborg *et al.*, 1982). However the theory does not explain the large drop in regenerative success with a relatively small increase of gap length. On its own, the neurotrophic theory cannot explain for the differences in clinical outcomes in using cell-permeable rather than protein-permeable chambers or insoluble devices with particular orientations.

#### 2.2.3.2 Contact Guidance Theory

According to the contact guidance theory, axons are guided across the gap via contact with and attachment to a substrate (Yannas, Zhang *et al.*, 2007). Insoluble substrates within the wound chamber, such as collagen-glycosaminoglycan (collagen-GAG) matrix filling, heavily influences the outcome of regeneration (Chamberlain, 1998; Spilker, 2000). The existence and structure of these substrates may be important in promoting regeneration because of adhesion of cytokines that support that mode of repair. However, this theory does not explain the superior regenerative activity of Schwann cell suspensions or of solutions of certain growth factors.

#### 2.2.3.3 Pressure Cuff Theory

The pressure cuff theory pinpoints the activity of force-exerting cells as the determinant in the healing outcome of wounded peripheral nerve tissue. Myofibroblasts are differentiated fibroblasts exhibiting a contractile phenotype and are found in two orientations in the nerve: axially aligned and circumferentially aligned (Chamberlain, 1996, 1998a; Chamberlain *et al.*, 1998b, 2000). The axially aligned cells are thought to exert a tensile force that may guide the regenerating nerve trunk across the gap, while having to compete with the circumferentially

aligned cells which form a contractile capsule around the proximal and distal nerve trunks to compress the regenerating nerve radially. The contractile forces are responsible for neuroma formation and the necking of the regenerate that is seen at the center of gap. The pressure cuff theory plausibly accounts for why regenerative success of nerve in spontaneous healing and induced regeneration studies is a function of gap length: as the gap length increases, contractile forces prevail over the axial forces to form a neuroma before the axons from the proximal end are able to elongate across to the distal target.

#### *2.2.3.4 Basement Membrane Microtubule Theory*

As experimentally observed in a nerve chamber, Schwann cells are found to migrate ahead of all cell types along the fibrin cable that forms following flow of wound exudate. In the absence of axons, basement membrane formation accompanying Schwann cell migration was documented (Zhao *et al.*, 1992). The two sets of data have led to the theory that Schwann cells migrate along the fibrin cable and synthesize 10-20 mm diameter cylindrical basement membrane microtubules in which axons can elongate and become myelinated (Yannas, Zhang *et al.*, 2007).

### **2.3 Early Fetal Repair as a Model for Regeneration**

#### *2.3.1 Spontaneous Late Fetal and Adult Wound Repair*

In all organ systems, spontaneous adult mammalian response to injury is a three stage process: inflammation, tissue formation, and remodeling (Gurtner *et al.*, 2008; Yannas, 2001). Inflammation occurs immediately after injury. Exudate, consisting of blood and extravascular tissue fluid, flows into the wound site along with cells from neighboring tissues. The exudate

carries cytokines released by the injured neuron to further the inflammatory response by attracting supporting cells, such as neutrophils and monocytes, and by promoting angiogenesis. Coagulation and immune response occur to stop blood and fluid losses, to remove dead tissues, and to prevent infection.

New tissue formation occurs a few days after injury and is characterized by cellular proliferation and infiltration by different cell types. Fibroblasts which are attracted from the edge of the wound are stimulated by pro-fibrotic cytokines released by differentiated monocytes, known as macrophages, and they themselves differentiate into myofibroblasts. The myofibroblasts produce and organize extracellular matrix (ECM), mainly consisting of collagen, forming scar tissue that lacks the architecture and function of normal nerve tissue (Yannas, 2001; Bottinger, 2008).

Remodeling of tissue begins a few weeks after injury and lasts for years. During this stage, the trauma-induced acute inflammatory processes cease. Endothelial cells, macrophages, and myofibroblasts undergo apoptosis or exit the wound (Gurtner *et al.*, 2008).

### 2.3.2 *Early Fetal Wound Healing*

Unlike adults, mammalian fetuses during the first two trimesters have the ability to spontaneously heal injuries by regeneration of tissue. During this early fetal stage, certain organs, such as skin and long bones, are observed to heal with minimal inflammatory response and without scar (Yannas *et al.*, 2007). The ability to restore tissue with the same morphology and functionality of the tissue existing prior to injury is of interest to the field of regenerative medicine. Thus, the mechanism of early fetal regeneration serves as a model to induced adult

regeneration, and differential protein observations found from early fetal to adult regeneration motivated the protein selection of this study.

Cytokines are an important part in transitioning early fetal regeneration to late fetal and adult repair. To better understand the mechanism of early fetal regeneration, investigators have studied molecules that are differentially expressed between early fetal and adult wounds. Observations have included decreased levels of pro-inflammatory cytokines including transforming growth factor beta 1 (TGF  $\beta$ 1) and 2 (TGF  $\beta$ 2), interleukin 6 (IL 6) and 8 (IL 8), platelet derived growth factor (PDGF), fibroblast growth factor (FGF), decorin, and tissue-derived inhibitor of metalloproteinases (TIMP) in early fetal wounds (Krummel *et al.*, 1988; Whitby *et al.*, 1996; Liechty *et al.*, 1998, 2000a; Beanes *et al.*, 2001; Dang *et al.*, 2003). The roles of these molecules include attracting fibroblasts and inflammatory cells, increasing collagen synthesis and deposition, and stimulating wound contraction (Yannas *et al.*, 2007). Alternatively, fetal wounds demonstrate higher levels of vascular endothelial growth factor (VEGF), hyaluronic acid, fibromodulin, metalloproteinases, TGF  $\beta$ 3, and IL 10 (Colwell *et al.*, 2005; Longaker *et al.*, 1991; Soo *et al.*, 2000, 2003; Liechty *et al.*, 2000b). The roles of these molecules include promoting vascularization, modulating extracellular matrix (ECM), and deactivating inflammatory cells (Yannas *et al.*, 2007).

### *2.3.3 Proteins Investigated in this Study*

This study chose to investigate differential TGF  $\beta$  and  $\alpha$  SMA expression in tissue regenerate induced by silicone or collagen tube treatment of peripheral nerve wounds. The reasons for this protein selection were numerous. First, TGF  $\beta$  has already been researched in wound repair across many organ types and this study serves as an extension of our knowledge of

its role in the PNS. Secondly, with an eye on the pressure cuff theory of wound healing, we are interested in the activity of fibroblasts, which are considered the major effector in scarless repair (Lorenz *et al.*, 1995). TGF  $\beta$  has many regulatory functions including the differentiation of adult and fetal fibroblasts to a myofibroblast phenotype that expresses  $\alpha$  SMA (Rolfe *et al.*, 2007). The roles of these proteins tie in nicely with our overall objective: to gain a better understanding of how to optimize *in vivo* induced regeneration. With this objective in mind, this proteomic study looks downstream from the genomic focus on TGF  $\beta$  and  $\alpha$  SMA done by Wong (2008).

#### 2.3.3.1 Transforming Growth Factor Beta (TGF $\beta$ ) Family

TGF  $\beta$  regulates the production and degradation of the ECM and the adhesive interactions between cells and the ECM in many cell types. Epithelial cells, fibroblasts, monocytes, and macrophages produce and respond to TGF  $\beta$  (Bottinger, 2008). Because of this, the protein family is responsible for the regulation of proliferation, apoptosis, differentiation, migration, cell attachment, wound healing, and fibrosis. The involvement of TGF  $\beta$  in wound repair first emerged over two decades ago when administration of TGF  $\beta$  to a wound chamber was found to promote repair (Sporn *et al.*, 1983). Since then, TGF  $\beta$ , its receptors, signaling molecules, and antibodies have been extensively studied for their roles in wound healing. TGF  $\beta$  is released from activated platelets aggregated at the wound sites, recruiting monocytes and macrophages. TGF  $\beta$  has been shown to induce fibroblasts to differentiate into their contractile phenotype *in vitro* and *in vivo* (Desmouliere *et al.*, 1993). Activated TGF  $\beta$  stimulates ECM production by fibroblasts and is responsible for the synthesis and deposition of ECM proteins including collagens, fibronectin, osteonectin, osteopontin, tenascin, thrombospondin, biglycan, and decorin (Schilling *et al.*, 2008). TGF  $\beta$ 1 has been shown to affect neuronal migration by up

regulating cell adhesion molecules, neural cell adhesion molecule, and integrin subunits (Siegenthaler and Miller, 2004). In both peripheral and central nervous system wounds, local delivery of antibodies against TGF  $\beta$  was found to reduce fibrotic response and maintain or restore functional integrity of the tissue (Nath *et al.*, 1998).

TGF  $\beta$ 1 and TGF  $\beta$ 2 are known as pro-fibrotic cytokines that promote deposition of ECM components and formation of scar during wound repair. Exogenous addition of neutralizing antibodies to these two cytokines in rat dermal wounds has shown to reduce the amount of neovascularization, monocyte and macrophage presence, and deposition of fibronectin, collagen I, and collagen III compared to control wounds (Shah *et al.*, 1995). TGF  $\beta$ 1 when added exogenously induces scar in early human fetal wounds and amplifies its own expression. TGF  $\beta$ 1 mRNA and protein and TGF  $\beta$ 2 mRNA have been found in higher concentrations in late fetal (day 19) than early fetal (day 16) rat skin injuries (Soo *et al.*, 2003). These findings contribute to the hypothesis that heightened TGF  $\beta$ 1 and TGF  $\beta$ 2 levels are involved in the transition from regenerative to nonregenerative wound repair.

Conversely, TGF  $\beta$ 3 may favor the regenerative healing process through reduction of scar. Topical application of TGF  $\beta$ 3 has been shown to inhibit scar formation related to TGF  $\beta$ 1 activity (Shah *et al.*, 1995). In support of TGF  $\beta$ 3's linkage to regeneration, Soo and colleagues found that there were more TGF  $\beta$ 3 mRNA and protein expression in dermal wounds inflicted on 16-day-old than on 19-day-old fetal rats (2003). In the study, day 16 rat skin wounds, which demonstrated prolonged and higher levels of TGF  $\beta$ 3 expression and decreased and transient levels of TGF  $\beta$ 1, repaired with organized collagen deposition, while the day 19 rat skin wounds healed with disorganized collagen architecture typical of late fetal fibrotic response. Despite some evidence in support of the regenerative role that TGF  $\beta$ 3 may play, the isoform is still

undergoing clinical investigations to determine whether it can prevent the pro-fibrotic activity of TGF  $\beta$ 1 (Bottinger, 2008).

The suggestive disparity between the isoforms' roles in wound healing is interesting given that the peptide structures of the three members of the TGF- $\beta$  family are highly similar. TGF  $\beta$ 1 is composed of 390 amino acids, while TGF  $\beta$ 2 and  $\beta$ 3 are slightly larger with 22 additional amino acids (Moses and Roberts, 2008). All the isoforms are composed of a N-terminal signal peptide of 20-30 amino acids required for cell secretion, a latency associated peptide (LAP), and a 112-114 amino C-terminus that becomes the mature TGF  $\beta$  molecule upon cleavage. The mature molecules form 25 kDa disulfide-linked homodimers (Roberts *et al.*, 1983) and show 64-82% identity (Moses and Roberts, 2008). In measuring each protein for this study, the homology between the three isoforms proved to be an obstacle that needed to be addressed through determination and usage of isoform-specific antibodies.

#### 2.3.3.2 Alpha Smooth Muscle Actin ( $\alpha$ SMA)

$\alpha$  SMA, a protein composed of 375 amino acids, is present in the stress fibers of smooth muscle cells, myofibroblasts, and pericytes (Skalli *et al.*, 1989). It was determined that the presence of this protein in a cell indicates the ability to exert contractile forces (Masur *et al.*, 1996).  $\alpha$  SMA is the most commonly used marker for myofibroblasts (Gabbiani *et al.*, 1998, 2002; Arora and McCulloch, 1999; Ronty *et al.*, 2006). Presence of  $\alpha$  SMA was previously shown in a capsule on the periphery of the wound regenerate, especially in 60 week silicone treated wounds where antibody stains were 10-15 cell layers thick, and sometimes in collagen wounds where stains were 1 cell layer thick (Chamberlain, 1998a; Chamberlain *et al.*, 1998b, 2000). In silicone treated wounds, the sheath of myofibroblasts has been observed throughout



the entire tabulated chamber, including around the proximal and distal stumps of the transected nerve.

#### *2.3.4 Transcriptional Comparison of Collagen versus Silicone Devices*

Previous experimental work investigating the TGF  $\beta$  and  $\alpha$  SMA mRNA expressions in collagen and silicone treated rat sciatic nerve wounds showed significant differences in mRNA levels at only a few time points when examined at 1, 3, 7, 14, and 21 days after implantation (Wong 2008). The graphical results from Wong's study were converted into significant percent increase statistics and tabulated in Table 2. A significant difference in TGF  $\beta$ 1 expression between silicone and collagen treated wounds only appeared on day 7 ( $p=.007$ ), and TGF  $\beta$ 2 expression between the two treatment groups were significantly different only on day 21 ( $p=.024$ ). TGF  $\beta$ 3 mRNA expression in collagen treated samples encountered a steep rise ( $p=.0001$ ) on day 14 that amounted to almost three times the level of expression in silicone treated samples at the same time point. Wounds from both treatment groups experienced a slow rise in  $\alpha$  SMA mRNA expression for the first few days; however, after a week into the wound healing response, the silicone treated samples encountered a significant increase in  $\alpha$  SMA mRNA expression ( $p=.0028$ ) that was as much as three times the levels observed in collagen treated samples by the third week ( $p=.0001$ ).

	Day 1	Day 3	Day 7	Day 14	Day 21
<b>TGF <math>\beta</math>1 mRNA</b>	-	-	44% more expression in silicone treated wounds	-	-
<b>TGF <math>\beta</math>2 mRNA</b>	-	-	-	-	70% more expression in silicone treated wounds
<b>TGF <math>\beta</math>3 mRNA</b>	-	-	-	170% more expression in collagen treated wounds	-
<b><math>\alpha</math> SMA mRNA</b>	-	-	150% more expression in silicone treated wounds	-	180% more expression in silicone treated wounds

**Table 2. Significant effects of treatment device (collagen or silicone tube) on TGF  $\beta$ 1, TGF  $\beta$ 2, TGF  $\beta$ 3, and  $\alpha$  SMA mRNA expression levels in whole peripheral nerve wounds (Wong 2008).**

## Chapter 3: Materials and Methods

### 3.1 Implant Preparation

To distinguish between a regenerative and nonregenerative outcome following peripheral nerve transection, one tubulation device with the consistent ability to reform nerve trunk across the wound gap and another tubulation device lacking such ability were prepared according to previous methods (Chamberlain 1998, Spilker 2000, Harley 2002, Wong 2008). Impermeable silicone tubes are mostly observed to induce only connective, nonneuronal tissue when bridging a nerve wound separated by a 10 mm gap, while porous, crosslinked collagen tubes are found to have a greater ability to regenerate neuronal tissue at this length. Due to the disparities in clinical outcomes as explained in Section 2.2.2, collagen and silicone were chosen as the implants to be compared for protein level differences in regenerative versus nonregenerative scenarios.

#### *3.1.1 Silicone Nerve Tube Preparation*

Silicone tubing (ID: 3.1 mm, Helix Medical, LLC, Carpinteria, CA) were cut with clean and sterilized microscissors into 16 mm segments to prepare the silicone nerve tubes (Appendix A.2). Each silicone segment was flushed twice with sterile phosphate buffered saline (PBS) and deposited into individual, unused glass vials (Short Form Style with Phenolic Cap, Cat. No. 66011-063, VWR International). The vials were placed in a vacuum oven for 48 hours at 120°C for dehydrothermal treatment (DHT) and sterilization. Upon removal from the vacuum oven, the vials were immediately sealed, collected into a larger autoclaved glass jar with a lid closure for secondary containment, and stored in a dessicator with DrieRite Absorbent (VWR International, Inc., San Diego, CA) until use in surgery.

### *3.1.2 Collagen Nerve Tube Preparation*

Collagen tubes were fabricated by lyophilization of a 5% collagen slurry in a method developed previously by Harley and used by Wong (Appendix A.1). 0.25 g of collagen I (Integra Life Sciences, San Diego, CA) was dissolved in 4 mL of degassed, distilled water in a 10 mL Luer Lock syringe (Cat. No. 309604, Becton Dickson & Co., Franklin Lakes, NJ). Gradually, 1.0 mL of glacial acetic acid (GAA, Mallinckrodt Chemical Co., Paris, KY) diluted to a 3.0 M concentration, was added and mixed into the collagen-water suspension via a 1 or 3 mL syringe with 22 gauge needle (Cat. No. 309574, Becton Dickinson & Co.). The 10 mL syringe was connected to an empty 10 mL syringe using a female-female Luer Lock assembly (Stainless steel Luer Lock tube fitting, female luer x female luer, Cat. No. 5194k12, McMaster-Carr Supply Company, New Brunswick, NJ) and used to homogenize the collagen slurry from the transfer of the slurry back and forth between the two syringes 10-15 times. The assembly was disassembled and the collagen slurry was given time to swell in the closed 10 mL syringe for 3 hours at room temperature. The swollen slurry was degassed by centrifugation at 4500 rpm for an hour total.

Approximately 0.25 mL of degassed slurry was injected into each cylindrical opening of a specially designed Teflon and aluminum mold (Figure 24 and Figure 25) to produce tubes with an outer diameter of 3.0 mm. Steel core mandrels (D: 0.032", Cat. No. GWXX-320-30, Small Parts, Inc., Miami Lakes, FL) with Teflon coating (O.D. 0.056", I.D. 0.032", PTFE Tubing, Cat. No. 06417-31, Cole-Parmer Instrument Company, Vernon Hills, IL) were inserted into the center of the cylindrical openings to produce collagen tubes with an inner lumen of 1.5 mm diameter. Teflon tubing (OD: 0.125", ID: 0.065", PTFE Tubing, Cat. No. 06407-42, Cole-Parmer Instrument Company) were used as end caps to keep the mandrels centered and in place. The

slurry-filled molds were placed in a freeze drier for 1 hour at -40°C before the frozen tubes were freed from the mold using clean forceps and a razor. With the mandrels and end caps intact, the tubes were placed onto an aluminum foil sheet and returned to the -40°C lyophilization chamber. A vacuum was then used to reach a pressure of 200 mTorr or less. At this lower pressure, the chamber was raised to 0°C and held at the temperature for 17 hours, after which it was raised to 20°C and the vacuum released for tube removal. The lyophilized tubes were carefully transferred off the mandrels and placed in open pouches made from folded aluminum foil and were ready for the subsequent cross-linking and sterilization process. The tubes underwent DHT for 48 hours at 120°C and approximately -29.8 mmHg. Upon removal from the vacuum oven, the packets were immediately sealed and placed in a dessicator containing DrieRite Absorbent.

Before surgery, the DHT crosslinked tubes were cut into 16 mm segments in a sterile biohood. The surface on which the tubes were placed and the forceps, microscissors, and razor used to manipulate and cut the tubes were sterilized with 70% ethanol. The tubes were cut using the central portion of the lyophilized product, omitting inconsistencies in the tube produced by compressed slurry at the mandrel interface and any defects caused by removal of the tube from the Teflon and aluminum mold. In the case that excess lyophilized collagen was attached to the outside of the tube as a result of the gap between the top and bottom halves of Teflon and aluminum molds, as much of the excess was carefully removed from the outside of the tube using microscissors.

### **3.2 Implant Characterization**

The purpose of this study was to investigate the proteomic disparities between a peripheral nerve wound that healed with regeneration after treatment with a collagen tube and

one that healed without regeneration after using a silicone tube. The silicone and collagen devices have dissimilar biomaterial properties, such as mechanical stress and strain characteristics, permeability, degradation rate, swelling, protein adsorption affinity, that undoubtedly have an effect on the *in vivo* immunological response. It has been shown that altering properties such as pore size and extent of crosslinking even while keeping the biomaterial composition constant can result in improvement or decline in the device's regenerative ability (Chang 1991; Yannas 2001; Harley 2002). The porosity of the collagen tube is a large determinant of the biological activity of the tube because pore size dictates whether the device is cell or protein permeable and defines the surface density of ligands onto which cells can bind and use in migration. Duration and temperature of dehydrothermal crosslinking treatments have an effect on the structural rigidity of the collagen tube and in turn acts as resistance to degradation of the tube *in vivo*. Therefore, it is of the utmost importance to state the characteristics of the devices used in this study for experimental reproducibility and to define the parameters responsible for the clinical results later shown.

The silicone tubes used in all surgeries were prepared from the same lot of tubing and were considered consistent throughout this study. However, collagen tubes, while fabricated as described in Section 3.1.2 from collagen provided by Integra, were made from different lots and by different research assistants over a span of three years. The collagen tubes used in the ELISA and immunoblotting studies were produced by Eric Soller and/or Kelly Chien from 2006 to 2007, while those used in the immunofluorescence study were produced by Kathy Miu in 2009. Both sets of nerve tubes were produced under the optimal protocol determined by Harley but with the following changes: lyophilizer model (VirTis Genesis EL versus LE) and closure mechanism used on mold (c-clamps versus screws). The lyophilizer model used to produce the

2009 tubes (VirTis EL) is much more efficient at a vacuum pressure of less than 200 mTorr (minutes rather than hours). In addition, the VirTis EL is a more advanced model with computerized controls and recorded thermocouple data. Due to these reasons, the VirTis EL was a superior choice over the VirTis LE for current and future collagen tube fabrication. The 2009 implants used c-clamp closure over the screw to provide slightly more clearance for the lyophilization of the tube. This resulted in fabrication of collagen tubes that were less prone to sticking to the Teflon surface and fracturing upon removal from the mold.

Characterization was performed on the tubes produced from 2006 onwards (Table 3) in order to confirm that the tubes implanted were consistent with those tested by Harley as having regenerative properties. Microscopic techniques were used to determine the porosity of 2006 collagen tubes that were remaining in the dessicator in addition to newly fabricated 2009 nerve tubes in the two lyophilizer models. The results were then compared to those empirically determined by Harley (2002).

<b>Group</b>	<b>Fabricated by</b>	<b>Year of Fabrication</b>	<b>Lyophilizer Used</b>	<b>Description</b>
A	Kelly Chien, Eric Soller	2006	VirTis Genesis LE	48 hour DHT crosslinked; horizontal orientation; mold with unknown closure
B	Kathy Miu	2009	VirTis Genesis LE	48 hour DHT crosslinked; horizontal orientation; mold with screw closure
C	Kathy Miu	2009	VirTis Genesis EL	48 hour DHT crosslinked; vertical orientation; mold with c-clamp closure

**Table 3. 48 hour 120C DHT crosslinked collagen tubes (groups A, B, and C) used in pore size characterization**

The tube types A and C studied were chosen on the basis of gathering information on the devices implanted in surgeries from 2006 to 2009. However, characterizing tubes used in pre-2009 studies proved to be a challenge because examining tubes fabricated in 2006 (group A) for

properties it had in 2007-2008 has its share of problems. Tubes in group A were kept in an aluminum foil packet in a dessicator with modest changes of DrieRite Absorbent over the course of three years. Gelatinization and degradation of these tubes were highly probable given the extent of storage. Thus tubes in group B were fabricated in the same lyophilizer and with the same mold closure in an attempt to reproduce what is believed the tubes in group A should have looked like and behaved closer to the time of implantation. The C tubes fabricated in the VirTis Genesis LE were used in 2009 immunofluorescence surgeries. Tubes B and C were characterized to confirm regenerative activity of the implants used in the proteomic investigation.

### *3.2.1 Determining Collagen Device Porosity*

Scanning electron microscopy (SEM) was used to perform qualitative analyses of the surfaces of the dry collagen tubes. 1-3 mm nerve tube segments were imaged with a LEO VP438 microscope using the LEO Scanning Electron Microscope software. The tubes were viewed from the cross sectional, outer lateral, and inner lateral perspectives under variable pressure using the backscatter detector. The outer and inner surface views were achieved by cutting segments laterally with a razor and placing each half in the appropriate orientation on a small mounting stub. Qualitative analyses of the segments were made from visually inspecting the tubes under 20x, 100x, and 200x magnifications.

To be more quantitative in characterizing the tubes, the porosity of the collagen devices was determined with JB-4 embedded sections of nerve tubes per previously used methods (Harley, 2002). Embedding the tubes with reagents from a JB-4 Kit (Cat. No. 00226-1, Polysciences, Inc., Warrington, PA) allowed for thin slices (~6  $\mu\text{m}$ ) of the tubes to be sectioned



and stained for approximately single layers of collagen. In the JB-4 embedding protocol described in Appendix A.9, DHT crosslinked nerve tubes were cut into 3-5 mm segments and rotated overnight in 1.5 mL eppendorf tubes filled with 100% ethanol at 4°C. The nerve tubes were transferred into new eppendorf tubes filled with an equilibrium solution composed of 50% ethanol/50% catalyzed JB-4 A and rotated for 12 hours at 4°C. To allow for infiltration of the embedding medium into the devices, the collagen tubes were moved into new eppendorf tubes filled with 100% catalyzed JB-4 A solution and rotated over the course of three days at 4°C with changes of fresh solution every 12 hours. The infiltrated tubes were then added to 2 mL of catalyzed 96.2% JB-4 A solution/3.8% JB-4 B solution in a mold (Polyethylene Molding Cup Trays, 6x12x5mm, Cat. No. 16643A-1, Polysciences, Inc., Warrington, PA) that was kept chilled over ice due to the exothermic reaction that occurs during embedding. The tubes were manipulated or held in the embedding medium to ensure the proper orientation for cross sectional and lateral sections using a 21 gauge needle. After 15 minutes, a plastic block holder (Cat. No. 15899-50, Polysciences, Inc., Warrington, PA) was added to each sample and the mold was moved to 4°C where the JB-4 embedding medium was allowed to harden for 24 hours. The samples were removed from the mold and allowed to air dry at room temperature while protected from light. A microtome (Shandon Finesse ME, Thermo Fisher Scientific, Inc.) was used to section approximately 6 µm thick samples that were subsequently mounted on glass slides with 10% ammonium hydroxide. After overnight drying, the slides were stained with aniline blue and coverslipped. An Olympus BX51 microscope was used to capture the scaffold slices at 4x, 10x, and 20x magnifications. The linear intercept method (Appendix A.10) was used to calculate the pore size from the 10x images.

### 3.2.2 Results

The collagen tubes made in 2006 and left in the dessicator (group A) were studied under light microscopy and SEM as a means of retroactively characterizing the collagen devices implanted from 2006 to 2008. Using both imaging techniques, the group A tubes were found under cross-section to have a collapsed pore structure. Lateral views indicated a sheet-like exterior and inner lumen. The gelatinization kinetics of the

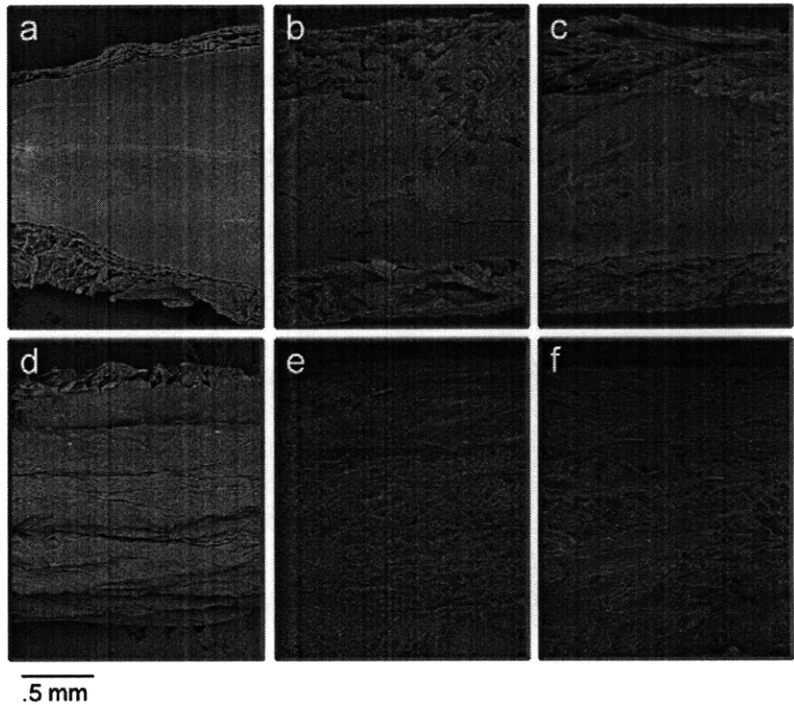


**Figure 3. SEM images of collagen tubes from group A (a,d), group B (b,e), and group C (c,f). (a-c) Lateral, inner surface view of nerve tubes. (d-f) Lateral, outer surface view of nerve tubes.**

tube under dessication has not been studied, and it is unclear how much of the biological activity of the tube had been lost before implantation, especially in the later surgeries. While the group A tubes are probably no longer characteristic of the implanted tubes in the 2007-2008 surgeries, they demonstrate an extreme case of degeneration of tube quality and serve as an example of a poor choice to be used in in regeneration studies. It was previously stated (Harley, 2002) that these tubes could be stored indefinitely in a dessicator with DrieRight Absorbent. However, due to inefficiencies in the dessication method, e.g. the tightness of dessicator seal or frequency of dessicant changes, it is clear that the quality of tubes should be evaluated on a case by case basis.

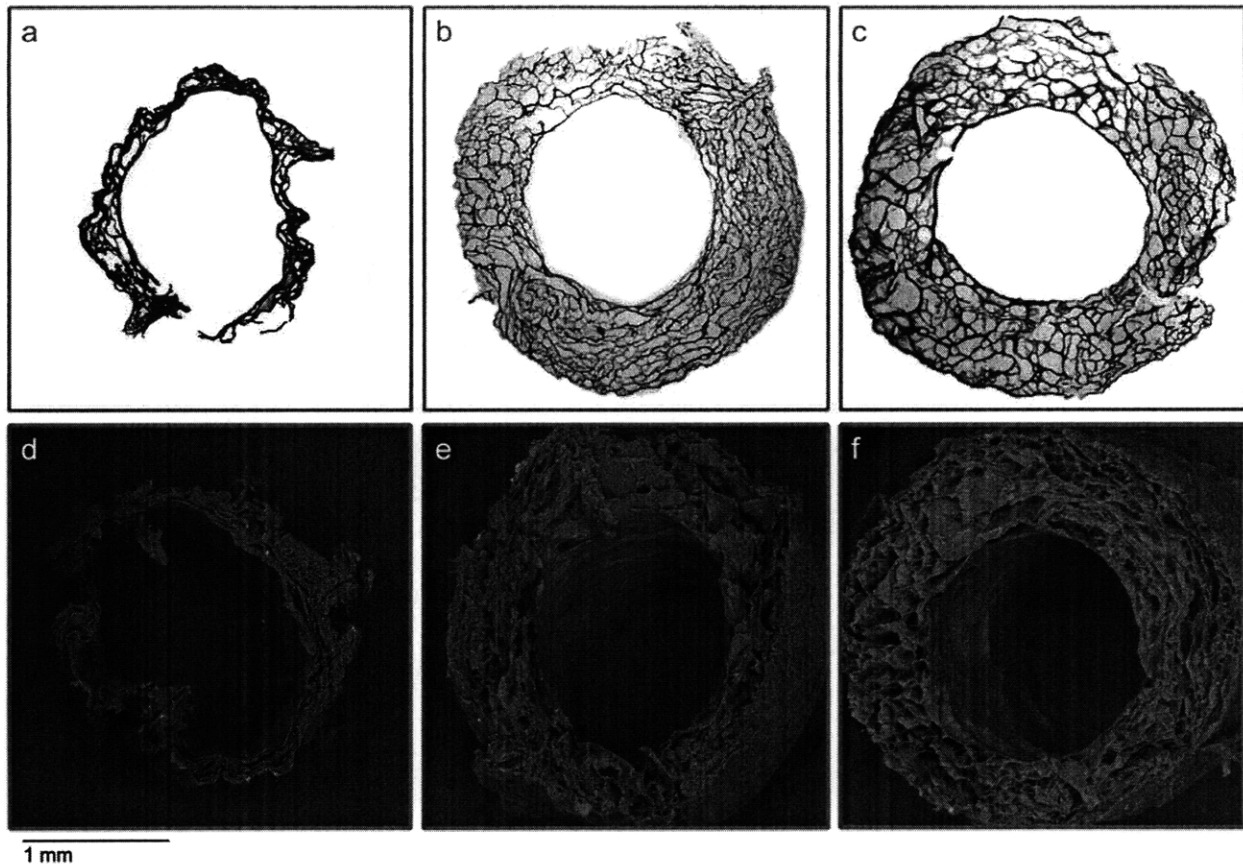


**Figure 4.** Cross sectional images of collagen tubes from groups A (a, d), B (b, e), and C (c, f). Aniline blue stained JB-4 embedded sections (a-c) and corresponding SEM images (d-f).

On the contrary, the cross sectional images of group B and group C tubes indicated open pore structures when viewed with SEM and light microscopy. Using the linear intercept method, it was found that tubes from group B were found to have a smaller pore size than tubes from group C. A significant difference in the mean pore sizes were determined through an unpaired T test ( $p < .0001$ ).

Using a subset of collagen tube devices with different crosslinking temperatures and times, Harley determined that out of the collagen tube devices he tested, the ones with the most regenerative ability were his tubes DHT crosslinked for 48 hours at 120°C and 90°C (2002). These devices had mean pore sizes of 70 to 100  $\mu\text{m}$ , respectively. While tubes used in this study

Device	Mean Pore Diameter $\pm$ SEM ( $\mu\text{m}$ )
B	72.5 $\pm$ 1.4
C	88.4 $\pm$ 1.3

Table 4. Average pore size for 48 hour 120°C DHT crosslinked collagen tubes used in 2008 and 2009 proteomic studies

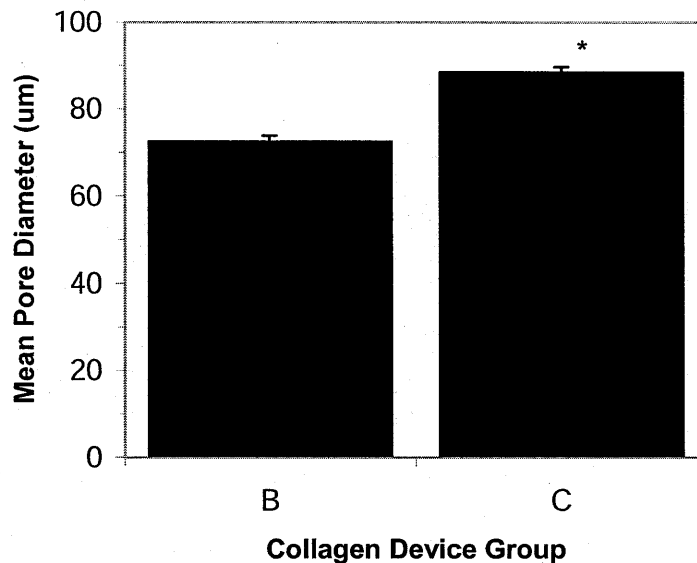


Figure 5. Pore diameter (mean  $\pm$  SEM) for 48 hour DHT crosslinked collagen tubes used in 2008 and 2009 proteomic studies

underwent 48 hour DHT crosslinking treatment at 120°C, the fabrication process involving different lyophilizers and slight differences in mold closures had an effect on the device porosity. However, despite the difference in porosity between the devices implanted in the ELISA and immunoblotting surgeries and those used in the immunofluorescence surgeries, both pore sizes fall in the range of the collagen tubes Harley found had regenerative activity.

### 3.3 Peripheral Nerve Regenerate Procurement and Storage

#### 3.3.1 Experimental Samples

Left sciatic nerve surgeries were performed on 17 adult female Lewis rats (150-200 g, Charles River Laboratories, Wilmington, MA) by Dr. Hu-Ping Hsu at the Boston VA Medical Center with the aid of Eric Soller in 2007 and both Soller and Miu in 2008. The surgical protocol, described in Sections 3.3.1-3.3.4, was adapted from the protocols of earlier researchers (Chamberlain, 1998a; Spilker, 2000; Harley, 2002; Wong, 2008). Eight animal wounds were

treated with collagen tubes fabricated in 2006 and 2007 by Soller and/or Kelly Chien (estimated mean pore diameter: 72.5  $\mu\text{m}$ ), while nine were treated with silicone nerve tubes. The processing of the explanted wound was developed by Soller and used by Wong (2008). When mass data for the samples, to be used as a means of normalization, was collected before tissue digestion, ELISA was performed. The resulting numbers of animals used in ELISA were seven for the collagen treated group and six for the silicone treated group. Due to normalization by cellular content rather than mass data with the immunoblotting assay, samples missing mass data were able to be included in the study. For immunoblotting, the collagen treated group had a sample size of eight and the silicone treated group had a sample size of nine. For both assays, animal wounds were sectioned into five segments as later described in Section 3.4. The ELISA and immunoblotting assays were performed on tissue segments from each animal wound (“per segment” analysis) and the measurements were pooled per animal and averaged for each treatment group (“whole wound” analysis).

In 2009, left sciatic nerve surgeries were performed on nine adult female Lewis rats (200-230 g) for an indirect immunofluorescence study. Five wounds were treated with collagen tubes fabricated in 2009 by Miu (mean pore diameter: 88.4  $\mu\text{m}$ ) and four were treated with silicone nerve tubes. The same surgical procedure as above was followed, though the processing of the explant differed (Section 3.3.6). 6  $\mu\text{m}$  thick cross-sectional slices of each nerve sample were compared at five locations along the nerve using immunofluorescent analysis.

		Treatment Group	
		Collagen Tube	Silicone Tube
Assay	ELISA	7	7
	Immunoblotting	8	9
	Immunofluorescence	5	4

Table 5. Sample sizes for treatment groups studied with ELISA, immunoblotting, and immunofluorescence.

### 3.3.2 Surgeries and Device Implantation

Surgeries took place at the Boston VA Medical Center. Sodium pentobarbital (50 mg/kg of animal) was used to anesthetize the Lewis rat prior to surgery. The left leg of the rat was shaved in addition to the area from the base of the tail to the middle of the back to expose the surgical region. The wounding and device implantation to follow were performed by the surgeon using sterilized equipment. An incision was made into the leg and the sciatic nerve was transected midway between the proximal nerve trunk and the distal bifurcation to produce the peripheral nerve wound. Marks were made 3 mm inwards from the nerve ends to indicate the site of attachment for the

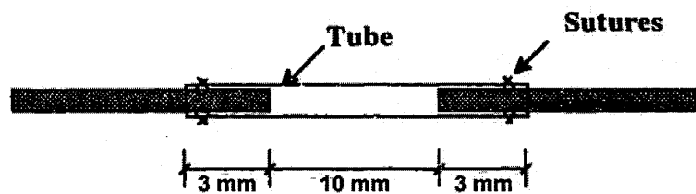


Figure 6. Use of implanted tube to bridge 10 mm gap between proximal and distal ends of sciatic nerve wound (adapted from Chamberlain, 1998).

nerve tube implant. The nerve ends were inserted into the implant and secured by 10-0 sutures that penetrated through both the epineurium and the tube. The leg was stitched and stapled to close the wound.

Rats were allowed to rest after surgery in individual recovery beds with delivery of oxygen through masks. Surgeries were performed on four or fewer rats per day. For each rat, subcutaneous injection of 0.1 mL of 0.15 mg/mL Ketofen, 0.1 mL of 100 mg/mL Cefazolin, and

1 mL Lactated Ringer's Solution were given. Once regaining consciousness, rats were moved to individual cages with fresh bedding, food, and water.

### *3.3.3 Post-Operative Care*

The subjects were visited by the graduate research assistant every 24 hours for 48 hours following the operation for post-operative care. During each visit, the rats received subcutaneous injections of 0.1 mL of 0.15 mg/mL Ketofen and 0.1 mL of 100 mg/mL Cefazolin.

### *3.3.4 14-Day Post-Operative Sacrifice*

A carbon dioxide chamber was used to sacrifice the rats 14 days after the device implantation. The leg wound was reopened, and the implant, enclosed nerve tissue and regenerate, and excess proximal and distal nerve tissue were excised. The distal end was marked with a tissue marker to denote the orientation of the explant. The explant was photographed and processed depending on the biological assay to follow suit.

### *3.3.5 Tissue Processing for ELISA and Immunoblotting*

For the samples used in the ELISA and immunoblotting studies, R-40 Peel-A-Way Embedding Molds (Cat No. 18646C-1, PolySciences, Inc., Warrington, PA), were labeled for the proximal and distal ends of the nerve wounds and were partially filled with room temperature optimal cutting temperature (OCT) compound. Samples (tissue and implant device) were deposited into the mold in the proper orientation, covered with additional OCT, and then immediately frozen in liquid nitrogen. This freezing method allowed for the collection of sample

tissue and exudate with minimal diffusion after excision. The samples were transferred to a -80°C freezer for long term storage.

When ready for sample segmentation, the OCT-embedded tissues were transferred from the -80°C freezer to a microtome-cryostat chamber equilibrated at -25°C. The R-40 Peel-A-Way Embedding Mold was stripped off each sample by cutting the containers at each corner with scissors. The OCT-embedded sample was then attached to a mounting block with addition of room temperature OCT and allowed to harden in the microtome-cryostat. The mounted sample was installed into the microtome, and the OCT was cut away in slices until the nerve sample and implant device were exposed. A razor was used to continue removing any excess OCT and to section the nerve sample into five segments.

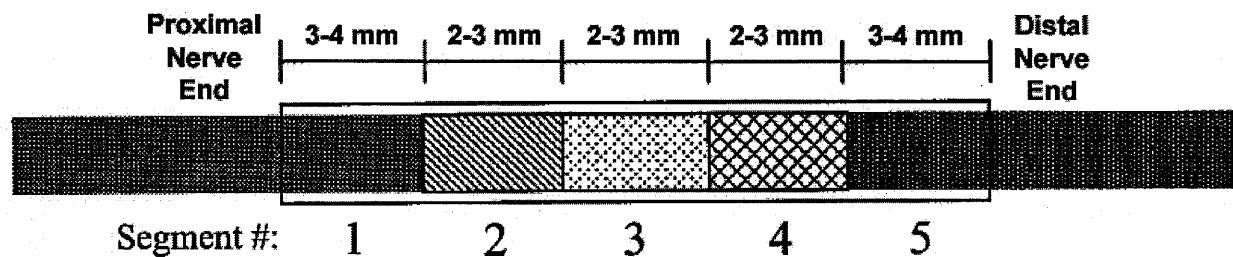


Figure 7. Segmentation of nerve samples into five ~3 mm segments with the requirement that segment 1 contain the proximal nerve stump and that segment 5 contain the distal nerve stump (adapted from Wong, 2008).

In accordance with Wong's protocol, segments 1 and 5 were cut such that their boundaries were defined by the proximal and distal nerve trunks, respectively. This methodology allowed for the segments to be more appropriately compared for cytokine content across different animals and treatment groups. Containing the nerve stumps in the end segments usually resulted in segments 1 and 5 being greater than 3 mm in length. Segments 2 through 4 were then ~.5-1 mm smaller, but equal and adjacent divisions of the explant existing in the remaining interneural wound gap. The segments were in most instances massed and in all



instances deposited into individual mini eppendorf tubes. For the silicone treated wounds, the segments were carefully removed from the silicone tube using sterile forceps before being massed and placed into individual containment. Due to the attachment of the nerve regenerate to the collagen device, collagen treated samples were processed with the implant intact. Masses of the nerve segments were calculated by subtracting the mass of the empty mini eppendorf tube from the mass of the tube after insertion of the nerve segment. Segments generated prior to this study were not massed because the Wong preparation did not use mass as a means of normalization. The mass data was collected after it was determined to be a useful statistic in normalizing the ELISA data. Therefore, some unused samples leftover from earlier studies could be used in the immunoblotting assay but not contribute data for ELISA.

### *3.3.6 Tissue Processing for Immunofluorescence*

Samples used in the immunofluorescence study followed an alternative processing protocol (Appendix A.8) in which the explants were formalin fixed and paraffin embedded. Formalin is an aldehyde fixative that achieves good penetration of tissues, forming crosslinks between basic amino acids to stabilize the proteins *in situ* (Millipore). After formalin fixation, paraffin is used to embed the tissue. Paraffin can be melted, dissolved by xylenes for infiltration of tissue, and then turned to solid state for structural support of the tissue during sectioning. Paraffin is the most commonly used embedding medium because it provides for excellent morphological detail and resolution in immunostaining techniques.

The peripheral nerve explants, cut with approximately 1 mm of excess tissue at each of the proximal and distal ends, were placed into specimen containers (4 ½ oz Graduated Wide Mouth with Screw Lid, Cat. No. 17000, Kendall Healthcare Products Co., Mansfield MA) with

20mL of Yanoff's fixative for 24 hours at 4°C. The explants were then moved to clean specimen containers with 20 mL of 10% buffered formalin for another 24 hours at 4°C. Lastly, the explants were rinsed with 70% ethanol, photographed, and stored in clean specimen containers with 70% ethanol at 4°C until ready to be processed for paraffin embedding.

Formalin-fixed samples were taken from the 70% ethanol solution used for storage and placed into individual TRUFLOW Tissue Cassettes (Cat. No. 15-200-403E, Thermo Fisher Scientific, Inc., Rockford, IL) that were placed into a TP 1020 tissue processor (Leica, Bannockburn, IL). The tissue processor dehydrated the fixed samples in a series of graded ethanol solutions and xylenes before infiltration in paraffin. The explants were removed from the machine, sectioned into five 3.5-4 mm pieces using a razor (Figure 8), and positioned distal end first into separate embedding molds of warm paraffin. The containers were cooled using a cold plate to preserve the orientation of the explants. The paraffin embedded samples were stored for 24 hours at -20°C, removed from the molds, and returned to -20°C until sectioning. The sections were made in 6 µm thick cuts and mounted as duplicates or triplicates onto microscope slides. The slides were air dried for an hour and then moved to a slide warmer for an additional hour before long term storage in a slide box at room temperature.

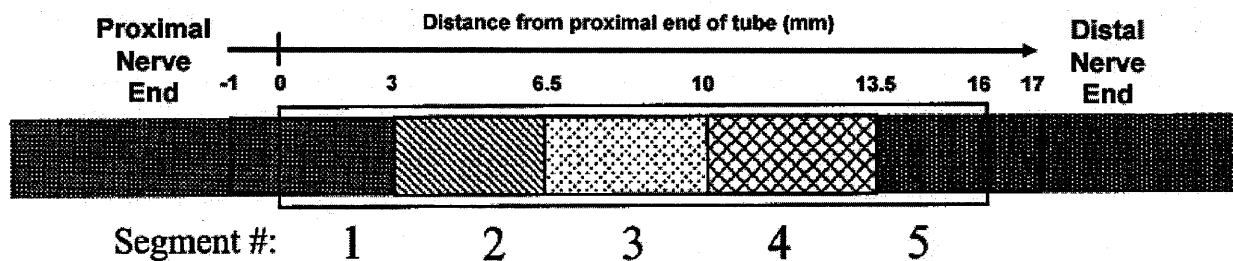


Figure 8. Segmentation of samples into five 3.5-4 mm pieces for paraffin embedding. Locations are in reference to proximal end of implant.

### **3.5 Enzyme-linked Immunosorbent Assay (ELISA)**

#### *3.5.1 Concept*

The ELISA method is used to quantify proteins based on the concentration-dependent absorbance properties of a solution. There are various forms of ELISA depending on whether the sample is bound to the plate and the antibody applied, or the antibody bound to the plate and the sample applied. In the method in used in this study, the sandwich ELISA, a primary antibody against the antigen of interest is coated onto a 96-well plate and is used to capture antigen in the sample. After the capture antibody is effectively bound to the wells of the plate, he samples to be analyzed are deposited into the wells. Any antigen present within the sample is given time to bind to the primary antibody. The unbound portion of the sample is then washed out, and another primary antibody, with a different epitope binding region than that of the capture antibody, sandwiches the antigen and is used as a detection antibody. A chromogenic reaction with the detection antibody is induced, and a set wavelength is used to test the absorbance of the solution in a plate reader, providing an optical density measurement.

A standard curve is developed by performing ELISA on graded concentrations of the protein of interest and generating a fitted curve from the optical density measurements for each known concentration. The optical densities from the unknown samples are compared to the plotted curve to back calculate the amount of antigen that was present in the well. Sample masses obtained prior to the tissue segment digestion were used to produce a protein content statistic normalized by mass.

### *3.5.2 Discussion of Assay Choice*

The ELISA method is the most quantitative way to determine protein concentration in unknown samples. The test results in samples are defined in absolute concentration of protein. To minimize error generated by differences in day-to-day test conditions, a standard curve is generated with each run so that the optical densities of the unknowns are always compared with the optical densities of the known wells for every test. The ELISA was thus explored as the primary assay of choice.

However there are disadvantages to the ELISA method that complicated its use. First, the antigen of interest must be extracted or produced as a recombinant protein and subsequently purified. The quantity of antigen amassed must be sufficient enough to be detected by ELISA and be used to produce a range that includes the quantity of protein in the unknown samples. Secondly, appropriate capture and detection antibodies for the antigen must be procured for the sandwich assay. The detection antibody must bind to an epitope site different from the capture antibody, and that site must remain freely accessible once the antigen has bound to the capture. The chromogenic reaction that follows should only be dependent on the concentration of detection antibody; this usually requires that the detection antibody generated from a different host species than the capture antibody. The choice of antibodies is critical because the sensitivity of the ELISA is determined by the binding properties of the primary antibodies to the antigen. Next, handling of the unknown samples for ELISA testing varies depending on whether the samples assayed are from cell culture or tissue lysate. If tissue lysate is used, as was the case in this study, the final absorbance measurement can be inaccurate based on the digestion buffer used to process the tissue. Therefore, there must be optimization for the digestion buffer to

produce the least background signal. For these reasons, it may not be possible to use ELISA to quantify all proteins.

### 3.5.3 ELISA Method

A rat-specific sandwich ELISA kit containing all the necessary solutions and antibodies for measuring TGF  $\beta$ 1 (Cat. No. MB100B, R&D Systems, Minneapolis, MN) was used to assess the concentration level differences in collagen versus silicone tube treated rat sciatic nerve samples. Digested tissue samples were taken from the  $-20^{\circ}\text{C}$  freezer and acidified for 15 minutes with 1 N HCl in order to activate any TGF  $\beta$ 1 to the mature form (Brown *et al.*, 1990). Tissue samples were then neutralized with 1 N NaOH and diluted with a calibration diluent. The samples and known concentrations of TGF  $\beta$ 1 standard ranging from 0 to 2000 pg/mL were added to wells of a 96-well plate pre-coated with TGF  $\beta$ 1 capture antibody. The TGF  $\beta$ 1 present in the sample and standards were given 2 hours to bind to the plate while shaking at room temperature. The wells were then emptied of liquid content and washed three times with wash buffer to remove any unbound material. A horseradish peroxidase (HRP) conjugated TGF  $\beta$ 1 detection antibody was added to the well to detect the antigen, and the plate was left shaking at room temperature for another 2 hours. The wash step was repeated three more times to remove unbound detection antibody. A concentration-dependent A+B color reagent was used to visibly indicate the levels of TGF  $\beta$ 1 conjugate bound to the antigen. The reaction was allowed to develop for 30 minutes at room temperature, and then finished by adding an acid stop. A SpectraMAX 340PC plate reader (Molecular Devices, Sunnyvale, CA) was used to analyze the optical density from the wells using a 450 nm wavelength as a measurement and 540 nm wavelength as a correction factor.

In this study, fabrication of sandwich ELISAs for TGF  $\beta$ 2 and TGF  $\beta$ 3 were attempted using high binding affinity 96 well plates, various combinations of monoclonal and polyclonal primary antibodies, a HRP-conjugated secondary antibody, and the color detection reagents left from the TGF  $\beta$ 1 kit. However, due to any number of complications specified in Section 3.1.1, a standard curve failed to be produced over a large concentration range over three orders of magnitude. Therefore, immunoblot analyses were the primary method of assessing the relative differences in TGF  $\beta$ 2 and TGF  $\beta$ 3 levels between collagen and silicone tube treated samples. ELISA was not performed for measurement of  $\alpha$  SMA due to the inability to purchase or purify protein standard.

#### 3.5.4 ELISA Data Analysis

As per the kit instructions, a standard curve was developed by fitting a 4-parameter logistic to the optical density data obtained from the plate readings of known TGF  $\beta$ 1. The optical densities from the rat tissue samples were compared to the standard curve to empirically determine the TGF  $\beta$ 1 concentration for each well. The digestion buffer of the rat tissue samples was optimized to produce the least background noise in this step. The concentration calculated was then converted to a ug TGF  $\beta$ 1 per g explanted tissue segment statistic by the method described in Appendix A.13 and summarized by the equation:

$$\frac{x}{m} = \frac{[x] \cdot V_f}{\chi_V \cdot m} \cdot 10^{-3},$$

where  $x$  is the mass of TGF  $\beta$ 1 present in the sample in ug,  $m$  is the mass of the explanted tissue segment in g,  $[x]$  is the concentration of TGF  $\beta$ 1 in the segment as determined by ELISA in ug/mL,  $V_f$  is the final volume of the diluted tissue sample prior to insertion into the wells, and

$\chi_v$  is the volume fraction of the aliquot taken from the digested sample. As earlier described in Section 3.4, the mass of the tissue segment,  $m$ , was calculated using the difference in masses between a mini eppendorf tube prior and after the deposition of the segment. The concentration of TGF  $\beta$ 1 in a segment sample,  $[x]$ , was determined using the standard curve described above, which was developed from plotting known concentrations of TGF  $\beta$ 1 against optical density measurements.  $V_f$  was the volume of the sample after the dilutions with 1 N HCl, 1 N NaOH, and calibration diluent.  $\chi_v$  was the volume ratio of the aliquot to the digested sample, which in this study was 1/5, after taking 10  $\mu$ L to test in ELISA from a 50  $\mu$ L sample stock. The  $10^{-3}$  was used in unit conversion to express the mass protein over mass tissue statistic in ug/g.

### **3.6 Immunoblot Assay**

#### *3.6.1 Concept*

The immunoblot technique can be used to semiquantitatively determine the amount of protein in a sample based on measuring a concentration-dependent chromogenic or chemiluminescent reaction that occurs at the site of interest. Electrophoresis is performed on the sample such that proteins in the test sample migrate through the gel based on molecular weight. A protein ladder containing proteins of known molecular weights is run simultaneously with the unknown samples to locate the approximate band site of the antigen. The proteins are transferred from the gel to a membrane onto which antibodies can be applied to the sample. A primary antibody against the protein of interest is used to locate the antigen, and a secondary antibody conjugated to a molecule involved in a color changing or light emitting reaction is used to detect the primary antibody. A chemiluminescent reaction, chosen to greater sensitivity, was induced and the light emission from the sample lanes are captured and compared. To normalize, an

immunoblot with a loading control is used to determine the amount of cellular content from each sample.

### *3.6.2 Discussion of Assay Choice*

Though the immunoblot technique is less quantitative than the ELISA method, the advantages the immunoblot technique has over the ELISA method allowed for the comparison of all proteins in this study. First, only one primary antibody is needed to detect the antigen; this eliminates complications with finding antibodies with epitope sites that do not conflict. The choice of antibody is further discussed in Section 3.6.2. Secondly, protein standard is not a requirement in relatively assessing the amount of protein in one sample from the next. Thus the immunoblot assay is apt for comparing protein concentrations in samples on a relative basis.

### *3.6.2 Assessment of Antibody Specificity*

The objective of the immunoblot assay is to measure the amount of a specific protein present in a sample; therefore it is in our interest to utilize the antibody with the highest binding affinity for the antigen while keeping cross-reactivity and nonspecificity minimal. Commercially available from numerous vendors are a plethora of antibodies that range from the animal source of the antigen that the antibody was raised against, the host species in which the antigen was introduced to produce an inflammatory response, and the clonality of cells that generated the immune response to the antigen. An  $\alpha$  SMA mouse monoclonal antibody (Cat. No. A5228, Sigma-Aldrich, St. Louis, MO) previously used in immunohistochemical stains by Chamberlain and Spilker, was tested with a human smooth muscle cell control in immunoblotting to confirm banding at the appropriate molecular weight location. Due to the homology of the TGF  $\beta$



isoforms, antibody specificity was a major concern. The determination of antibody specificity is commonly tested using dot blot tests (Ermens et al, 1997; Guo et al, 2006). Dot blot tests (Appendix A.14) with positive and negative controls (Table 6) were conducted for the TGF  $\beta$ 1, TGF  $\beta$ 2, and TGF  $\beta$ 3 primary antibodies considered candidates for the assay (Table 7). For each antibody, the isoform for it was raised was the positive control, bovine serum albumin (BSA) was the negative control, and binding to the other isoforms was in question. Strips of an Immobilon polyvinylidene fluoride (PVDF) membrane (Cat. No. IPSN07852, Millipore, Billerica, MA) were soaked in methanol for 20 seconds and rinsed in distilled water. An alcohol and waterproof marker was used to label each strip for the antibody to be applied in addition to the areas where each protein would be spotted. Using a pipette, proteins were spotted onto the PVDF strips according to their designated location and allowed to dry before proceeding.

<b>Antigen</b>	<b>Source</b>	<b>Vendor</b>	<b>Cat. No.</b>
TGF $\beta$ 1	Human recombinant	Peprtech	100-21
TGF $\beta$ 2	Human recombinant	Peprtech	100-35B
TGF $\beta$ 3	Human recombinant	Peprtech	100-36
BSA	Bovine	Roche Diagnostics	03116999001

**Table 6. Proteins used as positive and negative controls to assess TGF  $\beta$  antibody specificity.**

Once the protein spots were air dried, the strips were rotated in a 5% nonfat milk in Tris buffered saline (TBS) blocking solution. The blocked membrane strips were transferred into diluted primary antibody solution for an hour and washed three times with 0.5% Tween 20 in TBS wash buffer. Due to the heightened signal produced from polyclonal antibodies over monoclonal antibodies, the former were diluted 1:800 while the latter were diluted 1:500 in 0.33% BSA, 0.5% Tween 20 in TBS dilution buffer. The washed membrane strips were transferred to tubes filled with the relevant 1:5000 diluted HRP-conjugated secondary antibody for detection of the

mouse (Cat. No. 31340, Thermo Fisher Scientific, Inc., Rockford, IL), rabbit (Cat. No. 31460, Thermo Fisher Scientific, Inc.) or goat (Cat. No. 31402, Thermo Fisher Scientific, Inc.) primary antibodies.

Antibody	Isoform Specificity	Host	Clonality	Vendor	Cat. No.
A	TGF $\beta$ 1	Mouse	Monoclonal	Abcam	ab10517
B	TGF $\beta$ 1	Mouse	Monoclonal	Peprotech	500-M66
C	TGF $\beta$ 2	Mouse	Monoclonal	R&D Systems	MAB612
D	TGF $\beta$ 2	Rabbit	Polyclonal	Santa Cruz Biotechnology	sc-90
E	TGF $\beta$ 2	Goat	Polyclonal	Santa Cruz Biotechnology	sc-31610
F	TGF $\beta$ 3	Mouse	Monoclonal	R&D Systems	MAB643
G	TGF $\beta$ 3	Rabbit	Polyclonal	Santa Cruz Biotechnology	sc-82

**Table 7. Primary antibody candidates for use in TGF  $\beta$  immunoblots.**

After an hour of rotation in the solutions, the membrane strips were washed three times in wash buffer and exposed to 150  $\mu$ L of mixed 1:1 chemiluminescent reagent and enhancer (SuperSignal West Femto Chemiluminescent Substrate, Cat. No. 34095, Thermo Fisher Scientific, Inc.) for five minutes at room temperature on a microplate shaker. The resulting chemiluminescence from the strips were digitally captured using an FluorChem 8900 imager (Alpha Innotech, San Leandro, CA). Antibodies were evaluated qualitatively using the following metrics: isoform specific binding, cross reactivity to alternative isoforms, nonspecific binding to negative control, and background staining.

### 3.6.3 Antibody Choice

All antibodies, with the exception of one case (E), bound to their positive control spot (the isoform they were raised against) and did not bind to the negative control spot (BSA). The

goat anti-TGF  $\beta$ 2 antibody E failed to bind to any protein and was immediately discounted from use in the immunoblot assay. Polyclonal antibodies (D, G) had the strongest signal to the specific isoform they were raised against, but had high nonspecific binding to another isoform and moderate background noise. Typically, monoclonals (A, C, F) clearly showed specificity to their isoform but signal was oftentimes weaker than that generated from the polyclonal bound spot. An exception, monoclonal antibody B, produced very strong signal to its isoform, TGF  $\beta$ 1, but also to TGF  $\beta$ 2 and the blocked PVDF membrane.

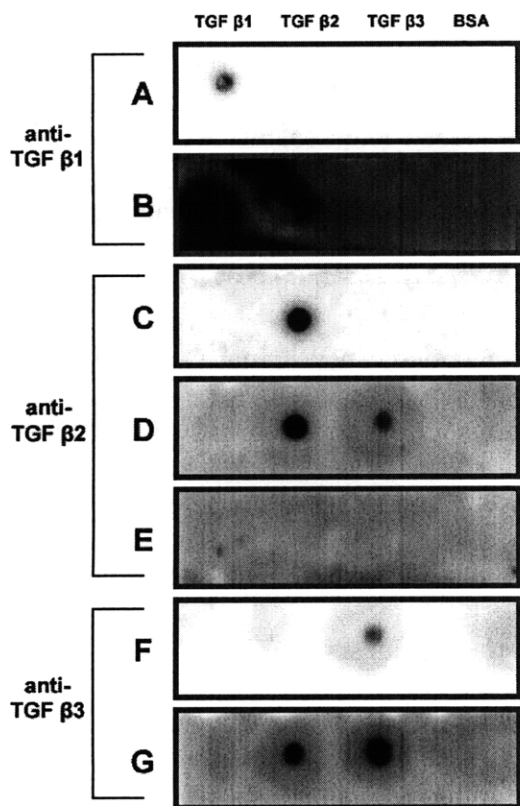


Figure 9. Dot blot results for antibody binding to TGF  $\beta$ 1, TGF  $\beta$ 2, TGF  $\beta$ 3, and BSA (negative control) protein spots.

Antibody	TGF $\beta$ 1 spot	TGF $\beta$ 2 spot	TGF $\beta$ 3 spot	BSA spot
A	+	-	-	-
B	++++	++	-	-
C	-	++	-	-
D	-	++	+	-
E	-	-	-	-
F	-	-	+	-
G	-	++	++	-

Table 8. Evaluation of antibody binding to protein spots in dot blot test. The number of pluses indicate relative amount of intensity, while a minus indicates no intensity from a spot.

Antibody	Background
A	-
B	+++
C	-
D	++
E	++
F	-
G	++

Table 9. Evaluation of antibody binding to the PVDF membrane. The number of pluses indicate relative amount of intensity, while a minus indicates no intensity from a spot.

Due to the goal of the study to quantify the isoform specific concentrations in the regenerative and nonregenerative wounds, the most specific primary antibodies would provide the most accurate results. Thus mouse monoclonal antibodies against each TGF  $\beta$  isoform (A, C, F) were chosen for use in the immunoblot measurements.

#### *3.6.4 Immunoblot Method*

In an immunoblotting protocol described in Appendix A.15, digested rat sciatic nerve samples from the  $-20^{\circ}\text{C}$  freezer were diluted 1:4 with distilled water and 1:2 with a previously diluted 2X Laemmli SDS-Sample Reducing Buffer (Cat. No. BP-110R, Boston BioProducts, Inc., Worcester, MA). The samples were vortexed, heated for five minutes at  $100^{\circ}\text{C}$ , and upon cooling, centrifuged for two minutes. The samples were loaded into separate wells of 4-15% Ready Gel Precast Gels (Cat. No. 161-1122, Bio-Rad Laboratories, Hercules, CA) and inserted into an electrophoresis/transfer module (Mini Protean Tetra Cell, Cat. No. 165-8030, Bio-Rad Laboratories). 35V was applied across the gel (300V Power Source, VWR International) in the electrophoresis setup to promote movement of the proteins in an arrangement by molecular weight. The gels were then moved to a blot transfer cassette and returned to the Mini Protean Tetra Cell where a 50 mA current was applied at  $4^{\circ}\text{C}$  for three to five hours as determined by previous optimization. Upon successful transfer, the protein lanes were bound to a PVDF membrane (Cat. No. IPSN07852, Millipore). Unbound areas of the membrane were blocked for an hour with 5% nonfat milk buffer in TBS to prevent the antibody from nonspecifically binding to the PVDF. Primary and secondary antibodies used in the immunoblotting study (Table 10) were all diluted with 0.33% BSA, 0.5% Tween 20 in TBS. The PVDF membrane was incubated at room temperature for two hours in a diluted primary antibody solution on a rocker and then

washed six times in 0.5% Tween 20 wash buffer at five minutes per wash. Exposure of the membrane to secondary antibody solution occurred at room temperature on a rocker for an hour followed by another six washes in wash buffer and one wash in distilled water to remove traces of Tween 20.

Antibody	Type	Dilution	Vendor	Cat. No.
Anti-TGF $\beta$ 1	Mouse monoclonal, primary	1:500	Abcam	ab10517
Anti-TGF $\beta$ 2	Mouse monoclonal, primary	1:500	R&D Systems	MAB612
Anti-TGF $\beta$ 3	Mouse monoclonal, primary	1:500	R&D Systems	MAB643
Anti- $\alpha$ SMA	Mouse monoclonal, primary	1:1000	Sigma-Aldrich	A5228
Anti- $\alpha$ Tubulin	Mouse monoclonal, primary	1:2000	Abcam	ab7291
Anti-mouse	Goat, secondary, HRP-conjugated	1:5000	Thermo Scientific	31340

**Table 10. Primary and secondary antibodies used for immunoblot detection**

Chemiluminescent reagent and enhancer (SuperSignal West Femto Chemiluminescent Substrate, Cat. No. 34095, Thermo Fisher Scientific, Inc.) were mixed 1:1 to make 1 mL of solution per blot and shaken with the membrane for five minutes at room temperature. The membrane was transferred to the FluorChem 8900 and captured at one, three, and ten minute exposures. The process was repeated for each sample using an antibody against  $\alpha$  Tubulin which, as a major component of microtubules, is a measure of cellular content and is commonly used in immunoblotting as a loading control. Normalization for amount of cells per sample was achieved using the chemiluminescence data gathered from blots probed for  $\alpha$  Tubulin at a one minute exposure.

### 3.6.5 Immunoblot Data Analysis

For the group of membranes to be analyzed for each protein, the length of exposure was chosen based on the intensity of the protein bands visible at B=0, W=255, G=1.0 settings in the

AlphaEaseFC software. The quality of the image was determined by visual inspection with confirmation from the histogram levels. Bands were checked for their sizes using lanes containing known molecular weight markers (Precision Plus Protein All Blue Standard, Cat. No. 161-0373, Bio-Rad Laboratories). The TGF  $\beta$  isoform bands were measured at 25 kDa and  $\alpha$  SMA was measured at 42 kDa. The rectangle tool was used to define the perimeter of the protein band or bands of interest in the sample lanes. Background intensity was automatically determined for each band as the average of the ten lowest intensities contained in the rectangle. The software generated an average intensity statistic per unit area for each protein band with subtraction of the background intensity. The intensities for each sample were compiled into a spreadsheet to be normalized with the corresponding spot densities from the  $\alpha$  Tubulin immunoblots.

Two-way ANOVA and student's T-tests were used to compare the effects of device and segment on protein expression from the intensities. The segment data were pooled by animal and then analyzed on a whole wound basis. The total wound protein expressions were compared using the student's T-test.

### **3.7 Direct Immunofluorescence Assay**

#### *3.7.1 Concept*

Direct immunofluorescent techniques utilize fluorophore-conjugated primary antibodies to visualize where antigens of interest are present within tissue. The excitation and emission spectra of the fluorophores are used to produce controlled fluorescence in the sample (see **Error! Reference source not found.** for the spectra related to the Cy3 fluorophore used in this study). A special filter set that allows the transmission of desired wavelengths within the peak of the

excitation spectra is installed to the microscope and is used to excite specifically the fluorophore involved with measuring the protein of interest. The resulting emission is captured with the filter set and the images are qualitatively or semiquantitatively analyzed.

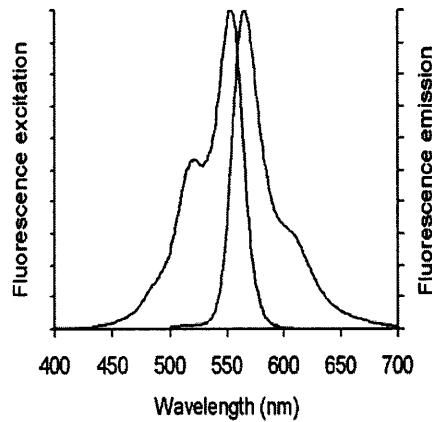


**Figure 10. Excitation and emission spectra of Cy3 fluorophore (Invitrogen). Maximal excitation of Cy3 occurs at 550 nm, with peak emission at 570 nm. Cy3 visualization can be visualized with traditional TRITC filter sets (nearly identical emission and excitation spectra).**

### *3.7.2 Discussion of Assay Choice*

Immunofluorescence is a visual assay which can be used to determine where proteins appear in the tissue spatially. This benefit allowed for the direct comparison of regenerate from the silicone treatment group with the regenerate from the collagen treatment group. In this and previous studies, the collagen device and the regenerated tissue are known to become interconnected over the course of the study so it is impossible to mechanically separate the tube from the sample (Harley 2002; Wong 2008). In the ELISA and immunoblot assay, the collagen tube is left intact with the regenerate and included in the protein measurements. The inclusion of the collagen tube in the other assays was of considerable concern with  $\alpha$  SMA quantification because an external scar which forms on the outside surface of all implants was still included in the collagen treated samples but omitted from the silicone treated samples. This external source

of  $\alpha$  SMA compromised the measurements in the immunoblot assays. Therefore, immunofluorescence was used in two ways: to generate a preliminary estimate for the correction factor for the  $\alpha$  SMA immunoblot, and to semiquantitatively compare  $\alpha$  SMA only within collagen treated and silicone treated regenerate.

One caveat of the immunofluorescence assay is that the exudate that is included with the samples analyzed in ELISA and immunoblotting is lost in the fixation and embedding process. While this assay was not used in this study to quantify the TGF  $\beta$  proteins, any cytokines present in the exudate would not have been measured by immunofluorescence.

### *3.7.3 Immunofluorescence Method*

The samples used in the immunofluorescence study were sectioned in 6  $\mu$ m slices using a microtome and mounted in triplicates on microscope slides (Superfrost Gold Plus, Cat. No. 15-188-48, Thermo Fisher Scientific, Inc.). Slides were air dried for an hour and placed on a slide warmer for an additional hour before storage in a slide holder. When ready for immunostaining (Appendix A.17), the slides were returned to the slide warmer for at least an additional hour. The warmed slides were immediately deparaffinized using xylene and rehydrated with graded ethanol solutions before a tap water wash. Slides were microwaved for ten minutes in a citrate-based antigen unmasking solution (Cat. No. H-3300, Vector Laboratories, Inc., Burlingame, CA) in order to expose epitope sites that may have become crosslinked in the fixation process. The slides were allowed to cool for 20 minutes before three washes in PBS. The samples were incubated overnight in Cy3 conjugated  $\alpha$  SMA antibody (Cat. No. C6198, Sigma-Aldrich, St. Louis, MO) at 4°C while stored in a humid chamber to prevent evaporation. Any unbound antibody after overnight incubation was removed with three washes of PBS. To stain for nuclei,



the samples were incubated with 200 ng/ml DAPI Nucleic Acid Stain (Cat. No. D1306, Invitrogen, Carlsbad, CA) at room temperature for 10 minutes. The samples were washed with PBS for a final three times and coverslipped with Shandon Immu-Mount (Cat. No. 9990402, Thermo Fisher Scientific, Rockford, IL).

The slides were allowed to dry for an hour before imaging with the Olympus BX60 microscope. Slides were chosen from the proximal nerve trunk, interneural wound gap, and distal nerve trunk. DAPI staining was visualized using the UV filter while Cy3 fluorescence was visualized using the TRITC filter. Due to the limited field of view of the camera attachment, images for each nerve cross section had to be stitched together using Adobe Photoshop.

#### *3.7.4 Immunofluorescence Data Analysis*

The immunofluorescent images offered a wealth of data pertaining to  $\alpha$  SMA expression in the wound site. For silicone treated wounds, the cross sections illustrated  $\alpha$  SMA in the regenerate expressed by contractile myofibroblasts and blood vessel pericytes. For collagen treated wounds, the cross sections illustrated  $\alpha$  SMA from three sources: scarring from the external surface of the device surface, myofibroblasts contained within the collagen tube, and the myofibroblasts and blood vessel pericytes from within the regenerate (Figure 11). In comparing  $\alpha$  SMA expression across treatment groups, the actual region of interest (ROI) was only the nerve regenerate. Thus, the use of image analysis software was crucial in accurately assessing  $\alpha$  SMA content in the regenerating wound.

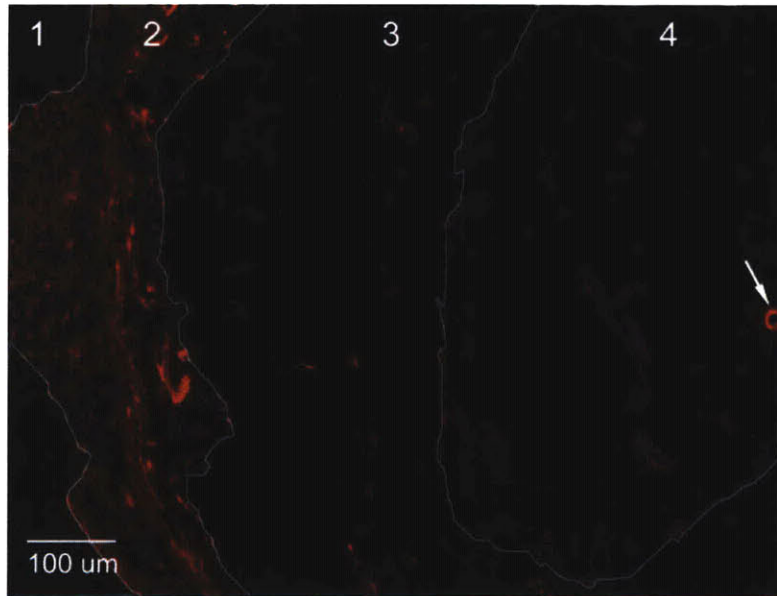


**Figure 11.** One 10x captured image of collagen treated wound cross section stained for  $\alpha$  SMA (red). Multiple 10x images are stitched together to create image of entire nerve cross section. White lines delineate borders between regions of the image. The background (region 1) is negative space on the slide containing no tissue. Scar and blood vessel formation (region 2) on the outside surface of the collagen tube stains highly for  $\alpha$  SMA. The collagen tube (region 3) is still intact at 2 weeks and harbors some contractile cells expressing  $\alpha$  SMA. The regenerate (region 4) has some  $\alpha$  SMA expression, with intense staining from blood vessels (arrow).

The first objective, to produce a preliminary correction factor for the  $\alpha$  SMA immunoblot assay, required determination of  $\alpha$  SMA expression from the regenerate as a percentage of the expression from the total cross section. This was done in ImageJ by thresholding the images and measuring the intensity of the  $\alpha$  SMA expression in the total image. A ROI was defined around the regenerate and the intensity from only the regenerate was measured.  $\alpha$  SMA expression of the regenerate was calculated as a percentage of total  $\alpha$  SMA expression. A similar process was followed using images from DAPI stained cross sections to determine the cellular content of the regenerate as a percentage of the total cross section. In ImageJ, the images were thresholded for nuclei and the ‘Analyze Particles’ function was used to count the number of nuclei in the entire cross section. A ROI was defined around the regenerate and ‘Analyze Particles’ was used again to count the number of nuclei only in the regenerate. This percentage was used to correct for the

normalization factor in the  $\alpha$  Tubulin data. Percentages of  $\alpha$  SMA expression and cellular content contributed by the regenerate alone were averaged across animals in the collagen tube treatment group, and the process was repeated at various data points to determine a scaling factor for the immunoblot  $\alpha$  SMA data as a function of distance along the length of the nerve.

The second objective involved determining the protein expression within a ROI in the nerve cross sections for the appropriate comparison of  $\alpha$  SMA between collagen and silicone treated samples.  $\alpha$  SMA is a component of both myofibroblasts and pericytes in the regenerating nerve, but the primary interest was to determine the amount of contractile capsule activity in the early stage wound. Chamberlain *et al.* previously found  $\alpha$  SMA expression as much as 10 to 15 cell layers in from the regenerate periphery in 30 to 60 week explants (1998a; 2000). Thus, a ROI from the edge of the nerve regenerate to about  $\sim 65 \mu\text{m}$  inwards was defined to include this region previously observed to contain contractile cells (proposed myofibroblasts). Within this region, images of the regenerate were quantified for intensity in the red channel as a function of radial distance away from the edge. Using image analysis software, a border was defined along the periphery of the regenerate. A program was run to sample the average intensity of pixels at the edge and subsequently in concentric shells shrunk 5 pixels inwards for the next 100 pixels. Based on the settings of the microscope and digital capture, this corresponded to the desired ROI from 0 to  $\sim 65 \mu\text{m}$  away from the edge. The average intensities from the ROI were summed and then a mean was generated for and compared between treatment groups. For each animal, this expression statistic was determined for five cross sections along the length of the nerve, and the statistics were averaged for animals of the same treatment group. Order 2 polynomials were used to create curve fits to describe protein expression versus location along nerve for silicone

and collagen treated wounds, and the areas underneath the curves were compared between treatment groups.

### 3.7.5 Correction Factor Results

Using immunofluorescence intensity as a relative quantifier of protein expression within regions of nerve cross sections,  $\alpha$  SMA expression from nerves treated with collagen or silicone tubes were divided as follows:

Treatment Device	Source	Percent contribution of $\alpha$ SMA expression in nerve cross sections (mean $\pm$ SEM)
Silicone	Regenerate	100%
Collagen	Regenerate	5.7% $\pm$ 2.3%
	External to Regenerate (Collagen Tube, Tube Outer Surface Scar)	95% $\mp$ 2.3%

**Table 11.** Percent contributions of  $\alpha$  SMA expression from sources internal and external to regenerate tissue.

For all animals, percentages of  $\alpha$  SMA from the regenerate and external to the regenerate tissue were sampled in four cross sections along the nerve and averaged to give the percentages pertaining to each treatment device. The difference in percent  $\alpha$  SMA expression contributed by the regenerate along the length of the nerve was not found to be statistically significant, and so the mean percent across all cross sections was used to generate the numbers in Table 11.

Based on the number of DAPI stained nuclei counted internally and externally to the regenerate tissue, percentages of cellular content were divided as follows:

Treatment Device	Source	Percent contribution of cellular content in nerve cross sections (mean $\pm$ SEM)
Silicone	Regenerate	100%
Collagen	Regenerate	35.3% $\mp$ 4.1%
	External to Regenerate (Collagen Tube, Tube Outer Surface Scar)	64.7% $\mp$ 4.1%

**Table 12. Percent contributions of cellular content from sources internal and external to regenerate tissue.**

Statistically significant differences were not found in cellular content as a function of location along the nerve. One would expect there to be less cellular content in the regenerate as the cross sections are taken from the center of the interneural wound gap. Statistical insignificance was perhaps due to high animal-to-animal variation and may require sampling from more animals for a more accurate correction factor. Because any difference found in the percent cellular content as a function of location within the nerve was not statistically significant, the percent cellular contents were averaged from all cross sections and used to generate the numbers in Table 12.

## Chapter 4: Results and Error Analysis

Protein expression levels in wounded nerve tissue treated with silicone or collagen tubes were compared on a “whole wound” basis to determine overall differences in the entire tissue and on a “per segment” basis to determine local differences in ~2-4 mm regions of tissue. Recall that in the ELISA and immunoblotting assays, the collagen treated wounds were digested with the collagen device which could not be mechanically removed from the regenerate. For all assays, wounds treated with silicone tube were removed from the silicone device. References to the explanted tissue mass in ELISA refer to the regenerate only in the silicone treated group or the regenerate and attached collagen tube in the collagen treated group. References to cellular content in immunoblot refer to the amount of  $\alpha$  Tubulin present in the regenerate only in the silicone treated group or the regenerate and attached collagen tube in the collagen treated group.

Immunofluorescence was used to visually determine the boundary between the regenerate and the collagen device, thus allowing for the direct comparison of regenerate only in both treatment groups. A region of interest (ROI) was defined from the regenerate periphery to ~65  $\mu\text{m}$  radially inwards where presence of a contractile capsule was previously noted and also observed in this study.

## 4.1 TGF $\beta$ 1 Expression

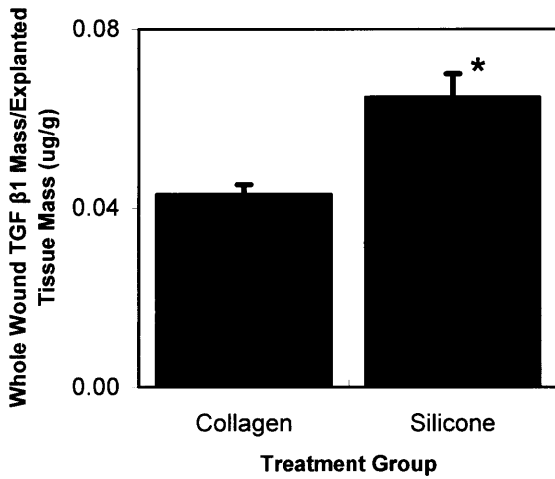


Figure 12. 14-day whole wound TGF  $\beta$ 1 expression (mean  $\pm$  SEM) as determined by ELISA. Expression was normalized by mass of the whole explanted tissue.

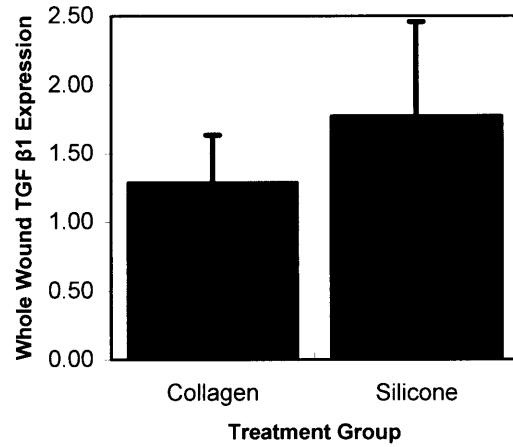
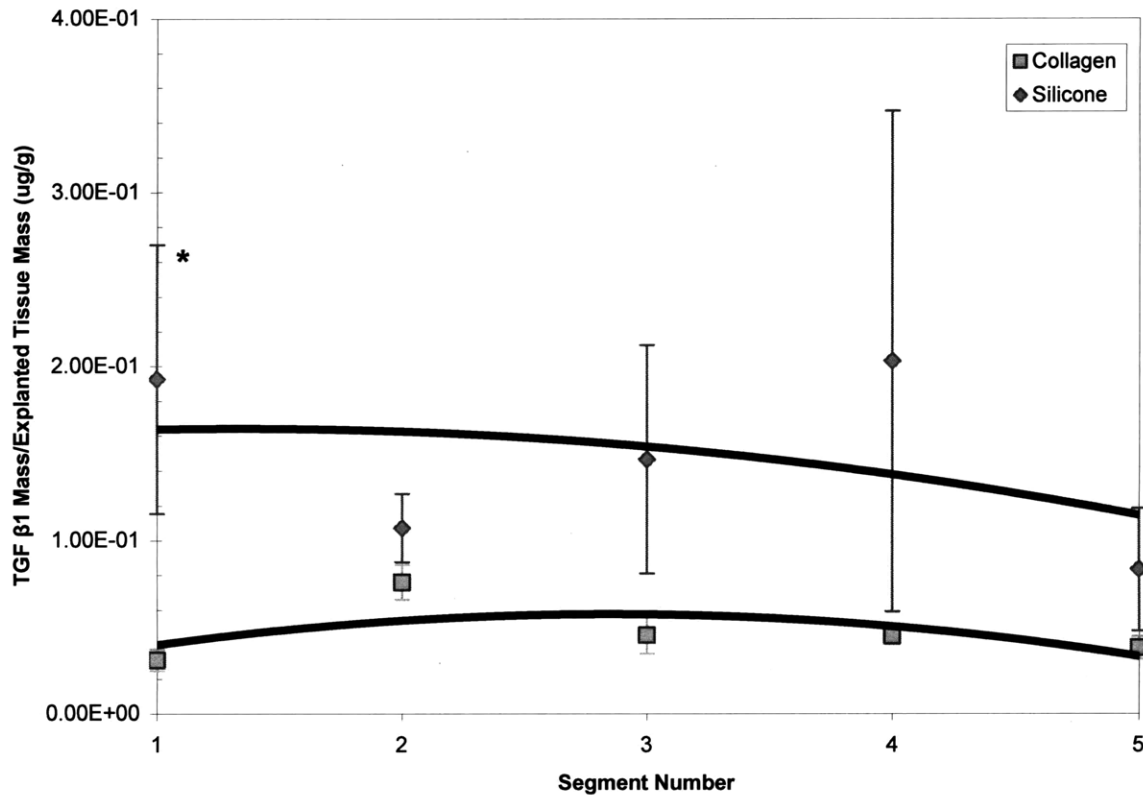


Figure 13. 14-day whole wound TGF  $\beta$ 1 expression (mean  $\pm$  SEM) as determined by average immunoblot intensity per unit area. Expression was normalized by cellular content.

Fourteen days after transection, the silicone treated peripheral nerve wounds demonstrated a possible increase in whole wound TGF  $\beta$ 1 expression over the collagen treated wounds. Measurement by ELISA determined a 50% increase of TGF  $\beta$ 1 levels on a mass protein per mass of explanted tissue that was statistically significant ( $p=.0021$ ). Immunoblot measurement of TGF  $\beta$ 1 normalized by cellular content similarly showed a 30% increase in total TGF  $\beta$ 1 expression in silicone treated wounds. However, the immunoblot result did not achieve statistical significance.

Differences in normalized TGF  $\beta$ 1 expression between the two treatment groups when observed on a per segment basis were most prevalent at the proximal and distal stumps. At the nerve trunks there was a possible 100% increase in TGF  $\beta$ 1 levels in the silicone treated from the collagen treated wounds, while in the center of the gap there was no difference. While ANOVA

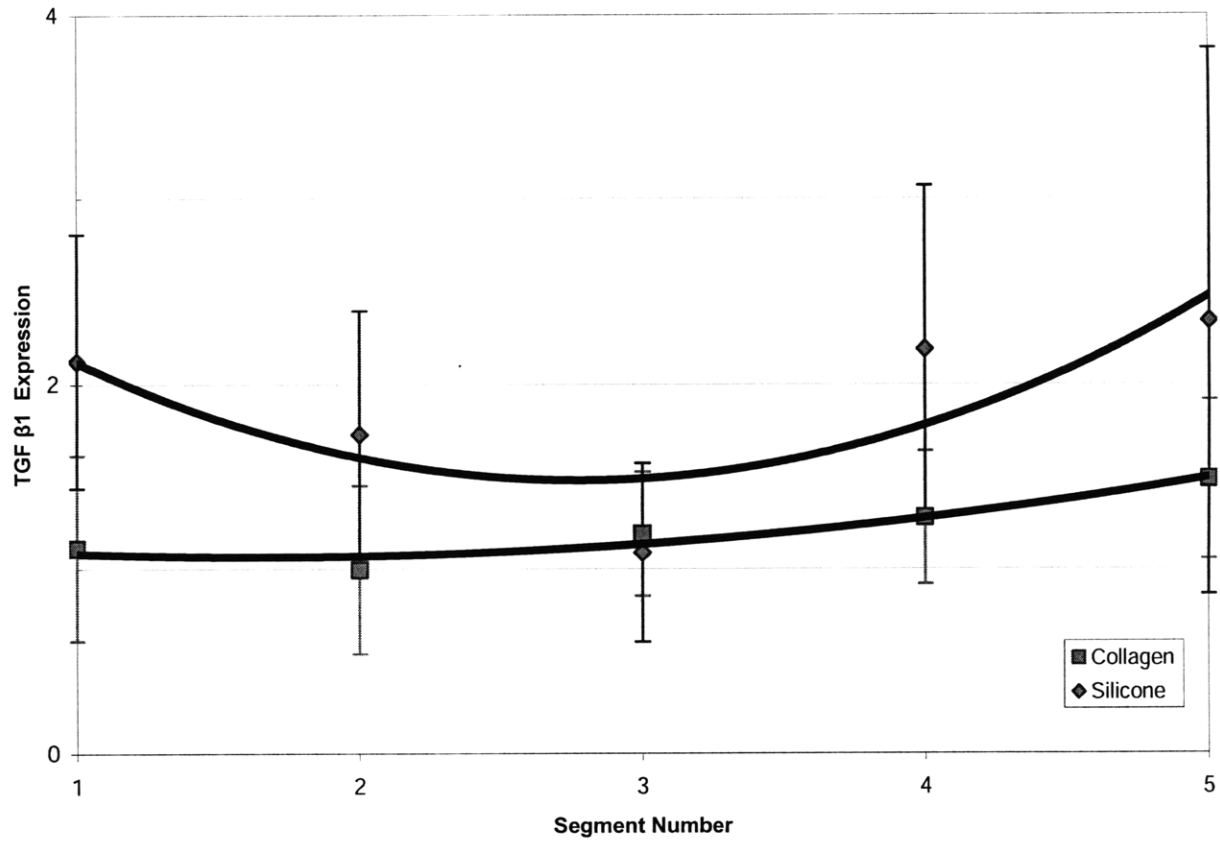
indicated a significant difference at the proximal stump from ELISA measurements, no significant differences were determined in any segment from the immunoblot data.



	Segment 1	Segment 2	Segment 3	Segment 4	Segment 5
<b>Collagen Treated</b>	0.03 ± 0.006	0.08 ± 0.01	0.05 ± 0.01	0.04 ± 0.005	0.04 ± 0.007
<b>Silicone Treated</b>	0.19 ± 0.08	0.11 ± 0.02	0.15 ± 0.07	0.20 ± 0.1	0.08 ± 0.04

Figure 14. 14-day TGF beta 1 expression (mean ± SEM) on per segment basis as determined by ELISA. Expression was normalized by mass of the explanted tissue segment.





	Segment 1	Segment 2	Segment 3	Segment 4	Segment 5
<b>Collagen Treated</b>	1.11 ± 0.50	0.99 ± 0.46	1.19 ± 0.34	1.28 ± 0.36	1.48 ± 0.43
<b>Silicone Treated</b>	2.12 ± 0.69	1.73 ± 0.67	1.09 ± 0.48	2.19 ± 0.88	2.34 ± 1.48

Figure 15. 14-day TGF β1 expression (mean ± SEM) on per segment basis as determined by average immunoblot intensity per unit area. Expression was normalized by cellular content.

## 4.2 TGF $\beta$ 2 Expression

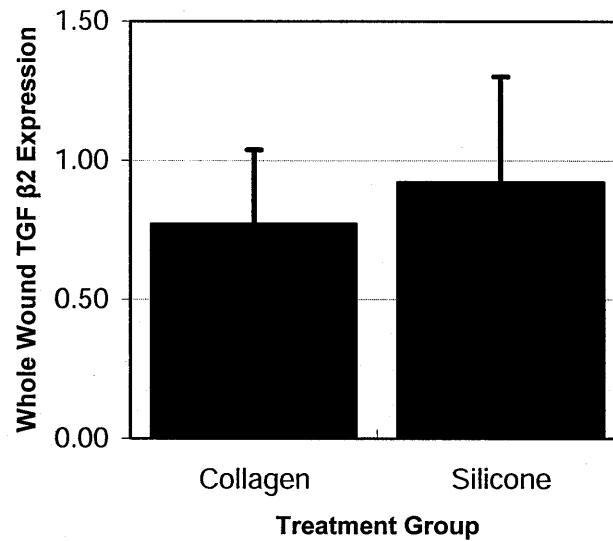
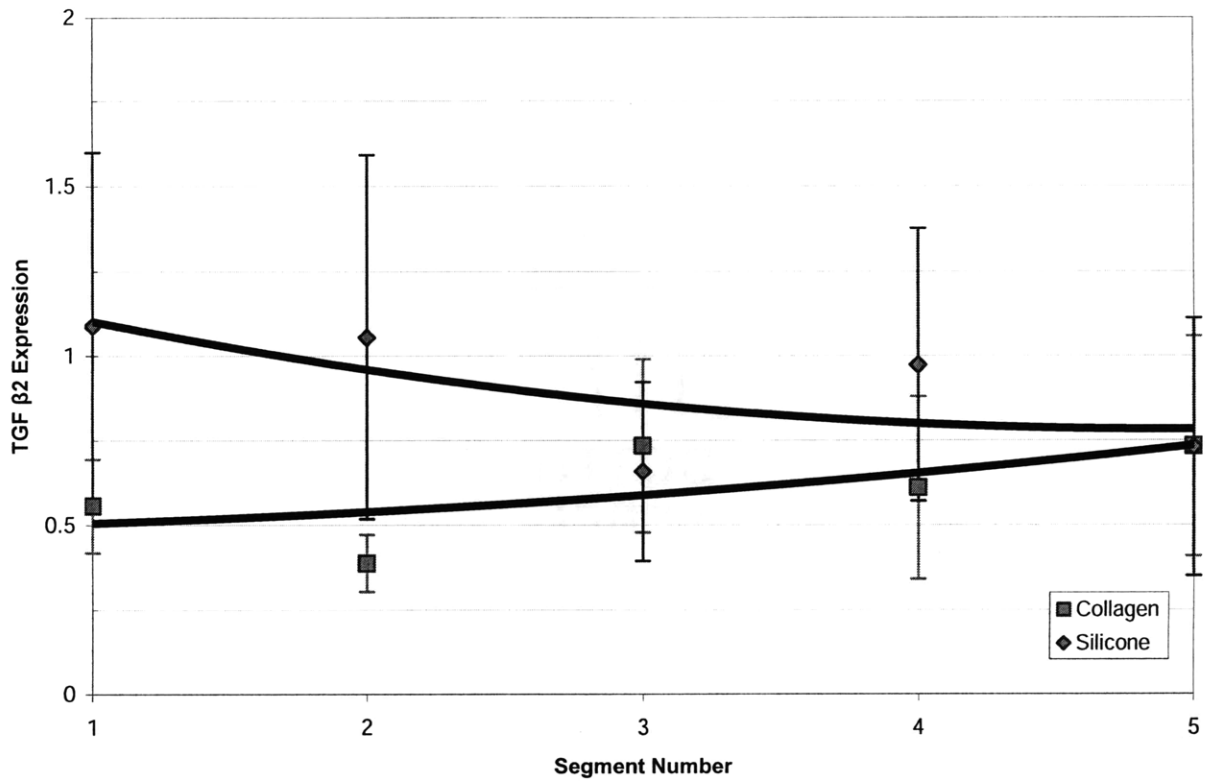


**Figure 16.** 14 day whole wound TGF  $\beta$ 2 expression (mean  $\pm$  SEM) as determined by average immunoblot intensity per unit area. Expression was normalized by cellular content.

Fourteen day sciatic nerve wounds treated with collagen and silicone devices showed no statistically significant difference in TGF  $\beta$ 2 expression when measured with immunoblot. Data from the wound segments alone showed possibly higher TGF  $\beta$ 2 expression in the silicone group in the most proximal segments. However, this result was statistically insignificant.



	Segment 1	Segment 2	Segment 3	Segment 4	Segment 5
<b>Collagen Treated</b>	0.56 ± 0.14	0.39 ± 0.08	0.73 ± 0.26	0.61 ± 0.27	0.73 ± 0.32
<b>Silicone Treated</b>	1.09 ± 0.51	1.05 ± 0.54	0.66 ± 0.26	0.97 ± 0.40	0.73 ± 0.27

**Figure 17. 14-day TGF β2 expression (mean ± SEM) on per segment basis as determined by average immunoblot intensity per unit area. Expression was normalized by cellular content.**

### 4.3 TGF $\beta$ 3 Expression

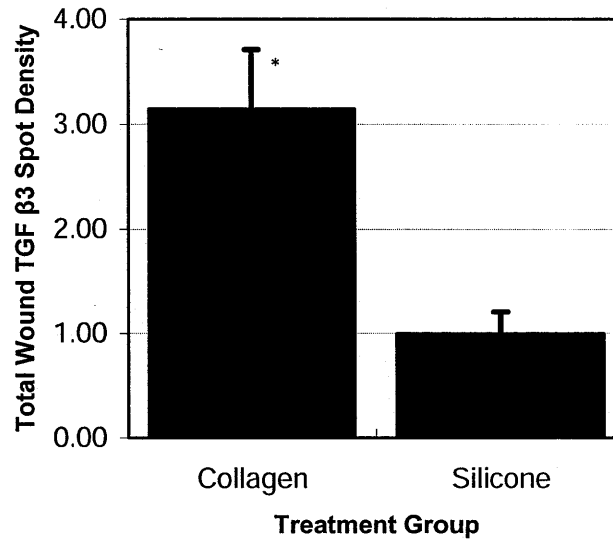
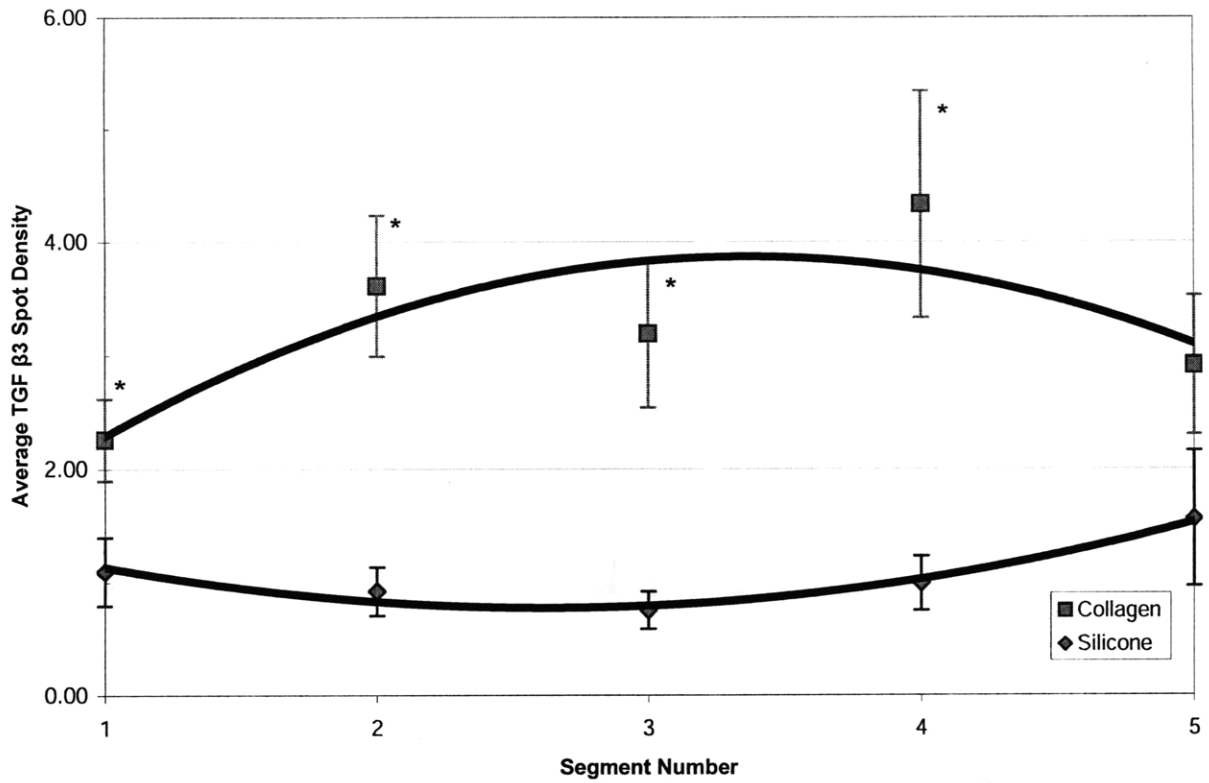


**Figure 18.** 14-day whole wound TGF  $\beta$ 3 expression (mean  $\pm$  SEM) as determined by average immunoblot intensity per unit area. Expression is normalized for cellular content.

Immunoblot assay showed three times the whole wound TGF  $\beta$ 3 expression in the collagen treatment group from the silicone treatment group ( $p=.002$ ). This difference was confirmed on a per segment basis. All five collagen treated segments had increased levels of TGF  $\beta$ 3 expression compared to the silicone treatment group, though statistical significance was only confirmed in the first four segments.



	Segment 1	Segment 2	Segment 3	Segment 4	Segment 5
<b>Collagen Treated</b>	2.26 ± 0.36	3.61 ± 0.62	3.19 ± 0.65	4.33 ± 1.00	2.91 ± 0.61
<b>Silicone Treated</b>	1.10 ± 0.30	0.92 ± 0.21	0.75 ± 0.17	0.99 ± 0.24	1.56 ± 0.60

**Figure 19. 14-day TGF β3 expression (mean ± SEM) on per segment basis as determined by average immunoblot intensity per unit area. Expression was normalized by cellular content.**

#### 4.4 $\alpha$ SMA Expression

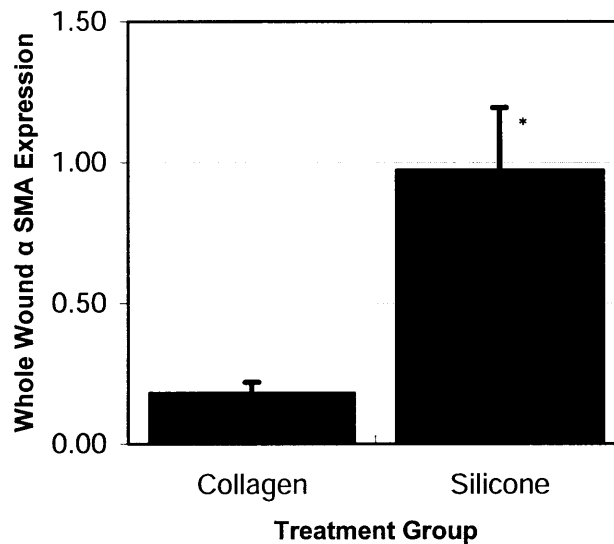
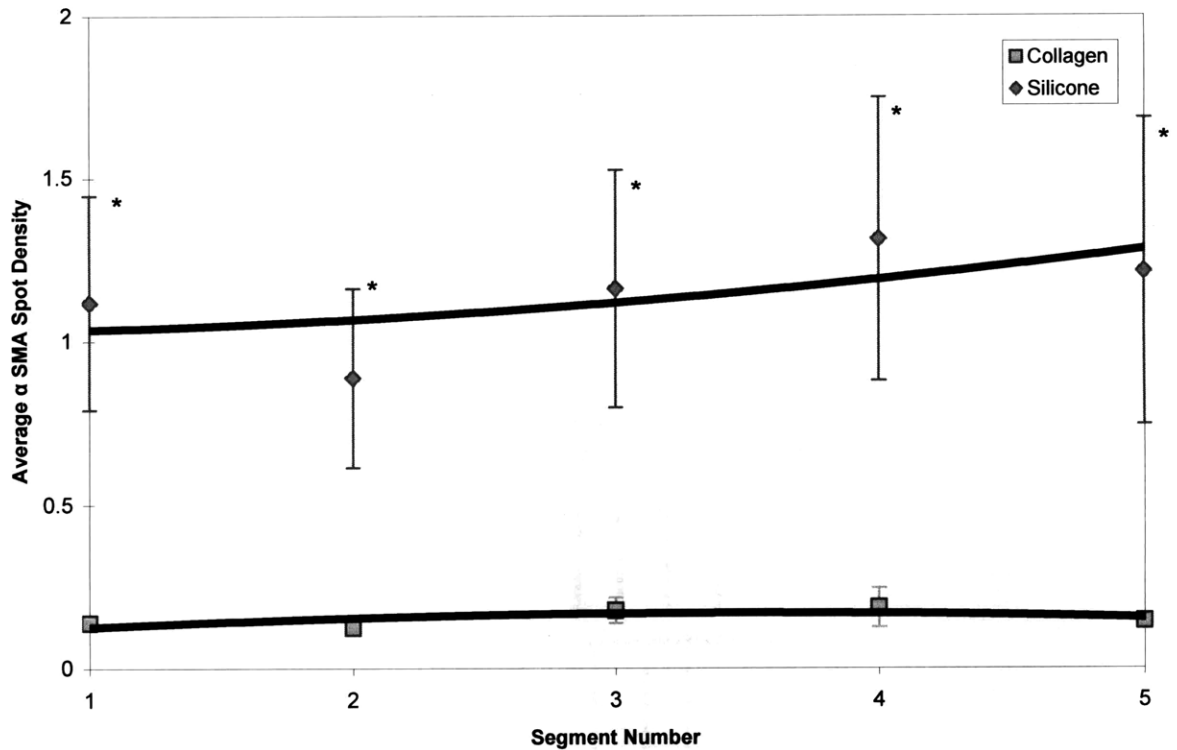


**Figure 20.** 14-day whole wound  $\alpha$  SMA expression (mean  $\pm$  SEM) as determined by average immunoblot intensity per unit area. Expression has been adjusted to reflect  $\alpha$  SMA expression inside the regenerate only with normalization by cellular content.

Recalling Section 3.7.5, expression of  $\alpha$  SMA in the collagen tube induced regenerate required correcting the immunoblot method for the tissue triage procedure that left the collagen tube in contact with the regenerate. Based on analysis from immunofluorescent images taken throughout different regions of the nerve, it was estimated that the immunofluorescent signal from the regenerate accounted for 5.7% of the total  $\alpha$  SMA expression and 35.3% of the total cellular content in the collagen treated wound. This correction factor was applied to the immunoblot data, and differences in  $\alpha$  SMA present only in the regenerate were compared across treatment groups. Whole wound  $\alpha$  SMA expression was 440% greater in the in silicone compared to collagen treated nerves ( $p=.0046$ ). The significant difference in  $\alpha$  SMA expression was also observed on a per segment basis across all segments.



	Segment 1	Segment 2	Segment 3	Segment 4	Segment 5
<b>Collagen Treated</b>	0.14 ± 0.02	0.12 ± 0.02	0.18 ± 0.04	0.18 ± 0.06	0.14 ± 0.02
<b>Silicone Treated</b>	1.12 ± 0.33	0.89 ± 0.27	1.16 ± 0.36	1.31 ± 0.43	1.21 ± 0.47

**Figure 21.** 14-day  $\alpha$  SMA expression (mean  $\pm$  SEM) on per segment basis as determined by average immunoblot intensity per unit area. Expression has been adjusted to reflect  $\alpha$  SMA expression inside the regenerate only with normalization by cellular content.

The level of  $\alpha$  SMA sampled in a region of interest (ROI) from the edge of the regenerate to  $\sim 65 \mu\text{m}$  radially inwards was used as a metric to determine the contribution of protein expression at the regenerate periphery (Figure 22). From plots of intensity as a function of radial distance from the edge, the first large magnitude gradient encountered from the edge, e.g. 0.5 intensity units/ $\mu\text{m}$ , corresponded to the boundary of contractile cell layers previously observed by Chamberlain *et al.* (1998, 2000). For cross sections from the silicone treatment group

sampled in the proximal and distal nerve trunk, contractile cell layers were almost as large as the entire radial distance assayed. Compared to the nerve stumps, silicone induced regenerate in the gap had a smaller thickness contractile cell layer (~5-10  $\mu\text{m}$ ) but more diffuse staining throughout the cross section. Cross sections in the collagen treatment group consistently had 0-10  $\mu\text{m}$  of staining on the regenerate periphery.

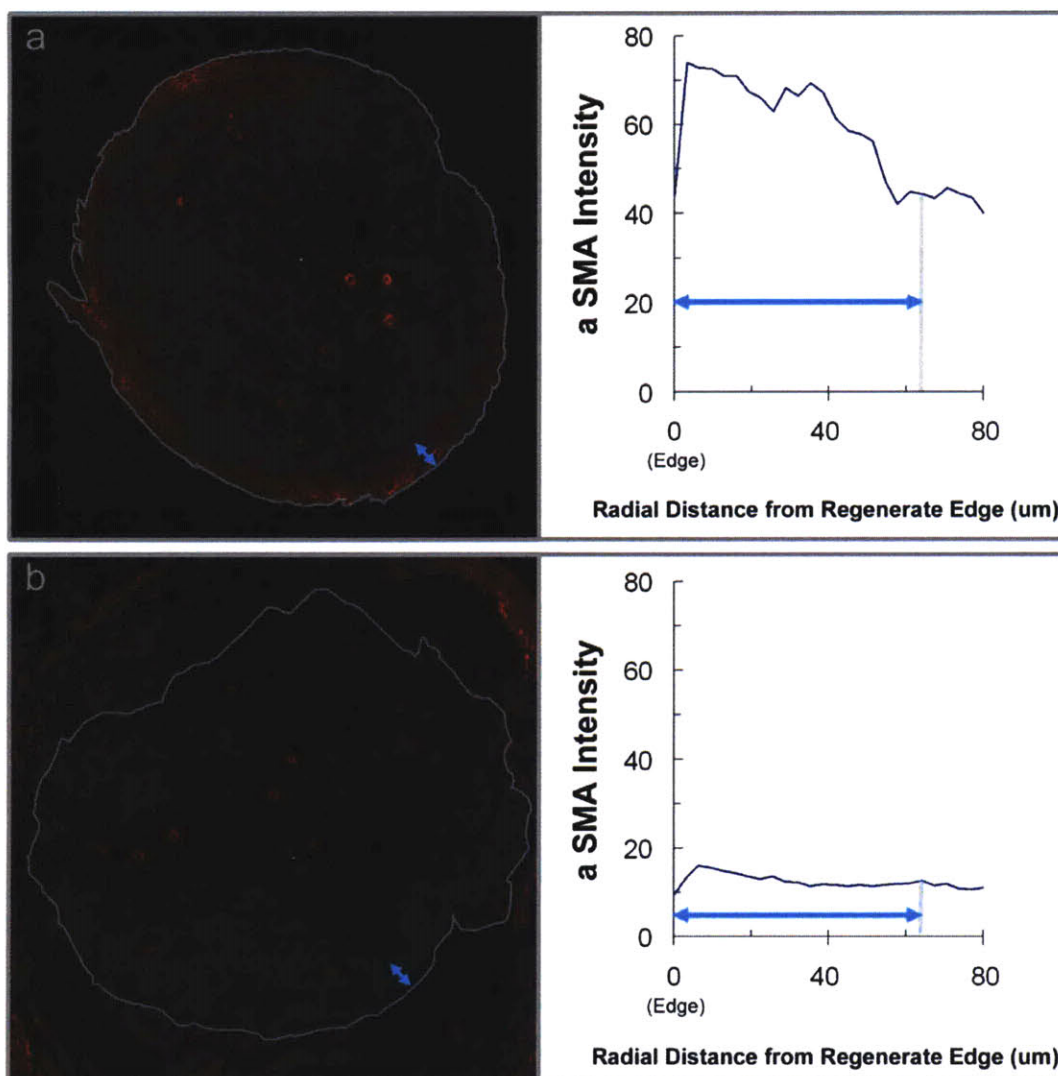
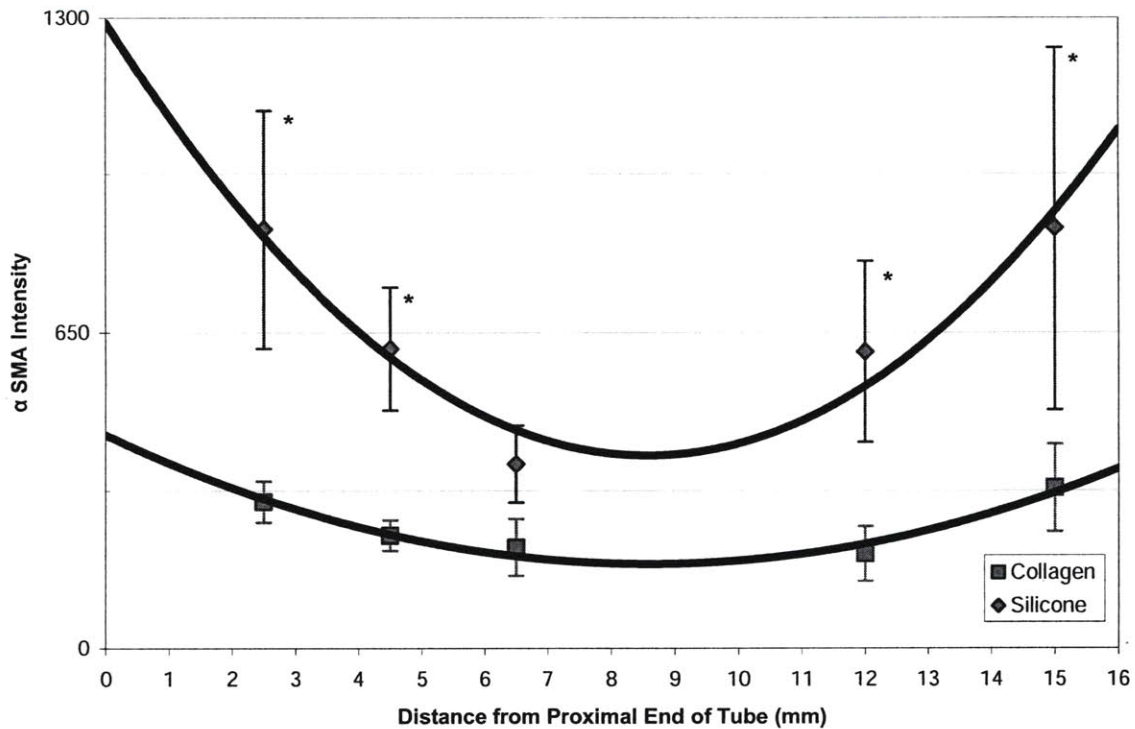


Figure 22.  $\alpha$  SMA expression in 14-day (a) silicone and (b) collagen treated peripheral nerve wounds. Cross sections were taken 2.5 mm from the proximal end of the tube, and intensity measurements were taken from the edge of the regenerate to ~65  $\mu\text{m}$  radially into the center of the cross section to capture  $\alpha$  SMA expression from circumferential contractile cell layers observed in silicone treated wounds by previous investigators.





	Immunofluorescence Intensity Units				
	x = 2.5 mm	x = 4.5 mm	x = 6.5 mm	x = 12 mm	x = 15 mm
<b>Collagen Treated</b>	302.7 ± 46.3	229.1 ± 23.5	176.0 ± 51.8	236.0 ± 33.0	356.2 ± 45.1
<b>Silicone Treated</b>	829.1 ± 252.1	611.3 ± 132.0	368.5 ± 90.4	622.5 ± 193.7	1011.2 ± 252.4

**Figure 23.** 14-day  $\alpha$  SMA expression (mean  $\pm$  SEM) for 5 locations sampled in nerve using immunofluorescence intensity as a metric. Intensity data for cross sections were summed over a concentric shell extending from the periphery to  $\sim 65 \mu\text{m}$  toward the center of the regenerate and averaged across treatment groups.

Immunofluorescent cross sectional analysis was conducted at five data points along the length of the nerve to compare  $\alpha$  SMA expression in the two treatment groups as a function of distance. Silicone treated wounds were found to express two to three times the level of  $\alpha$  SMA as did the collagen treated wounds. The significant differences between treatment groups occurred in the proximal (x=2.5 mm, p=0.024; 4.5mm, p=0.041) and distal (x=12 mm, p=0.04;

15 mm,  $p=0.002$ ) trunks, but not at the data point sampled in the interneural wound gap ( $x=6.5$  mm).

	<b>Best fit curve</b>	<b>R<sup>2</sup></b>	<b>Area under curve (Intensity Units)</b>
<b>Collagen Treated</b>	$4.0423x^2 - 66.174x + 442.1$	90.995	10887
<b>Silicone Treated</b>	$13.885x^2 - 227.4x + 1314.8$	0.973	4122

**Table 13. Polynomial order 2 best fit curve to describe peripheral  $\alpha$  SMA expression across the entire nerve.**

The  $\alpha$  SMA expression from the whole wound periphery (ROI evaluated across the entire nerve length) was quantified by integrating the order 2 polynomial best fit curves to the intensity data. In comparing the two treatment groups with this calculation, silicone treated wounds showed a 164% increase in the whole wound periphery expression of  $\alpha$  SMA from the collagen treated wounds.

## Chapter 5: Discussion

### 5.1 TGF $\beta$ 1 Expression

The pro-fibrotic cytokine TGF  $\beta$ 1 was measured in higher levels in silicone than collagen tube treated wounds, but statistical difference could only be achieved through an enzyme-linked immunosorbent assay (ELISA). ELISA indicated about a 50% increase of whole wound TGF  $\beta$ 1 levels in the silicone treatment group compared to the collagen treatment group ( $p=.0021$ ). Though immunoblotting showed a similar 30% increase in TGF  $\beta$ 1 in the silicone treatment group, the data did not show a statistically significant difference between silicone and collagen treated wounds.

There are a number of possibilities that may explain the apparent inconsistency between and the ELISA and immunoblot data. Differences in assay results may be due to the sensitivity of the antibody used. Immunoblotting was performed using a different antibody than those used provided in the ELISA kit. In addition, immunoblotting is a semiquantitative technique to compare relative amounts of protein between samples. The immunoblot assay produces more variation than the ELISA method due to the operator-dependent nature of selecting protein bands.

Wong found statistical difference in the levels of TGF  $\beta$ 1 mRNA expression by day 7 but not day 14 (2008). He observed about a 44% increase in mRNA expression that corresponds well with the possible 30-50% increase in protein expression that may occur a few days later in data obtained in this study. It is possible that the difference in TGF  $\beta$ 1 expression between treatment groups, if there is one, may have occurred maximally before day 14. If this is the case, then the relative levels of TGF  $\beta$ 1 between the silicone and collagen tube treated groups may have been too small to be proven for 14-day data by the immunoblotting technique.

The comparison of wounded day 16 rat fetal skin and day 19 rat fetal skin by Soo *et al.* (2003) serves as a benchmark for this study due to our interest to use differential cytokine expression in early fetal wounds as a model for regeneration in the peripheral nerve. TGF  $\beta$ 1 expression was found to be greater in magnitude and more prolonged for the late fetal scarring wound than that of the early fetal wound that heals by regeneration. While I cannot definitively state that there was a difference in TGF  $\beta$ 1 expression between silicone and collagen treated wounds on day 14 based on the data from the immunoblot assay, the research by Soo and colleagues points out that the differences in TGF  $\beta$ 1 expression are not only in magnitude but in duration. The differential expression of TGF  $\beta$ 1 expression in the regenerating versus nonregenerating nerve may occur at an earlier time point.

Due to the difference in conclusion reached by the use of two assays, this study can only conclude that the data suggest a 30-50% increase in TGF  $\beta$ 1 protein expression in the silicone treated wounds over collagen treated wounds by day 14. This suggested difference could be explored in future work with immunofluorescence. However, it may be more useful to spend more effort exploring TGF  $\beta$ 1 protein levels in the nerve wounds between the day 7 and day 14 time points which may contain the maximal difference between TGF  $\beta$ 1 expression.

## **5.2 TGF $\beta$ 2 Expression**

No statistical difference in TGF  $\beta$ 2 expression could be measured between the collagen and silicone treated wounds 14 days post-operatively. This was consistent with Wong's data, which did not find differences in TGF  $\beta$ 2 expression until another week into the wound healing process (2008). Soo *et al.* found an increase in TGF  $\beta$ 2 expression in late fetal over early fetal wounds in immunohistological determinations but not by RT-PCR techniques, which showed the

reverse at 24 and 72 hours post injury (2003). The protein level increase at the late fetal stage determined by immunohistochemistry was less than that observed for TGF  $\beta$ 1. The investigators hypothesized that the increase in TGF  $\beta$ 2 they observed may be a result of inflammatory infiltrate, and concluded that TGF  $\beta$ 2 transcription may not be important for scar formation. In another study by Broker *et al.*, comparison of fetal to adult fibroblasts in TGF  $\beta$ 2 expression showed no difference (1992). My study therefore concurs with the above studies in TGF  $\beta$ 2's diminished role in regenerative wound healing.

### **5.3 TGF $\beta$ 3 Expression**

Unlike the results for the other isoforms, a marked difference was found in TGF  $\beta$ 3 levels between day 14 collagen and silicone treated wounds. As quantified by immunoblot, collagen treated wounds expressed three times the levels of TGF  $\beta$ 3 than that of the silicone treated wounds ( $p=.0026$ ). This corresponds with the differential TGF  $\beta$ 3 mRNA expression observed by Wong which also showed three times the levels in collagen over silicone treated wounds (2008). This result suggests a transcriptional and protein level difference in TGF  $\beta$ 3 that may be important at the two-week time point for regenerative wound healing.

TGF  $\beta$ 3 has been implicated by other studies as having an anti-inflammatory role. This observation was upheld by Soo *et al.*, who similarly observed heightened and prolonged expression of this particular isoform in early fetal skin wounds over late fetal skin wounds (2003). This investigation is additional confirmation that TGF  $\beta$ 3 expression has influence on the determination of a regenerating wound.

#### 5.4 $\alpha$ SMA Expression

Immunoblot and immunofluorescent techniques showed a large and significant increase in day 14  $\alpha$  SMA expression in silicone treated versus collagen treated peripheral nerve wounds. Immunoblot results gave an estimate of ten times the amount of  $\alpha$  SMA in silicone treated wounds than collagen treated wounds. This estimate was gathered by applying a preliminary correction factor to the immunoblot data due to the external scar covering the collagen tube surface that could not be removed from the samples assayed. The correction amounted to considering only  $\alpha$  SMA that accumulated around the regenerated nerve rather than including  $\alpha$  SMA that had accumulated around the still undegraded collagen device. A more accurate correction factor can be determined in future work requiring more numerous sampling across the nerve regenerate.

A measurement of  $\alpha$  SMA expression in only the regenerate was determined using immunofluorescence, in which the spatial distribution of the protein was mapped as a function of distance from the nerve periphery. At a 14 day time point, significant increases in levels of  $\alpha$  SMA in silicone treated wounds occurred in cross sections taken at every location assayed along the nerve wound except at the one data point taken in the interneural wound gap ( $x=6.5$ ). The largest increase in expression between the two treatment groups was about 170-180% and occurred at the proximal and distal nerve trunks ( $p=.0243$ ;  $p=.0021$ ). At the nerve stump cross sections, silicone treated wounds had a thick layer of very bright  $\alpha$  SMA staining that was sometimes as thick as 65  $\mu\text{m}$ , while collagen treated nerve wounds showed occasional intense  $\alpha$  SMA staining that, when present, was only 5-10  $\mu\text{m}$  thick. This amount of  $\alpha$  SMA staining was consistent in the collagen treated nerve wounds in cross sections taken along the length of the nerve. A statistically significant difference could not be shown in the  $\alpha$  SMA expression

between treatment groups at the cross section taken from the interneural wound gap. There was only a thin ~400  $\mu\text{m}$  diameter tissue regenerate that spanned the gap from the proximal to the distal end of the silicone treated wound by two weeks post-operative from injury. The thin tissue regenerate from the silicone treated wounds showed only ~5-10  $\mu\text{m}$  of intense  $\alpha$  SMA staining at the periphery, but a basal level of  $\alpha$  SMA staining into the center of the regenerate, as expression of  $\alpha$  SMA is much more diffuse in the early stages of wound healing.

Consistent with Wong's (2008) and the data of Chamberlain *et al.* (1998b, 2000), presence of  $\alpha$  SMA in the collagen treated wounds was far less than that in the silicone treated wounds. This study, which sampled nerves at a 14-day time point, adds to our understanding of contractile cell presence at the early wound healing stage. The immunofluorescent staining used in this investigation gave more insight on the spatial distribution of  $\alpha$  SMA, which was valuable in developing a metric that focused on the region of myofibroblast concentration.

Presence of myofibroblasts in both early fetal and adult wounds was observed in previous wound healing studies (Rolfe *et al.*, 2007). However, in the study by Rolfe and colleagues, fetal dermal fibroblast (FDF) response to TGF  $\beta$ 1 was shown to be much more rapid and short lived than the response of adult dermal fibroblasts. Differentiated FDF also failed to produce increased levels of ECM component deposition as do their adult counterparts. My study concludes that nerve wounds treated by the regenerative collagen device do express some levels of  $\alpha$  SMA that correspond to blood vessels and an occasional, but small layer of contractile cells at the periphery of the regenerate. The lower expression of  $\alpha$  SMA at the periphery of the collagen induced regenerate implies a smaller extent of myofibroblast activity than that present in the contractile capsule formed around the regenerate induced by the silicone treatment.

## Chapter 6: Summary

The rat model serves as a good basis for comparing regenerative and nonregenerative wound healing outcomes in the adult. This study attempted to explain regenerative versus nonregenerative healing in peripheral nerve through a proteomic analysis. The outcomes of wound healing were observed in a rat model using a well defined defect involving complete transection of the sciatic nerve. The nerve ends were bridged with a silicone or collagen tubulation device, previously shown to have poor and good ability, respectively, in regenerating nerve trunk across a 10 mm gap.

This study assayed the wounds of the two treatment groups for relative amounts of TGF  $\beta$ 1, TGF  $\beta$ 2, TGF  $\beta$ 3, and  $\alpha$  SMA, which are known to play important roles in wound healing, especially with respect to the pressure cuff theory that points to myofibroblast activity as a determinant for regenerative versus nonregenerative outcomes in peripheral nerve healing. The peripheral nerve wounds from the collagen treatment group expressed upregulated levels of TGF  $\beta$ 3, lower  $\alpha$  SMA levels, and possibly decreased levels of TGF  $\beta$ 1 compared to the silicone treatment group. The proteomic trends observed between wounds treated with the collagen regenerative device versus the silicone nonregenerative device are also observed between wounds undergoing early fetal regeneration versus adult nonregenerative repair. Results from this study concur with the use of early fetal regeneration as a model for induced adult regeneration in the peripheral nerve.



## References

- Affi AK and RA Bergman.** Functional neuroanatomy, 2nd ed.: text and atlas. New York: McGraw-Hill Medical Publishing, 2005.
- Archibald SJ, Krarup C, Shefner J, Li ST, Madison RD** (1991). A collagen-based nerve guide conduit for peripheral nerve repair: an electrophysiological study of nerve regeneration in rodents and nonhuman primates. *J Comp Neurol.* 306(4):685-696.
- Beanes SR, Dang C, Soo C, Wang Y, Urata M, Ting K, Fonkalsrud EW, Behnaim P, Hedrick MH, Atkinson JB, Lorenz, HP** (2001). Down-regulation of decorin, a transforming growth factor-beta modulator, is associated with scarless fetal wound healing. *J Pediatr Surg.* 36: 1666-1671.
- Bottinger, EP** (2008) "Tgf- $\beta$  and fibrosis" In The tgf-beta family. (Derynck R, Miyazono K, Eds.) New York: Cold Spring Harbor Laboratory Press, pp. 989-1022.
- Broker BJ, Chakrabarti R, Blynman T, Roesler J, Wang MB, Srivatsan ES** (1999). Comparison of growth factor expression in fetal and adult fibroblasts: a preliminary report. *Arch Otolaryngol Head Neck Surg.* 125:676-680.
- Brown PD, Wakefield LM, Levinson AD, Sporn MB** (1990). Physiochemical activation of recombinant latent transforming growth factor- $\beta$ s 1, 2, and 3. *Growth Factors* 3:35-43.
- Chamberlain LJ** (1996). Long term functional and morphological evaluation of peripheral nerves regenerated through degradable collagen implants. SM thesis, Massachusetts Institute of Technology, Cambridge, MA.
- Chamberlain LJ** (1998a). Influence of implant parameters on the mechanisms of peripheral nerve regeneration. PhD thesis, Massachusetts Institute of Technology, Cambridge, MA.
- Chamberlain LJ, Yannas IV, Arrizabalaga A, Hsu H-P, Norregaard TV, Spector M** (1998b). Early peripheral nerve healing in collagen and silicone tube implants: Myofibroblasts and the cellular response. *Biomaterials* 19:1393-1403.
- Chamberlain LJ, Yannas IV, Hsu H-P, Spector M** (2000). Connective tissue response to tubular implants for peripheral nerve regeneration: the role of myofibroblasts. *J Comp Neurol.* 417:415-430.
- Clark RAF and Henson PM.** The molecular and cellular biology of wound repair. New York: Plenum Press, 1998.
- Cowell AS, Beanes SR, Soo C, Dang C, Ting K, Longaker MT, Atkinson JB, Lorenz HP** (2005). Increased angiogenesis and expression of vascular endothelial growth factor during scarless repair. *Plast Reconstr Surg.* 115: 204-212.

**Colwell AS, Longaker MT, Lorenz HP** (2005). Mammalian fetal organ regeneration. *Adv Biochem Eng Biotechnol.* 93:83-100.

**Dang CM, Beans SR, Lee H, Zhang X, Soo C, and Ting K** (2003). Scarless fetal wounds are associated with an increased matrix metalloproteinase-to-tissue inhibitor of metalloproteinase ratio. *Plast Reconstr Surg.* 111:2273-2285.

**Dellon AL** (1990). Wound healing in nerve. *Clin Plast Surg.* 17:545-570.

**Desmouliere A, Geinoz A, Gabbiani F and Gabbiani G** (1993). Transforming growth factor-beta 1 induces alpha-smooth muscle actin expression in granulation tissue myofibroblasts and in quiescent and growing cultured fibroblasts. *J Cell Biol.* 122:103-111.

**Ermens AAM, Bayens AJM, van Gemert ACM, van Duijnhoven LP** (1997). Simple dot-blot method evaluated for detection of antibodies against extractable nuclear antigens. *Clin Chem.* 12:2420-2422.

**Fields RD, LeBeau JM, Longo FM, and Ellisman MH** (1989). Nerve regeneration through artificial tubular implants. *Prog Neurobiol.* 33:87-134.

**Freyman TM** (2001). Development of an *in vitro* model of contraction by fibroblasts. PhD thesis, Massachusetts Institute of Technology, Cambridge, MA.

**Fu SY and Gordon T** (1997). The cellular and molecular basis of peripheral nerve regeneration. *Mol Neurobiol.* 14:67-116.

**Guo L, Benlian Y, Zhou J, Li X, and Xing WD** (2006). Development of rabbit monoclonal and polyclonal antibodies for detection of site-specific histone modifications and their application in analyzing overall modification levels. *Cell Res.* 16:519-527.

**Gurtner GC, Werner S, Barrandon Y, Longaker MT** (2008). Wound repair and regeneration. *Nature.* 453: 314-321.

**Harley BA** (2002). Peripheral nerve regeneration through collagen devices with different *in vivo* degradation characteristics. SM thesis, Massachusetts Institute of Technology, Cambridge, MA.

**Herpin A, Lelong C, Favrel P** (2004). Transforming growth factor-beta-related proteins: an ancestral and widespread superfamily of cytokines in metazoans. *Dev Comp Immunol.* 28(5): 461-85.

**Kemp SWP, Syed S, Walsh SK, Zochodne DW, Midha R** (2009). Collagen nerve conduits promote enhanced axonal regeneration, schwann cell association, and neovascularization compared to silicone conduits. *Tissue Eng.* 15(00):1-14.

**Krummel TM, Michna BA, Thomas BL, Sporn MB, Nelson JM, Salzberg AM, Cohen IK, Diegelmann RF** (1988). Transforming growth factor beta (TGF-beta) induces fibrosis in a fetal wound model. *J Pediatr Surg.* 23: 647-652.

**Lee SK and Wolfe SW** (2000). Peripheral nerve injury and repair. *J Am Acad Orthop Surg.* 8(4):243-252.

**Liechty KW, Crombleholme TM, Cass DL, Martin B, Adzick NS** (1998). Diminished interleukin-8 (IL-8) production in the fetal wound healing response. *J Surg Res.* 77:80-84.

**Liechty KW, Adzick NS, Crombleholme TM** (2000a). Diminished interleukin 6 (IL-6) production during scarless human fetal wound repair. *Cytokine* 12:671-676.

**Liechty KW, Kim HB, Adzick NS, Crombleholme TM** (2000b). Fetal wound repair results in scar formation in interleukin-10-deficient mice in a syngeneic murine model of scarless fetal wound repair. *J Pediatr Surg.* 35:866-872; discussion 872-863.

**Lin RY, Sullivan KM, Argenta PA, Meuli M, Lorenz HP, Adzick NS** (1995). Exogenous transforming growth factor-beta amplifies its own expression and induces scar formation in a model of human fetal skin repair. *Ann Surg.* 222(2):146-154.

**Longaker MT, Chiu ES, Adzick NS, Stern M, Harrison MR, Stern R** (1991). Studies in fetal wound healing. V. A prolonged presence of hyaluronic acid characterizes fetal wound fluid. *Ann Surg.* 213:292-296.

**Lorenz HP, Lin RY, Longaker MT, Whitby DJ, Adzick NS** (1995). The fetal fibroblast: the effector cell of scarless fetal repair. *Plast Reconstr Surg.* 96:1251-1259.

**Lundborg G, Dahlin LB, Danielsen N, Gelberman RH, Longo FM, Powell HC, Varon S** (1982). Nerve regeneration in silicone chambers: Influence of gap length and of distal stump components. *Exp Neurol.* 76:361-375.

**Madison RD, Archibald SJ, Krarup C** (1992). Peripheral nerve injury. In *Wound Healing, Biochemical and Clinical Aspects* (Cohen IK, Diegelmann RF, Lindblad WJ, Eds.), pp 450-487.

**Millipore.** "Immunostaining techniques." <<http://www.millipore.com/immunodetection/id3/immunostainingtechniques>>

**Moses, HL and Roberts AB** (2008) "The discovery of  $\text{tgf-}\beta$ : A historical perspective" In The  $\text{tgf-}\beta$  family. (Derynck R, Miyazono K, Eds.) New York: Cold Spring Harbor Laboratory Press, pp. 1-28.

**Nath, RK, Kwon B, Mackinnon S, Jenson JN, Reznik S, Boutros S** (1998). Antibody to transforming growth factor beta reduces collagen production in injured peripheral nerve. *Plast & Recon Surg.* 102(4):1100-1106.

**Pelton R, Saxena B, Jones M, Moses H, and Gold L (1991).** Immunohistochemical localization of tgfb1, tgfb2, and tgfb3 in the mouse embryo: Expression patterns suggest multiple roles during embryonic development. *J Cell Biol.* 115(4):1091-1105.

**Rolfe K, Richardson J, Vigor C, Irvine L, G Addie, Linge C (2007).** A Role for TGF- 1- Induced Cellular Responses during Wound Healing of the Non-Scarring Early Human Fetus?. *J Inv Derm.* 127:2656–2667.

**Schilling SH, Hjelmeland AB, Rich JN, Wang XF (2008).** “Tgf- $\beta$ : a multipotential cytokine” In The tgfbeta family. (Derynck R, Miyazono K, Eds.) New York: Cold Spring Harbor Laboratory Press, pp. 45-77.

**Shah M, Foreman DM, Ferguson MW (1995).** Neutralisation of tgfbeta1 and tgfbeta 2 or exogenous addition of tgfbeta 3 to cutaneous rat wounds reduces scarring. *J Cell Sci.* 108:983-1002.

**Siegenthaler JA and Miller MW (2004).** Transforming growth factor  $\beta$ 1 modulates cell migration in rat cortex. *Cerebral Cortex* 14:791-802.

**Skalli O, Pelte MF, Pecllet MC, Gabbiani G, Gugliotta P, Bussolati G, Ravazzola M, Orci L (1989).** Alpha-smooth muscle actin, a differentiation marker of smooth muscle cells, is present in microfilamentous bundles of pericytes. *J Histochem Cytochem.* 37(3):315-321.

**Soo C, Beans SR, Hu F-Y, Zhang X, Dang C, Chang G, Wang Y, Nishimura I, Freymiller E, Longaker MT, Lorenz HP, Ting K (2003).** Ontogenetic transition in fetal wound transforming growth factor- $\beta$  regulation correlates with collagen organization. *Am J Path.* 163(6):2459-2476.

**Spilker MH (2000).** Peripheral nerve regeneration through tubular devices: a comparison of assays of device effectiveness. PhD thesis, Massachusetts Institute of Technology, Cambridge, MA.

**Sporn MB, Roberts AB, Shull JH, Smith JM, Ward JM, Sodek J (1983).** Polypeptide transforming growth factors isolated from bovine sources and used for wound healing in vivo. *Science.* 219(4590):1329-31.

**Whitby DJ and Ferguson MW (1991).** Immunohistochemical localization of growth factors in fetal wound healing. *Dev Biol.* 147: 207-215.

**Wong MQ (2008).** Transcriptional analysis of the healing response of wounded nerves treated with collagen and silicone tubes. SM thesis, Massachusetts Institute of Technology, Cambridge, MA.

**Yannas, IV.** Tissue and Organ Regeneration in Adults. New York: Springer-Verlag, 2001.

**Yannas, IV** (2005). Similarities and differences between induced regeneration in adults and early fetal regeneration. *J R Soc Interface* 22:403-417.

**Yannas IV, Kwan MD, Longaker MT** (2007). Early fetal healing as a model for adult organ regeneration. *Tissue Eng.* 13(8):1789-1797.

**Yannas IV, Zhang M, Spilker MH** (2007). Standardized criterion to analyze and directly compare various materials and models for peripheral nerve regeneration. *J Biomater Sci. Polymer Edn.* 18(8):943-966.

**Zhao Q, Dahlin LB, Kanje M, Lundborg G** (1992) The formation of a 'pseudo-nerve' in silicone chambers in the absence of regenerating axons. *Brain Res.* 592:106-114.

## Appendix A: Protocols

### A.1 5% Collagen Tube Fabrication Protocol

adapted from Harley, 2000

#### SUPPLIES

- 0.25 g Type I Collagen (Integra)
- 150  $\mu$ L Glacial Acetic Acid (GAA, Mallinckrodt)
- 22 Gauge Needle (Cat. No. 309574, Becton Dickinson)
- 10 mL Syringes (Cat. No. 309604, Becton Dickinson)
- Female-female Luer Lock Assembly (Stainless steel Luer Lock tube fitting, female luer x female luer, Cat. No. 5194k12, McMaster-Carr)
- Stainless Steel Wire (0.032" D., Cat. No. GWXX-320-30, Small Parts)
- Teflon Tubing, O.D. 0.056", I.D. 0.032" (PTFE Tubing, Cat. No. 06417-31, Cole-Parmer)
- Teflon Tubing, O.D. 0.125", I.D. 0.065" (PTFE Tubing, Cat. No. 06407-42, Cole-Parmer)
- Two Teflon and Aluminum Molds (see Figure 24 and Figure 25)

#### SOLUTIONS

- Acetic Acid, 3.0 M: 300  $\mu$ L glacial acetic acid, 1.7 mL distilled water

#### EQUIPMENT

- Centrifuge (Heraeus Labofuge 400R)
- Lyophilizer (VirTis Genesis EL or LE)

---

#### PROCEDURE

##### PREPARATION

- Assemble mandrels using a stainless steel wire core surrounded by Teflon tubing (O.D. 0.056", I.D. 0.032"). The length of the mandrel should be several mm larger than the length of the mold.
- Spacers, to be used at the ends of mandrels, are made out of Teflon tubing (O.D. 0.125", I.D. 0.065") and are on the order of 5-10 mm long.
- Autoclave mandrels and spacers before use.
- Clean two Teflon and aluminum molds with acetic acid. Per the protocol to follow, approximately 12 tubes (6 tubes per mold) can be made.

##### TUBE FABRICATION

- Fill two 15 mL Falcon tubes with approximately 5 mL of distilled water. Leave both tubes uncapped and centrifuge at 4500 rpm for 10-15 minutes to degas.
- Draw 3.0 M acetic acid into 3 mL syringe with 22 gauge needle

- Weigh 0.25 g Type I Collagen (Integra Life Sciences, San Diego, CA). Place collagen into 10 mL syringe that has Parafilm covering luer-lock end. Add 4 mL degassed, distilled water and mix thoroughly with forceps.
- Insert plunger into syringe and invert syringe, allowing collagen mixture to fall away from the syringe tip. Remove Parafilm and mix collagen slurry by moving stopper up and down. Purge air out from tip, bringing plunger up so that slurry comes up to the tip.
- Slowly inject 1 mL 3.0 M acetic acid into collagen, placing the needle from the 3 mL syringe through the tip of the 10 mL syringe with collagen-water suspension. Add the 1 mL acetic acid slowly while mixing with needle tip and pulling back on the 10 mL syringe plunger.
- Blend slurry well until a homogenous mixture is achieved. Attach 10 mL syringe with collagen slurry to another 10 mL syringe with a female-female Luer Lock assembly and mix by injecting collagen slurry from one syringe to another. Mix back and forth 10-15x, until collagen fibers begin to hydrate and solution appears uniform.
- Try to make sure as much of the collagen slurry is in only one of the 10 mL syringes. Remove empty syringe and Luer Lock fitting. Seal the tip of the full syringe with multiple layers of Parafilm to ensure that the collagen does not escape during centrifugation.
- Do not remove plunger. Let slurry mixture sit for 3 hours at room temperature to allow for the collagen fibers to swell.
- After 3 hours, remove plunger, but keep Parafilm over syringe tip. Cut a small notch in on the side of the black rubber material using a razor.
- Set lyophilizer to  $-40^{\circ}\text{C}$  (it takes  $\geq 1$  hr for chamber to reach set temperature).
- Centrifuge the collagen slurry in the syringe in order to degas the collagen so that it homogenizes without any macroscopic air bubbles. Place the syringe into a 50 mL Falcon tube, using a moist, folded paper towel to brace the syringe along the central axis of the conical tube.
- Mass the Falcon tube-syringe system and make the counterweight of the same mass using a Falcon tube filled with water.
- Centrifuge the Falcon tubes at 4500 rpm (3940xG) at  $25^{\circ}\text{C}$  for 30 minutes. Check to make sure that the syringe is still centrally aligned in the Falcon tube; if not, make the appropriate adjustments. Return the Falcon tube-syringe system to the centrifuge and spin at 4500 rpm (3940xG) at  $25^{\circ}\text{C}$  for 30 minutes.
- Take the molds and align the top and bottom. Close molds using screw mechanism or 4 c-clamps.
- Remove the syringe from the centrifuge. Slowly return the plunger to the syringe while removing the parafilm seal.
- Slowly inject the centrifuged slurry ( $\sim 0.25$  mL per tube) into closed molds until slurry is apparent on other side. Insert mandrel into slurry, rotating mandrel during insertion so as to keep the mandrel centered and to maintain a uniform deposition of collagen throughout the mold. Cap the free ends of the mandrel with the spacers after the mandrel is fully inserted. Repeat step, filling as many holes possible of each mold.
- Place molds in lyophilizer for 1 hour. Depending on the shelf height, the molds will be placed horizontally or vertically on the shelf. Be sure to note which orientation was used.

- After freezing, remove the molds from the lyophilizer and split them. Gently remove the tubes using clean forceps and a razor. Keep the mandrels inside the tubes. Place tubes with mandrels back into the lyophilizer (at  $-40^{\circ}\text{C}$ ).
- Pull vacuum in lyophilizer until both readouts are below 200 mTorr.
- Raise temperature to  $0^{\circ}\text{C}$  and leave overnight under vacuum in lyophilizer (17 hours).
- Raise temperature to  $20^{\circ}\text{C}$  and release vacuum.
- Create aluminum foil packet by tearing a large sheet of aluminum foil and folding it in half once in one direction, and once in half in the other direction. The walls of the packet should now be two sheets thick. For two of the three open edges, fold over the sheet twice approximately 8 mm each time to create a durable closure. The open edge is for deposition of the collagen tube. Using a lab marker, label the package with the following information:
  - Collagen I Nerve Tubes
  - $T_f = -40^{\circ}\text{C}$
  - Investigator Name, Date of Fabrication
- Remove tubes (Figure 26 for final dimensions) with mandrels from lyophilizer and place into aluminum foil packets. Close the open edge by folding it over twice. Store packets in dessicator with DrieRite Absorbent (VWR International,

## ASSOCIATED FIGURES

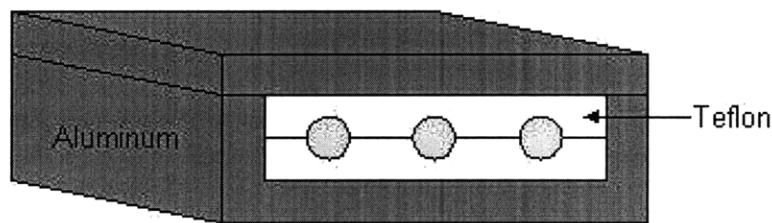


Figure 24. Teflon and aluminum mold schematic

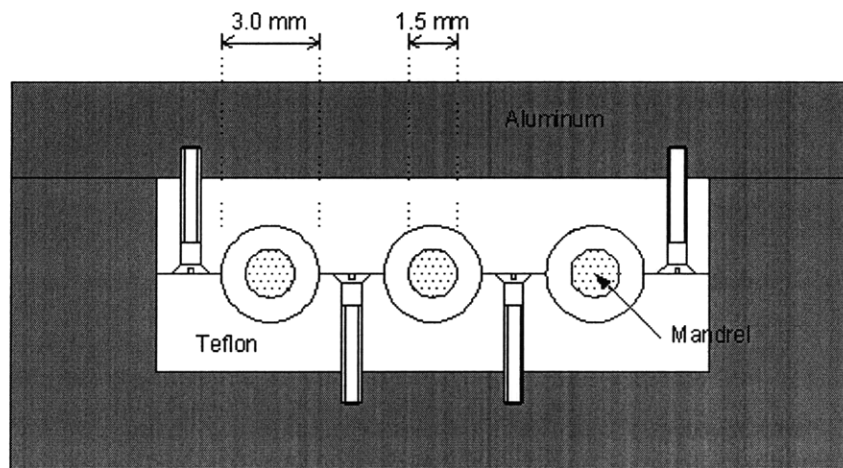
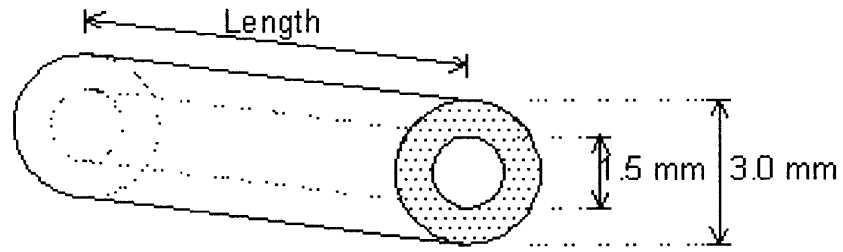


Figure 25. Teflon and aluminum mold (side view) with inserted mandrels





**Figure 26. Collagen nerve tube produced from Teflon and aluminum mold**

## A.2 Dehydrothermal Treatment (DHT) of Implant Devices

adapted from Harley, 2000

### SUPPLIES

- Silicone tubing (ID: 3.1 mm, Helix Medical, LLC, Carpinteria, CA)
- Razor
- Phosphate buffered saline (PBS) (Cat. No. BM-220S, Boston BioProducts)
- Teflon sheet
- Ruler
- Razor
- 500 mL glass jar with lid
- Glass vials (Short Form Style with Phenolic Cap, Cat. No. 66011-063, VWR)
  - 1 for each silicone device
- Lyophilized collagen tubes, contained within aluminum foil packet

### EQUIPMENT

- Vacuum oven (Isotemp Model 201, Fisher Scientific)
- 

### PROCEDURE

DHT is performed on silicone and collagen tubes used for implantation. They do not have to be, and usually are not, treated at the same time. Silicone tubes are treated 1-2 days before surgery while collagen tubes should be treated immediately after lyophilization.

### PREPARATION

- All metal instruments should be cleaned with 70% ethanol.
- The glass vials, jars, and lids should be autoclaved.
- For silicone tube DHT
  - Prepare silicone tube implants in a clean environment by measuring 16 mm of silicone tubing on a Teflon sheet. Cut with a razor. Flush each segment twice with PBS and place in individual glass vials without the cap on.
- For collagen tube DHT
  - Obtain collagen tubes contained inside aluminum foil packet immediately after lyophilization step or with little time spent in storage with desiccant (do not store for more than 24 hours prior to DHT). Open the top edge of the foil packet.
- Place vials and caps or packet in the vacuum oven at the established set temperature.

### DHT PROTOCOL

<u>Set Temperature</u>	<u>Exposure Time</u>
120 °C	48 hours

- Turn purge valve off and vacuum valve on. Flip the switch on the vacuum to turn it on. The vacuum oven should reach a final pressure of approximately -29.7 mmHg.

- At the end of the exposure period, turn off the vacuum and vent the chamber. Open the vacuum door and immediately seal the vials or aluminum foil packet. The tubes should only be handled under sterile conditions from now on.
- Place the silicone tube vials in the 500 mL glass jar and close the lid.
- Store the tube in a desiccator with Drierite Absorbent (VWR International, Inc., San Diego, California). Crosslinked matrices can remain for a few months in a desiccator prior to testing or use.

### **A.3 Sterile Procedure and Implant Assembly for Surgery Preparation**

adapted from Chamberlain, 1998, Spilker, 2000; Harley, 2002

#### **SUPPLIES**

- Jewelers Forceps
  - Regular Forceps (2)
  - Large Forceps
  - Surgical Blade Holder
  - Needle Holder
- 

#### **PROCEDURE**

To be carried out 1-2 days before implantation

#### **IMPLANTATION DEVICES**

- Dehydrothermally Treat (DHT) tubes (Appendix A.2)
  - Silicone tubes in individual glass vials.
  - Collagen tubes in packets
- Bring the DHT crosslinked collagen tubes to a sterile biohood. Using a Teflon sheet, ruler, forceps, and razor that have been sprayed with 70% ethanol, cut the collagen tubes into 16 mm segments. Place each segment into an individual aluminum foil packet. Close the packets.
- Store all implant devices in dessicator until transportation to VA Medical Center.

#### **SURGICAL TOOLKIT**

- Autoclave surgical instruments in autoclave bags.

## A.4 Surgical Protocol

Chamberlain, 1998; Spilker, 2000; Harley, 2002

### SUPPLIES

- Order animals: Adult, female Lewis rats 150 – 200 g, from Charles River Laboratories. Animals must arrive at least one week in advance of surgery to reduce the stress placed on the animal due to travel.

- Sterilize the necessary items:

Metal Bowl	Large Scissors
Gauze	Surgical (Tenotomy) Scissors
Surgical Blade Holder	Paper Clip Retractors (2)
Microneedle Holder	Forceps (2)
Microscissors	Needle Holder
Jewelers Forceps (2)	Animal Skin Staples
Large Forceps	Wooden Rods (cotton swabs)

- Ready other sterile items:

Table Covering	Pen
Scalpel Blades (4 #15 blade, 1 #11 blade)	10-0 Sutures
Bottle of PBS	4-0 Sutures
Iodine Sponge	1 mL Syringes
Draping	
Implants	
Bottle of Sodium Pentobarbital (Nembutal), 50 mg/ml	
Small Piece of Wood (e.g. from tongue depressor)	

- Ready other non-sterile items:

Surgical Board	Numbered Ear Tags
Rubber Bands (4)	Microsurgery Glasses (Loops)
Ear Tagging Tool	Hair Clippers

---

### PROCEDURE

- Weigh animal on an approximately sized balance. Record the weight and determine anesthetic dosage based on the pre-operative weight.
- Anesthetize animal with injection of sodium pentobarbital (50 mg of solution per kg of animal). Allow 10-15 minutes for anesthesia to take effect. Each animal reacts differently to the anesthetic and in some cases, more time may be required.
- Meanwhile, arrange the surgical area so that the table is at a comfortable level for the surgeon, and the tools are conveniently located.
- The surgeon should be sterilely dressed in scrub shirt and pants, hat and mask.

- When ready, shave the animal using the animal hair clippers from the base of the tail up to the middle of the back. The leg receiving the prosthesis should be shaved carefully and completely.
- Place the animal on the surgical board in the prone position and secure the fore and hind limbs to the board using rubber bands. The hind legs should be in 30° abduction. Place a piece of gauze under the appropriate thigh to elevate the leg slightly.
- Connect the animal to O<sub>2</sub> mask for the duration of the surgical procedure.
- Clean the shaved portion of the animal vigorously with the iodine sponge to disinfect the area. At this point, the surgeon should put on the sterile gloves and remain sterile for the rest of the procedure. Cut a hole in the sterile draping small enough so that only the leg is exposed. Place the draping over the animal.
- Using the # 15 scalpel, make a 4 cm incision along the leg of the animal. Separate the skin from the muscle along the incision by cutting through the connective tissue with the surgical scissors.
- Using the surgical scissors, separate the muscles until the sciatic nerve is visible. Carefully cut back the muscle along the skin incision line exposing the sciatic nerve.
- Place the paper clip retractors inside the muscle to separate the wound edges. Anesthetize the nerve by placing a few drops of Lidocaine directly on the area. Cut away the fascia surrounding the sciatic nerve carefully so that the nerve is free from constraint.
- Place the sterile wood piece underneath the nerve and carefully transect the nerve midway between the proximal nerve trunk and the distal bifurcation using the scalpel.
- Measure the prosthesis and make a mark on the nerve stumps 3 mm from each end. If necessary, trim prosthesis to appropriate length using microscissors.
- Place the tube in the gap and insert the proximal nerve stump 3 mm into the tube end, as marked. Secure the nerve in place by using two 10-0 sutures which travel through the epineurium and then through the tube. Inject enough sterile PBS into proximal end of prosthesis to fill the device using the 1 cc syringe. Tie the sutures with four single knots. Insert the distal nerve end 3 mm into the other end of the tube and secure in the same manner.
- Remove the paper clip retractors and close the muscle layer using three 4-0 sutures. Close the skin using skin staples.
- Place the animals on heating pads with O<sub>2</sub> masks and monitor until they are mobile.

## **A.5 Post-Operative Care and Supervision Protocol**

adapted from Spilker, 2000; Harley, 2002

### **SUPPLIES**

- Ketofen, 0.15 mg/mL
  - Cefazolin, 100 mg/mL
  - 1 mL TB Syringes
- 

### **PROCEDURE**

- Monitor rats immediately following surgery. Analgesic is to be started immediately following surgery while the rat is still under anesthesia. Inject 0.1 mL of 0.15 mg/mL Ketofen and 0.1 mL of 100 mg/mL Cefazolin subcutaneously every 24 hours for the next 72 hours. For hydration, make a one-time injection of 1 mL sterile Lactated Ringer's solution immediately following surgery.
- Place rats into individual cages following surgery. Place food onto floor of cage for the rat immediately following surgery.
- Continue to monitor eating and drinking and general condition of animals.

## A.6 Animal Sacrifice

Soller, 2007

### SUPPLIES

- Sterile Surgical Equipment
  - Surgery Board
  - #15 Scalpel Blade
  - Forceps
- Tissue marker

### EQUIPMENT

- Carbon dioxide chamber
  - Camera
- 

### PROCEDURE

- Sacrifice animals by placing in carbon dioxide chamber for 3-5 minutes.
- Open the original wound with a #15 scalpel blade. The wound can be located by identifying the dermal scar or skin staples.
- Open the fascia and muscle to locate the tube implant and adjacent nerve stumps.
- Photograph the experimental wound space in situ prior to removing the implant. Note connective tissue response.
- Remove the entire tube implant as well as at least 5 mm of proximal and distal nerve tissue. Mark the proximal stump with the tissue marker.
- Photograph the explant on the sterile surgery board to capture the gross morphology.



## **A.7 Optimal Cutting Temperature (OCT) Embedded Tissue Processing Protocol**

adapted from Soller, 2007

### **SUPPLIES**

- Insulated Container with liquid nitrogen
  - Rectangular R-40 Peel-A-Way® Embedding Molds (PolySciences, Inc., Warrington, PA)
  - Optimal Cutting Temperature (OCT) Embedding medium
  - Tissue marker
  - Freezer packs
  - Portable Cooler
- 

### **PROCEDURE**

#### **TISSUE EMBEDDING**

- Fill the bottom of the Rectangular Embedding mold with OCT.
- Carefully place explant (nerve stumps + prosthesis) on top of OCT layer as flatly as possible. Maintain sample orientation by labeling the side of the mold that is closest to the proximal nerve stump.
- Slowly cover the explant with OCT until the mold is mostly filled and the sample is completely covered. Mold dimensions are 22mm wide x 40mm long x 20mm deep.
- Using forceps, carefully lower mold into liquid nitrogen and allow the OCT to freeze. Do not completely immerse the mold to avoid quenching. Wait until freezing is complete before moving mold to cooler filled with freezer packs.
- Store OCT-embedded samples in their molds in a -80°C freezer for future analysis.

## **A.8 Formalin-Fixed Paraffin-Embedded (FFPE) Tissue Processing Protocol**

adapted from Chamberlain, 1998

### **Materials**

- Specimen Containers (Cat. No. 17000, Kendall)
- TRUFLOW Tissue Cassettes (Cat. No. 15-200-403E, Fisher Scientific)
- Biopsy Foam Pads (Cat. No. 22038221, Fisher Scientific)
- Microscope Slides (Superfrost Gold Plus, 15-188-48, Fisher Scientific)
- Monobasic Sodium Phosphate  $\text{NaHPO}_4$  (Sigma)
- Dibasic Sodium Phosphate  $\text{Na}_2\text{HPO}_4$  (Cat. No. S-0876, Sigma)
- Glutaraldehyde, EM Grade, 25% (Cat. No. 01909-10, Polysciences)
- 10% Buffered Formalin Phosphate (Cat. No. SF100-4, Fisher Scientific)
- Ethyl Alcohol EtOH (Histoprep)
- Xylene (Histoprep)
- Paraffin (Cat. No. 23-021-401, Fisher Scientific)

### **Solutions**

- Stock A: .04175 g  $\text{Na}_2\text{HPO}_4$ , .22375 g  $\text{Na}_2\text{HPO}_4$ , 240 mL distilled water, 10 mL 25% glutaraldehyde
- Stock B: 250 mL 10% formalin phosphate, .6125 g  $\text{Na}_2\text{HPO}_4$
- Yannoff's fixative = 1:1 mixture of Stock A:Stock B
- EtOH, 70%, 80%, 90%, 95%

### **Equipment**

- Tissue Processor (TP1020, Leica)
- Embedding Center (Shandon Histocentre 2, Thermo Fisher Scientific, Inc.)

---

### **TISSUE FIXATION**

- Explant the sciatic nerve from sacrificed animal and place tissue into individual specimen containers with 20 mL of Yanoff's fixative for 24 hours at 4°C. Label each specimen container lid with the animal number information.
- Transfer tissue into individual specimen containers with 20 mL of 10% neutral buffered formalin solution for 24 hours at 4°C. Reuse container lids with animal information.
- Remove tissue from formalin and rinse in 70% EtOH.
- Photograph the nerve to capture the gross morphology of the tissue.
- Tissue can be stored in individual specimen containers with 20 mL of 70% EtOH until ready for paraffin embedding. Reuse container lids with animal information.

### **PARAFFIN EMBEDDING**

- Put nerves in tissue cassettes, sandwiched by two biopsy foam pads, and label the cassettes with sample information, date, and investigator name in pencil. Keep the tissue cassettes in 70% EtOH.

- Dehydrate and paraffinize nerves by placing the cassettes into the tissue processor with the following program:

Reagent	Vacuum	Duration (min)	Temperature
EtOH, 70%	No	10	RT
EtOH, 80%	No	90	RT
EtOH, 95%	No	90	RT
EtOH, 95%	No	90	RT
EtOH, 100%	No	90	RT
EtOH, 100%	No	90	RT
EtOH, 100%	Yes	90	RT
Xylene	No	90	RT
Xylene	No	90	RT
Xylene	No	90	RT
Paraffin	Yes	180	58°C
Paraffin	Yes	180	58°C

**Table 14. Tissue processor settings for paraffin embedding**

- Remove cassettes from tissue processor and place them in warm paraffin in paraffin machine.
- Remove tissues from cassettes and section tissue in five 3-4 mm segments (record stump location and lengths of segments).
- Place segment distal end down in embedding mold such that cross-sectional sections will be later made with the microtome. Embed segment in paraffin. On top of the warm paraffin, quickly add the cassette with the sample information written on it. Add more warm paraffin on top of the cassette so that it will be attached to the sample.
- Cool embedded segment on cold plate for an hour before moving to -20°C freezer.
- After at least 24 hours, pop the paraffin-embedded sample from the mold. Remove any excess paraffin from the cassette and return to -20°C freezer.

## SECTIONING

- Section paraffin embedded sample with a microtome at 6µm slices. Make a ribbon of several sections.
- Place ribbon of sections on surface of water bath. Separate sections in duplicates or triplicates. Position microscope slide underneath the sections and retrieve the sections using a pencil as a guide.
- Shake off excess water from the microscope slide. Let air dry for 1 hour.
- Transfer slide to slide warmer for 1 hour. Store in slide box.

## A.9 JB-4 Embedding, Staining, and Imaging for Pore Analysis

adapted from Freyman, 2001; O'Brien, Harley *et al.*, 2004; O'Brien, Harley *et al.*, 2005

### SUPPLIES

- JB-4 A monomer solution (Cat. No. 0226A-800, Polysciences)
- JB-4 A catalyst, (Benzoyl Peroxide, plasticized, Cat. No. 02618-12, Polysciences)
- JB-4 B embedding solution (Cat. No. 0226B-30, Polysciences)
- Ethyl alcohol EtOH (PHARMCO-AAPER)
- Ammonium Hydroxide  $\text{NH}_3$  (aq) (Cat. No. 30501, Fluka)
- Microscope Slides (Superfrost Plus White, Cat. No. 22-034-979, Thermo Fisher Scientific)
- Aniline Blue (Cat. No. A-967, Thermo Fisher Scientific)
- Glacial Acetic Acid (Cat. No. A A507-500, Thermo Fisher Scientific)
- Cyto seal 60 (Cat. No. 18006, Electron Microscopy Sciences)
- Cover slips (Fisherfinest Premium Cover Glasses, Cat. No. 12-548-5M, Thermo Fisher Scientific)

### SOLUTIONS

- Infiltration Solution: 0.3125 g of catalyst dissolved in 25 mL JB-4 solution A.
- Equilibration Solution: 50:50 solution of infiltration solution and 100% ethanol
- Embedding Solution: 1 mL of JB-4 B embedding solution dissolved in 25 mL freshly made infiltration solution
- $\text{NH}_3$  (aq), 10% (v/v): 10 mL ammonium hydroxide, 90 mL distilled water
- EtOH, 95% (v/v)
- Aniline Blue: 2.5 g aniline blue, 2 mL glacial acetic acid, 100 mL distilled water
- Acetic Acid, 1 % (v/v): 1 mL acetic acid, 99 mL distilled water

### EQUIPMENT

- Microtome (Shandon Finesse ME, Thermo Fisher Scientific)
- Light Microscope (Olympus BX51) with Camera (Olympus U-CMAD3)
- Rotator (VWR)

---

### PROCEDURE

For each change of solution, collagen tubes are transferred in new 1.5 mL eppendorf tubes filled with solution.

### DEHYDRATION AND INFILTRATION

- DHT collagen tubes are dehydrated by rotation in 100% alcohol overnight at 4°C.
- Samples are equilibrated for 12 hours at 4°C while rotating in a solution 50% ethanol/50% catalyzed JB-4 solution A.
- Infiltrate tubes in 100% catalyzed JB-4 solution A by rotation for 3 days at 4°C. Change solution every 12 hours.

### EMBEDDING

- Prepare the plastic molds by placing over an icepack in fumehood. Pipet about 1.5 to 2 mL of embedding solution into plastic molds.
  - Place samples in appropriate orientation in plastic molds. Ensure that sample orientation is maintained.
  - Solution begins to harden in approximately 30 minutes.
  - After the JB-4 mixture becomes viscous enough that the samples do not float, place labeled metal or plastic block holders onto each well and place the plastic mold tray in a refrigerator (4°C) and wait overnight.
- Pop the blocks from the mold. Let the samples dry at room temperature for 1 day

## **SECTIONING**

- Section embedded tube very slowly with a microtome at 6um slices.
- Place a drop of 10% ammonium hydroxide where the section is to put on the microscope slide. Position the section on top of the drop. More than one section can fit per microscope slide.
- When the slide is done, let dry on a slide warmer for 30 minutes.
- Store overnight in slide holder before staining with aniline blue.

## **ANILINE BLUE STAINING**

- Dip in aniline blue solution for 2 min
- Place in 1% acetic acid solution for 1 min.
- Dip 5-10x in 95% EtOH until most of background staining goes away. Dip 5-10x in 100% EtOH.
- Mount with Cytoseal 60 and coverslip.
- Dry in hood for 1 hour before imaging with light microscope.

## **IMAGING**

- Bring stained slides to Olympus BX51 microscope (VA Medical Center, D1-147) and locate sections with minimal air bubbles, contaminants, etc.
- Digitally capture the sections using the camera connected to the computer with PictureFrame software. With gain at 4.9102 and target intensity at 75%, click on “Full Image Find Exposure” button. Set correct scale under configurations. Take images at 4x, 10x, and 20x magnifications using “Snap” button.
  - 10x images were used in linear intercept analysis of collagen tube cross-sectional porosity.

## A.10 Linear Intercept Method for Pore Size Analysis

adapted from Harley, 2002; Freyman, 2001

### SOFTWARE

- Adobe Photoshop
- Scion Image
- Microsoft Excel

---

### PROCEDURE

#### IMAGE EDITING

- Open image in Adobe Photoshop. Select Image>Adjustments>Threshold. Change threshold values until optimal image of collagen struts is visible. Clean up any remaining spots using eraser tool.
- Change image size to 640x480. Save the image as an edited .tif file.

#### PORE ANALYSIS

- Open edited image in Scion Image. Go to Special>Load Macros and open "pore characterization macros.txt" (code to follow).
- Set the scale for the analysis using Analyze>Set Scale. The scale is determined as follows when taking the images with the Olympus BX51 (VA Medical Center, D1-147) and having reduced the image size to 640x480:
  - 4X: 214 px/mm
  - 10X: 535 px/mm
  - 20X: 1070 px/mm
  - 40X: 2140 px/mm
- Select an area of the image to be analyzed using the oval drawing tool. Try to get as much of tube enclosed within the curve.
- Go to Special > Linear Intercept. This calculates the distance between the pore walls along lines at various angles emanating from the center of the selected region. Next, run Special > Plot Intercepts. This macro will plot the average pore radii into a best-fit ellipse and will calculate linear intercept coefficients  $C_0$ ,  $C_1$ , and  $C_2$ .
- Transfer  $C_0$ ,  $C_1$ , and  $C_2$  data to an Excel spreadsheet. Calculate the minor (a) and major (b) axes of the ellipse using the following equations:

$$a = \frac{1}{\sqrt{C_0 + \sqrt{C_1^2 + C_2^2}}}$$
$$b = \sqrt{\frac{\sqrt{C_1^2 + C_2^2}}{C_0 \sqrt{C_1^2 + C_2^2} + C_2^2 - C_1^2}}$$

- Calculate the average pore diameter using the following equation. The two scaling factors are for a scaling factor associated with the analysis (1.5\*) and to change from pore radius to pore diameter (2\*):

$$\text{Pore Diameter} = 1.5 \cdot 2 \cdot \sqrt{\frac{a^2 + b^2}{2}}$$

## ASSOCIATED CODE

### Codes contained inside pore characterization macros.txt

```
macro 'Linear Draw'
{This macro is used for testing different line drawing routines for use
with the macro 'Linear Intercept'}
var
  left,top,width,height,MinDim,nx,ny,i,j,k:integer;
      ThetaStep,NSteps,PI,x1,x2,y1,y2,dy,dx:real;
  Theta, valx, valy, plength, scale, AspectRatio:real;
  IntLength, LineSum:real;
  Intercepts:integer;
  switch, indicator:boolean;
  unit:string;
begin
  GetRoi(left,top,width,height);
  if width=0 then begin
    PutMessage('Selection required. ');
    exit;
  end;
  if width<height then MinDim:=width
  else MinDim:=height;
  PI:=3.141592654;
  GetScale(scale,unit,AspectRatio);
  NSteps:=GetNumber('Enter theta steps between 0 and 90 deg.',3,0);
  ThetaStep:=PI/(2*NSteps);
  for j:=0 to 2*NSteps-1 do begin
    x1:=left;
    y1:=top;
      Theta:=j*ThetaStep;
    nx:=5*sin(Theta)*width/height;
    ny:=5*abs(cos(Theta));
    for i:=0 to nx do begin
      if Theta=0 then begin
        x1:=left;
        x2:=x1+width;
      end else begin
        x1:=left+(width*i/(nx+1))+width/(2*(nx+1));
        x2:=x1+(height*cos(Theta)/sin(Theta));
      end;
      y2:=top+height;
      if x2>=left+width then begin
        x2:=left+width;
        y2:=y1+(x2-x1)*sin(Theta)/cos(Theta);
      end else if x2<left then begin
        x2:=left;
        if Theta>PI/2 then y2:=y1+(x2-
x1)*sin(Theta)/cos(Theta);
      end;
      {plength is the length of the line to be drawn in pixels}
      plength:=sqrt(sqr(x2-
x1)+sqr((y2-y1)/AspectRatio));
    end;
  end;
end;
```

```

    valx:=x1;
    dx:=(x2-x1)/plength;
    dy:=(y2-y1)/plength;
    switch:=true;
    if plength>=MinDim then begin
        PutPixel(x1+k*dx,y1+k*dy,255);
    end;
end;
for i:=1 to ny do begin
    if Theta<=PI/2 then begin
        x1:=left;
        x2:=left+width
    end else begin
        x1:=left+width;
        x2:=left;
    end;
    y1:=top+height*i/(ny+1);
    y2:=y1+(width*sin(Theta)/abs(cos(Theta)));
    if y2>top+height then begin
        y2:=top+height;
        x2:=x1+((y2-y1)*cos(Theta)/sin(Theta));
    end;
    {plength is the length of the line to be drawn in pixels}
    plength:=sqrt(sqr(x2-
x1)+sqr((y2-y1)/AspectRatio));
    valx:=x1;
    dx:=(x2-x1)/plength;
    dy:=(y2-y1)/plength;
    switch:=true;
    if plength>=MinDim then begin
        PutPixel(x1+k*dx,y1+k*dy,255);
    end; {if}
end; {i}
end; {j}
end;

```

```

macro 'Linear Intercept'
{This macro measures the linear intercept distance over a giver ROI
at intervals of angle}
var
    left,top,width,height,MinDim,nx,ny,i,j,k:integer;
    ThetaStep,NSteps,PI,x1,x2,y1,y2,dy,dx:real;
    Theta,valx,valy,plength,scale,AspectRatio:real;
    IntLength,LineSum,dummy:real;
    Intercepts:integer;
    switch,indicator:boolean;
    unit:string;
begin
    SetOptions('User1;User2');
    GetRoi(left,top,width,height);
    if width=0 then begin

```



```

    PutMessage('Selection required. ');
    exit;
end;
if width<height then MinDim:=width
    else MinDim:=height;
PI:=3.141592654;
GetScale(scale,unit,AspectRatio);
NSteps:=18;{GetNumber('Enter # steps between 0 and 90 deg.',3,0);}
ThetaStep:=PI/(2*NSteps);

{block out next line when doing cumulative measurements}

SetCounter(2*NSteps);
SetUser1Label('Theta(rad) ');
SetUser2Label('Lx10^3');
for j:=0 to 2*NSteps-1 do begin
    LineSum:=0;
    Intercepts:=0;
    x1:=left;
    y1:=top;
        Theta:=j*ThetaStep;
nx:=10*sin(Theta)*width/height;
ny:=10*abs(cos(Theta));
    for i:=0 to nx do begin
        if Theta=0 then begin
            x1:=left;
            x2:=x1+width;
        end else begin
            x1:=left+(width*i/(nx+1))+width/(2*(nx+1));
            x2:=x1+(height*cos(Theta)/sin(Theta));
        end;
            y2:=top+height;
                if x2>=left+width then begin
                    x2:=left+width;
                    y2:=y1+(x2-x1)*sin(Theta)/cos(Theta);
                end else if x2<left then begin
                    x2:=left;
                    if Theta>PI/2 then y2:=y1+(x2-
x1)*sin(Theta)/cos(Theta);
                end;
                    {plength is the length of the line to be drawn in pixels}
                    plength:=sqrt(sqrt(x2-
x1)+sqrt((y2-y1)/AspectRatio));
                    valx:=x1;
                        valy:=y1;
                    dx:=(x2-x1)/plength;
                    dy:=(y2-y1)/plength;
                    switch:=true;
                    if plength>=MinDim then begin
                        LineSum:=LineSum+(plength/scale);
                            for k:=0 to plength do begin
                                if GetPixel(x1+k*dx,y1+k*dy)>0
                                    then indicator:=true
                                        else indicator:=false;
                                if (switch=true) and (indicator=true) then begin
                                    Intercepts:=Intercepts+1;
                                    switch:=false;

```

```

        end;
        if (indicator=false) then switch:=true;
    end;
end;
end;
end;
for i:=1 to ny do begin
    if Theta<=PI/2 then begin
        x1:=left;
        x2:=left+width
    end else begin
        x1:=left+width;
        x2:=left;
    end;
    y1:=top+height*i/(ny+1);
    y2:=y1+(width*sin(Theta)/abs(cos(Theta)));
    if y2>top+height then begin
        y2:=top+height;
        x2:=x1+((y2-y1)*cos(Theta)/sin(Theta));
    end;
    {length is the length of the line to be drawn in pixels}
    length:=sqrt(sqr(x2-
x1)+sqr((y2-y1)/AspectRatio));
    valx:=x1;
    valy:=y1;
    dx:=(x2-x1)/length;
    dy:=(y2-y1)/length;
    switch:=true;
    if length>=MinDim then begin
        LineSum:=LineSum+(length/scale);
        for k:=0 to length do begin
            if GetPixel(x1+k*dx,y1+k*dy)>0
                then indicator:=true
                else indicator:=false;
            if (switch=true) and (indicator=true) then begin
                Intercepts:=Intercepts+1;
                switch:=false;
            end;
            if (indicator=false) then switch:=true;
        end;
    end;
end; {i}
IntLength:=LineSum/Intercepts;
dummy:=rUser2[j+1];
rUser1[j+1]:=180*Theta/PI;

```

{to do cumulative measurements, type in 'dummy+ before Intlength in the next line}

```

    rUser2[j+1]:=IntLength*1000;
end; {j}
ShowResults;
end;

```

```

macro 'Linear Intercept +'
{This macro measures the linear intercept distance over a giver ROI
at intervals of angle}
var

```

```

left,top,width,height,MinDim,nx,ny,i,j,k:integer;
      ThetaStep,NSteps,PI,x1,x2,y1,y2,dy,dx:real;
Theta, valx, valy, plength, scale, AspectRatio:real;
  IntLength, LineSum, dummy:real;
Intercepts:integer;
switch, indicator:boolean;
unit:string;
begin
  SetOptions('User1;User2');
  GetRoi(left,top,width,height);
  if width=0 then begin
    PutMessage('Selection required. ');
    exit;
  end;
  if width<height then MinDim:=width
    else MinDim:=height;
  PI:=3.141592654;
  GetScale(scale,unit,AspectRatio);
  NSteps:=18;{GetNumber('Enter # steps between 0 and 90 deg.',3,0);}
  ThetaStep:=PI/(2*NSteps);

{block out next line when doing cumulative measurements}

  {SetCounter(2*NSteps);}
  SetUser1Label('Theta(rad)');
  SetUser2Label('Lx10^3');
  for j:=0 to 2*NSteps-1 do begin
    LineSum:=0;
    Intercepts:=0;
    x1:=left;
    y1:=top;
      Theta:=j*ThetaStep;
    nx:=10*sin(Theta)*width/height;
    ny:=10*abs(cos(Theta));
    for i:=0 to nx do begin
      if Theta=0 then begin
        x1:=left;
        x2:=x1+width;
      end else begin
        x1:=left+(width*i/(nx+1))+width/(2*(nx+1));
        x2:=x1+(height*cos(Theta)/sin(Theta));
      end;
      y2:=top+height;
      if x2>=left+width then begin
        x2:=left+width;
        y2:=y1+(x2-x1)*sin(Theta)/cos(Theta);
      end else if x2<left then begin
        x2:=left;
        if Theta>PI/2 then y2:=y1+(x2-
x1)*sin(Theta)/cos(Theta);
        end;
        {plength is the length of the line to be drawn in pixels}
        plength:=sqrt(sqrt(x2-
x1)+sqrt((y2-y1)/AspectRatio));
        valx:=x1;
        valy:=y1;
        dx:=(x2-x1)/plength;

```

```

dy:=(y2-y1)/plength;
switch:=true;
if plength>=MinDim then begin
LineSum:=LineSum+(plength/scale);
                                for k:=0 to plength do begin
        if GetPixel(x1+k*dx,y1+k*dy)>0
            then indicator:=true
            else indicator:=false;
        if (switch=true) and (indicator=true) then begin
            Intercepts:=Intercepts+1;
            switch:=false;
        end;
        if (indicator=false) then switch:=true;
    end;
end;
end;
for i:=1 to ny do begin
    if Theta<=PI/2 then begin
        x1:=left;
        x2:=left+width
    end else begin
        x1:=left+width;
        x2:=left;
    end;
    y1:=top+height*i/(ny+1);
    y2:=y1+(width*sin(Theta)/abs(cos(Theta)));
                                if y2>top+height then begin
        y2:=top+height;
        x2:=x1+((y2-y1)*cos(Theta)/sin(Theta));
    end;
    {plength is the length of the line to be drawn in pixels}
    plength:=sqrt(sqrt(x2-
x1)+sqrt((y2-y1)/AspectRatio));
    valx:=x1;
                                valy:=y1;
    dx:=(x2-x1)/plength;
    dy:=(y2-y1)/plength;
    switch:=true;
    if plength>=MinDim then begin
LineSum:=LineSum+(plength/scale);
                                for k:=0 to plength do begin
        if GetPixel(x1+k*dx,y1+k*dy)>0
            then indicator:=true
            else indicator:=false;
        if (switch=true) and (indicator=true) then begin
            Intercepts:=Intercepts+1;
            switch:=false;
        end;
        if (indicator=false) then switch:=true;
    end;
end;
end;
end;{i}
IntLength:=LineSum/Intercepts;
dummy:=rUser2[j+1];
rUser1[j+1]:=180*Theta/PI;

```

{to do cumulative measurements, type in 'dummy+ before Intlength in the next line)

```

    rUser2[j+1]:=dummy+IntLength*1000;
end; {j}
ShowResults;
end;

```

Macro 'Plot Intercepts'

{This macro plots the linear intercept distance as a function of angle in cylindrical coordinates  
It then finds the best-fit ellipse to a set of linear intercept distance vs. angle data  
using multiple linear regression of the equation  $Y=C0+C1*X+C2*Z$ , where  $Y=1/L^2$ , where L is one half the linear intercept distance at Theta  
 $X=\cosine(2*Theta)$ ,  $Z=\sine(2*Theta)$   
 $C0=(Mii+Mjj)/2$ ,  $C1=(Mii-Mjj)/2$ ,  $C2=Mij$ .  
The objective is to solve for M11, Mjj, and Mij  
The best-fit ellipse it then plotted on top of the linear intercept measurements}

var

```

left,top,width,height,X0,Y0,X1,Y1,i,n:integer;
pscale,aspectRatio,dx1,dx2,dy1,dy2,maxdim:real;
unit:string;
sumX,sumY,sumZ,sumXZ,sumXY,sumYZ,sumZsqr,sumXsqr:real;
C0,C1,C2,Mii,Mjj,Mij,Y,X,Z,PI,Thetal,Theta2,L1,L2:real;

```

begin

```

    PI:=3.141592654;
SaveState;
SetForegroundColor(255);
SetBackgroundColor(0);
width:=400;
height:=400;
maxdim:=0;
for i:=1 to rCount do begin
    if rUser2[i]>maxdim then maxdim:=rUser2[i];
end;
pscale:=.8*(width+height)/(2*maxdim);
SetNewSize(width,height);
MakeNewWindow('Linear Intercepts vs. Theta');
SetLineWidth(1);
X0:=(width/2);
Y0:=(height/2);
MakeLineROI(0,Y0,width,Y0);
Fill;
MakeLineROI(X0,0,X0,height);
Fill;
for i:=1 to rCount do begin
    dx1:=pscale*0.5*rUser2[i]*cos(rUser1[i]*PI/180);
    dy1:=pscale*0.5*rUser2[i]*sin(rUser1[i]*PI/180);
    if i<rCount then begin
        dx2:=pscale*0.5*rUser2[i+1]*cos(rUser1[i+1]*PI/180);
        dy2:=pscale*0.5*rUser2[i+1]*sin(rUser1[i+1]*PI/180);
    end else begin
        dx2:=-pscale*0.5*rUser2[1]*cos(rUser1[1]*PI/180);

```

```

        dy2:=-pscale*0.5*rUser2[1]*sin(rUser1[1]*PI/180);
    end;
    MoveTo(X0+dx1,Y0+dy1);
    LineTo(X0+dx2,Y0+dy2);
    MoveTo(X0-dx1,Y0-dy1);
    LineTo(X0-dx2,Y0-dy2);
end;
n:=rCount;
sumX:=0;
sumY:=0;
sumZ:=0;
sumXY:=0;
sumYZ:=0;
sumXZ:=0;
sumZsqr:=0;
sumXsqr:=0;
for i:=1 to n do begin
    Y:=1/(sqr(rUser2[i]/2));
    X:=cos(2*PI*rUser1[i]/180);
    Z:=sin(2*PI*rUser1[i]/180);
    sumX:=sumX+X;
    sumY:=sumY+Y;
    sumZ:=sumZ+Z;
    sumXY:=sumXY+(X*Y);
    sumYZ:=sumYZ+(Y*Z);
    sumXZ:=sumXZ+(X*Z);
    sumZsqr:=sumZsqr+sqr(Z);
    sumXsqr:=sumXsqr+sqr(X);
end;
C1:=((sumXY*sumZsqr)-(sumXZ*sumYZ))/((sumXsqr*sumZsqr)-sqr(sumXZ));
C2:=((sumYZ*sumXsqr)-(sumXY*sumXZ))/((sumXsqr*sumZsqr)-sqr(sumXZ));
C0:=(sumY/n)-C1*(sumX/n)-C2*(sumZ/n);
for i:=1 to rCount do begin
    Theta1:=rUser1[i]*PI/180;
    if i<rCount then Theta2:=rUser1[i+1]*PI/180
    else Theta2:=rUser1[1]*PI/180;
    L1:=1/sqrt(C0+C1*cos(2*Theta1)+C2*sin(2*Theta1));
    L2:=1/sqrt(C0+C1*cos(2*Theta2)+C2*sin(2*Theta2));
    dx1:=pscale*L1*cos(Theta1);
    dy1:=pscale*L1*sin(Theta1);
    if i<rCount then begin
        dx2:=pscale*L2*cos(Theta2);
        dy2:=pscale*L2*sin(Theta2);
    end else begin
        dx2:=-pscale*L2*cos(Theta2);
        dy2:=-pscale*L2*sin(Theta2);
    end;
    MoveTo(X0+dx1,Y0+dy1);
    LineTo(X0+dx2,Y0+dy2);
    MoveTo(X0-dx1,Y0-dy1);
    LineTo(X0-dx2,Y0-dy2);
end;
NewTextWindow('Results');
write('C0 = ',C0:8:8);
write('C1 = ',C1:8:8);
write('C2 = ',C2:8:8);
end;

```

```

macro 'Count Black and White Pixels [B]';
{
Counts the number of black and white pixels in the current
selection and stores the counts in the User1 and User2 columns.
}
begin
  RequiresVersion(1.44);
  SetUser1Label('Black');
  SetUser2Label('White');
  Measure;
  rUser1[rCount]:=histogram[255];
  rUser2[rCount]:=histogram[0];
  UpdateResults;
end;

```

```

macro 'Compute Percent Black and White';
{
Computes the percentage of back and white pixels in the
current selection. This macro only works with binary images.
}
var
  nPixels,mean,mode,min,max:real;
begin
  RequiresVersion(1.44);
  SetUser1Label('Black');
  SetUser2Label('White');
  Measure;
  GetResults(nPixels,mean,mode,min,max);
  rUser1[rCount]:=histogram[255]/nPixels;
  rUser2[rCount]:=histogram[0]/nPixels;
  UpdateResults;
  if (histogram[0]+histogram[255])<>nPixels
    then PutMessage('This macro requires a binary image.');
```

```

end;

macro 'Compute Area Percentage [P]';
{
Computes the percentage of foreground
pixels in the current selection.
}
var
  mean,mode,min,max:real;
  i,lower,upper,fPixels,nPixels,count:integer;
begin
  RequiresVersion(1.50);
  SetUser1Label('%');
  Measure;
  GetResults(nPixels,mean,mode,min,max);
  GetThresholds(lower,upper);
  if (lower=0) and (upper=0) and
    ((histogram[0]+histogram[255])<>nPixels)
  then begin
    PutMessage('This macro requires a binary or thresholded image.');
```

```

        exit;
    end;
if nPixels=0 then begin
end;
if (lower=0) and (upper=0) then begin
    if nPixels=0
        then rUser1[rCount]:=0
        else rUser1[rCount]:=(histogram[255]/nPixels)*100;
    UpdateResults;
    exit;
end;
fPixels:=0;
nPixels:=0;
for i:=0 to 255 do begin
    count:=histogram[i];
    nPixels:=nPixels+count;
    if (i>=lower) and (i<=upper)
        then fPixels:=fPixels+count;
end;
rUser1[rCount]:=(fPixels/nPixels)*100;
UpdateResults;
end;

```



## A.11 Tissue Digestion for ELISA and Immunoblotting Quantification

Amit Roy, 2008

### SUPPLIES

- Tissue segments (stored in mini eppendorf tubes at -80°C)
- 50mM Tris-HCl/150mM NaCl (pH7.5) (Boston BioProducts)
- .5M EDTA pH 8.0 (Cat. No. BM-150, Boston BioProducts)
- 200 U/mg Collagenase I (Cat. No. Ls 4196, Worthington)

### EQUIPMENT

- Centrifuge
  - Incubator
- 

### PROCEDURE

- Prepare digestion buffer cocktail:
  - Per each segment to digest, prepare 50  $\mu$ L of 50 mM Tris-HCl/150mM NaCl/5mM EDTA/10 U Collagenase I
- Let tissue segments thaw at room temperature for 10 minutes.
- Add 50  $\mu$ L of digestion buffer to each tissue segment.
- Incubate segments at 38°C for 8 hours.
- Aspirate any undigested tissue to break up mechanically. Centrifuge for 10 min at 8000  $\text{min}^{-1}$ .
- Save supernatant in new eppendorf tubes and store at -20°C until further use.

## A.12 TGF $\beta$ 1 Enzyme-Linked Immunosorbent Assay (ELISA)

adapted from R&D Systems MB100B data sheet

### SUPPLIES

- Digested tissue samples
- Mouse/Rat/Porcine/Canine TGF-beta 1 Quantikine ELISA Kit (Cat. No. MB100B, R&D Systems)
- Hydrochloric Acid HCl, 1N (contained within Cat. No. MB100B, R&D Systems)
- Sodium Hydroxide NaOH, pellets (Cat. No. 7708, Mallinckrodt)

### SOLUTIONS

- Sodium Hydroxide NaOH, 1N: 10g NaOH in distilled water, final volume 250 mL

### EQUIPMENT

- Microplate shaker (Cat. No. 12620-926, VWR)
  - Microplate reader (SpectraMAX 340PC, Molecular Devices)
- 

## PROCEDURE

### PREPARATION

- Dilute kit wash buffer and calibrator diluent to 1X.
- Reconstitute control.
- Prepare protein standards ranging from 31.2 pg/mL to 2000 pg/mL through six serial 1:2 dilutions.
  - The standard curve will be later constructed using the known TGF  $\beta$ 1 concentrations: 31.2 pg/mL, 62.5 pg/mL, 125 pg/mL, 250 pg/mL, 500 pg/mL, 1000 pg/mL, 2000 pg/mL

### SAMPLE ACTIVATION AND DILUTION

- Aliquot 10  $\mu$ L of each digested tissue sample into an individual mini eppendorf tube.
- Add 4  $\mu$ L of 1 N HCl to each tube to activate any latent TGF  $\beta$ 1. Lightly vortex the samples. Let incubate at room temperature for 15 minutes.
- Neutralize samples by adding 4.2  $\mu$ L 1 N NaOH to each tube. Lightly vortex the samples.
  - Some reagents, such as distilled water, are slightly acidic. The volume of 1 N NaOH needed to neutralize the sample was therefore greater than the volume of 1 N HCl added and was determined using litmus tests
- Dilute samples with 181.8  $\mu$ L of calibrator diluent. There should be enough volume in each sample to run duplicates in the ELISA.

### ELISA

- Remove excess microplate strips from the plate frame, return them to the foil pouch containing the desiccant pack, and reseal.
- Add 50  $\mu$ L of assay diluent to each well.

- Add 50  $\mu\text{L}$  of protein standard, control, blank or activated sample per well. Prepare wells in duplicates. Tap the plate gently for one minute. Cover with the adhesive strip provided. Incubate for 2 hours at room temperature while shaking.
- Aspirate each well and wash by filling each well with 400  $\mu\text{L}$  wash buffer using a squirt bottle. Complete removal of liquid at each step is essential to good performance. Wash 3x. After the last wash, remove any remaining Wash Buffer by aspirating or decanting. Invert the plate and blot it against clean paper towels.
- Add 100  $\mu\text{L}$  of TGF-B1 conjugate to each well. Cover with a new adhesive strip. Incubate for 2 hours at room temperature while shaking.
- Repeat the aspiration/wash 3x.
- Add 100  $\mu\text{L}$  of substrate solution to each well. Incubate for 30 minutes at room temperature. Protect from light.
- Add 100  $\mu\text{L}$  of stop solution to each well. Gently tap the plate to ensure thorough mixing.
- Determine the optical density of each well within 30 minutes, using a microplate reader set to 450 nm. Set wavelength correction to 540 nm.

## A.13 Calculating ELISA Mass Protein per Mass Tissue Statistic

### SOFTWARE

- SpectraMAX Pro Software
  - Microsoft Excel
- 

### PROCEDURE

- Configure the SpectraMAX Pro software to produce the averaged duplicate readings for each standard, control, and sample; the software will also subtract the average zero standard optical density.
- Create a standard curve by generating a four parameter logistic (4-PL) curve-fit to the data in the software. The program will determine the concentration of the diluted sample by reading off the concentration from the curve that corresponds to the measured optical density reading.
- Export the data to an Excel spreadsheet and compile with sample mass and dilution information.
- Apply the following equation to the sample data to determine  $x/m$ , the mass TGF  $\beta 1$  per mass explanted tissue segment (ug/g):

$$\frac{x}{m} = \frac{[x] \cdot V_f}{\chi_v \cdot m} \cdot 10^{-3},$$

where  $x$  is the mass of TGF  $\beta 1$  present in the sample in ug,  $m$  is the mass of the explanted tissue segment in g,  $[x]$  is the concentration of TGF  $\beta 1$  in the segment as determined by ELISA in ug/mL,  $V_f$  is the final volume of the diluted sample prior to insertion into the wells, and  $\chi_v$  is the volume fraction of the aliquot taken from the digested sample. The  $10^{-3}$  was used in unit conversion to express the mass protein over mass tissue statistic in ug/g.

## A.14 Dot Blot Technique for Antibody Cross-Reactivity Assessment

### SUPPLIES

- Protein positive and negative controls
  - TGF  $\beta$ 1 (Cat. No. 100-21, Peprotech)
  - TGF  $\beta$ 2 (Cat. No. 100-35B, Peprotech)
  - TGF  $\beta$ 3 (Cat. No. 100-36, Peprotech)
  - BSA (Cat. No. 03116999001, Roche)
- Primary antibodies to test
  - Anti-TGF  $\beta$ 1 (Cat. No. ab10517, Abcam; Cat. No. 500-M66, Peprotech)
  - Anti-TGF  $\beta$ 2 (Cat. No. MAB612, R&D Systems; Cat. Nos. sc-90 & sc-31610, Santa Cruz Biotechnology)
  - Anti-TGF  $\beta$ 3 (Cat. No. MAB643, R&D Systems; Cat. Nos. sc-82, Santa Cruz Biotechnology)
- HRP-conjugated secondary antibodies
  - Goat Anti-mouse (Cat. No. 31340, Thermo Fisher Scientific)
  - Goat Anti-rabbit (Cat. No. 31460, Thermo Fisher Scientific)
  - Rabbit Anti-goat (Cat. No. 31402, Thermo Fisher Scientific)
- .05% Tween-20 in Tris-buffered Saline (TBS), 10X (Cat. No. IBB-181-1L, Boston BioProducts)
- Instant dry non-fat milk (Carnation)
- Methanol (Cat. No. 3016-16, Mallinckrodt)
- Immobilon PVDF membrane (Cat. No. IPSN07852, Millipore)
- SuperSignal West Femto Chemiluminescent Substrate (Cat. No. 34095, Thermo Fisher Scientific)

### SOLUTIONS

- Non-fat milk blocking buffer, 5% (%w/v): .5g instant dry non-fat milk in TBS; final volume of 100mL
- Wash buffer: 100 mL of .05% Tween-20 in TBS (10X) in 900 mL distilled water
- Antibody diluent: .33g BSA in wash buffer, 1X; final volume of 100 mL

### EQUIPMENT

- Rotator
- Shaker
- Camera apparatus and Alpha Innotech FluorChem8900 image acquisition software

---

### DOT BLOT

- Cut the Immobilon membrane into approximately 10mm x 40mm strips using a razor and straight edge. Cut the upper right corner to denote orientation. Make one strip per each antibody tested. Use a special lab marker or pen to denote the locations of the protein spots and to label the strips for the antibody to be used. Wet the strips in methanol for 15 seconds. Rinse with distilled water.

- Using a 1  $\mu$ L pipet, spot the protein positive and negative controls onto each strip in a straight line. Let the spots soak into the strip and air dry.
- After the strips are dry, let them rock in non-fat milk blocking buffer for 1 hour.
- Use the diluent to make the appropriate dilution of primary antibody, e.g. 1:500 for monoclonals, 1:800 for polyclonals.
- Put each strip into a 5 mL test tube with the diluted primary antibody solution added to the container. Rotate the tube in the diluted primary antibody solution for 1 hour at room temperature.
- Fill new 5 mL tubes with the wash buffer and dip the strips 10-15x. Empty the tubes, refill with new wash buffer, and dip the strips an additional 10-15x. Repeat the last step for a total of 3 washes.
- Prepare the diluted secondary antibody solution using the antibody diluent. For example, a 1:2000 dilution of goat anti-mouse IgG (H+L), peroxidase conjugated is recommended. Incubate the membrane in a 5 mL test tube with diluted secondary antibody solution for 1 hour at room temperature.
- Fill new 5 mL tubes with the wash buffer and dip the strips 10-15x. Empty the tubes, refill with new wash buffer, and dip the strips an additional 10-15x. Repeat the last step for a total of 3 washes.
- Transfer the system to the Dedon Lab (500 Tech Sq) for imaging. Be sure to bring the luminol and enhancer solution, a Falcon tube, aluminum foil, and clear sheet protector in a chilled Styrofoam box.
- Combine .5 mL of the luminol solution with .5 mL of the enhancing solution.
- Incubate all membrane strips in the mixed luminol-enhancer solution for 5 minutes while covered. Shake at room temperature.
- Put all strips in between two slices of a cut sheet protector. Place on top of a clear Petri dish. Remove as many air bubbles as possible with a Kim wipe.

## IMAGING

- Place the sheet protector-blot sandwich into the Alpha Innotech FluorChem 8900.
- Make sure the iris is fully open, and zoom all the way in on a subject. Adjust the focus. Zoom out to see the whole membrane.
- Close the bottom door of the FluorChem 8900, but leave the top door open. Leave at position 1 (no filter).
- Open up the FluorChem 8900 software. Choose the highest resolution and chemidisplay. Test a few exposure times (1, 3 minutes). Put the warning sign on the bottom door so that no one will open it while the camera is operating.

## A.15 Immunoblot Detection of Protein in Tissue Samples

adapted from S. Gallagher, D. Tzeranis

### SUPPLIES

- Protein samples
  - Digested tissue samples (Appendix A.11)
  - Note: during the first run test a control, e.g. human smooth muscle extract
- Laemmli's reducing SDS Buffer 4X (Cat. No. BP-110R, Boston BioProducts)
- Glycerol (Cat. No. 16374, usb)
- Sodium Hydroxide (Cat. No. 7708, Mallinckrodt)
- Ready Gel Tris-HCl gel, 4-15%, 15-well 15  $\mu$ L (Cat. No. 161-1122, Bio-Rad Laboratories)
- Tris-Glycine-SDS Running Buffer 10X (Cat. No. BP-150, Boston BioProducts).
- Precision Plus All Blue standards (Cat. No. 161-0373, Bio-Rad Laboratories).
- Primary antibody for antigen of interest
  - E.g.  $\alpha$ -SMA monoclonal Ab (mouse IgG2a) (Cat. No. 2547-2ML, Sigma)
- HRP-conjugated secondary antibody
  - Goat Anti-mouse (Cat. No. 31340, Thermo Fisher Scientific)
- Transfer buffer, 10X (Cat. No., BP-100, Boston BioProducts)
- .05% Tween-20 in Tris-buffered Saline (TBS), 10X (Cat. No. IBB-181-1L, Boston BioProducts)
- Instant dry non-fat milk (Carnation)
- Methanol (Cat. No. 3016-16, Mallinckrodt)
- Immobilon PVDF membrane (Cat. No. IPSN07852, Millipore)
- SuperSignal West Femto Chemiluminescent Substrate (Cat. No. 34095, Thermo Fisher Scientific)

### SOLUTIONS

- Sample loading buffer (2X): 5 mL Laemmli's SDS buffer (4X), 4 mL distilled water, 1 mL glycerol
- 1N Sodium hydroxide: 10g NaOH in distilled water, final volume 250 mL
- Running buffer: 100 mL Tris-Glycine-SDS running buffer (10X), 900 mL distilled water
- Transfer buffer: 100 mL Transfer buffer (10X), 900 mL distilled water

### EQUIPMENT

- Mini Protean Tetra Cell for Ready Gel Precast Gels and Mini Trans-Blot Module (Cat. No. 165-8030, Bio-Rad Laboratories)
  - Dry Bath Incubator (Fisher Scientific)
  - Power Source (300 V, VWR)
  - Magnetic Stirrer
  - Rocker
  - Camera apparatus and Alpha Innotech FluorChem8900 image acquisition software
-

## **PROCEDURE**

### **PREPARATION**

- Rinse the Mini-PROTEAN Tetra cell with de-ionized water.
- Turn on the dry heating block and set the temperature at 95°C.

### **GEL POSITIONING**

- Using a razor, score neatly (from right to left) the topmost edge of the black line located on the ready gel. Remove slowly and carefully the sticker underneath the line (from left to right) using the pull tab.
- Place the ready gel in the electrophoresis cell so that the smaller plastic plate faces the inner side of the electrophoresis cell. Secure the gel using the two handles.
  - Use the cell that contains two electric plugs on the top, if 1 or 2 gels will be run. Use the second cell (doesn't contain plugs) if more than 2 gels will be run.
  - When running 1 or 3 ready gels, use the provided buffer dams to cover the extra empty spot of the cell.
- Place the cell-ready gel-dam assembly inside the tank.
  - Make sure that red/black plugs are on the red/black marked sides of the tank.
- The space between two gels or between a gel and a dam forms an inner well. Add running buffer in the inner well until the gel wells are fully covered.
- Add running buffer to the tank (outside of the assembly) up to the level indicated for running 1-2 or 3-4 gels.

### **SAMPLE PREPARATION**

- Prepare the samples inside clean .5 mL eppendorf tubes. Use one tube per sample. Dilute 4x with distilled water.
- In a new eppendorf tube, take 1 part of the 1:4 diluted sample and add 1 part of sample loading buffer.
  - Check and correct if necessary the pH of the samples using drops of 1N NaOH. The color of the samples should be dark blue (same as the Laemmli buffer).
- Store the 1:8 diluted samples at 4 deg until use.

### **LOAD THE GEL**

- Heat the electrophoresis protein samples in the heat block (95 deg) for 5 minutes.
- Let the electrophoresis protein samples cool for 10 minutes.
- Micro-centrifuge the electrophoresis protein samples for 1 minute.
- Use a thin tipped pipette to load each electrophoresis protein sample (max 15  $\mu$ L) inside a well of the ready gel.
- Load 7  $\mu$ L protein standard to one or two gel wells.

### **START ELECTROPHORESIS**

- Place the lid of the assembly on top on the tank-cells.
- Connect the electrodes to the power supply using the cables.
- Turn on the power supply and select the applied voltage and electrophoresis time.



- The gels run within approximately 6h when 35V is applied.

### **BLOT TRANSFER PREPARATION**

- 1 hour before the electrophoresis will finish, begin soaking the transfer cassette, filter paper, and fiber pads (Mini Trans-Blot Cell) in transfer buffer for 1 hour in a large rectangular container (e.g. clean Rubbermaid container). Remove any air bubbles in the fiber pads.
- 15 minutes before the electrophoresis will finish, pre-wet the Immobilon membrane in methanol for 15 seconds. Wash with distilled water, and let sit in transfer buffer.

### **FINISH ELECTROPHORESIS**

- After the gel has finished running, drain the running buffer (it can be disposed in the sink) or store it at 4 deg so that it can be re-used (up to 3 times total).
- Unsecure the handles and remove the ready gels from the electrophoresis cell.
- Remove the sticker that connects two plastic covers. Gently separate the two plastic covers, carefully using a razor if necessary. The polyacrylamide gel will remain attached to one of the two plastic covers.

### **BLOT TRANSFER**

- Assemble the blotting sandwich. Place one pre-wetted fiber pad on top of the black side of the open cassette. Add a sheet of filter paper. Carefully add the gel, and remove any air bubbles. Place the membrane on top of the gel. Note that the membrane is cut smaller than the gel, so make sure it covers the appropriate area. Place another sheet of filter paper on top, followed by a second fiber pad. Close the cassette firmly while keeping the contents stable. Place the blotting sandwich in the transfer module, with the black side of the cassette facing the black plate of the module.
- Fill the tank with some transfer buffer. Place the module in the tank. Add a standard stir bar to help maintain even temperature and ion distribution. Completely fill the rest of the tank with transfer buffer.
- Put on the tank lid and move stirring and tank assembly to 4°C fridge. Set the stirrer on a very fast speed (speed setting 8). Plug the transfer cell cables into the power supply (should be outside of the fridge) and run the blot at constant current (25 mA).
  - Previously determine the optimal running time of transfer (3 hours TGF  $\beta$ , 5 hours  $\alpha$  SMA), by running gels in different transfer times and performing the rest of the immunoblot protocol for strongest signal
- Turn off the power supply after optimal running time has passed. Disassemble the blotting sandwich in a rectangular container with transfer buffer and carefully remove the membrane. Place the membrane in a small container with enough 5% nonfat milk in TBS blocking buffer to immerse the membrane.
- Clean the transfer cell, fiber pads, and cassettes being sure to rinse well with deionized water.

### **IMMUNOBLOT DETECTION**

- Let the membrane rock in the blocking buffer for 1 hour at room temperature.

- Use antibody diluent to make the appropriate dilution of primary antibody. For example, dilute the  $\alpha$ -SMA primary antibody 1:1000 with the diluent (1.5 mL). Ensure homogeneity of solution with end to end shaking.
- After the membrane is satisfactorily blocked, rinse the membrane in a small amount (1 mL) of antibody diluent. Empty the rinse. Then add the diluted primary antibody solution to the container. Let the membrane rock in the diluted primary antibody solution for 1 hour at room temperature.
- Add in approximately 5 mL of wash buffer into the small container with the membrane. Let shake for 5 minutes at room temperature. Empty the container of the wash buffer and wash again repeatedly for a total of 6 washes.
- Dilute the secondary antibody using the antibody diluent. For example, a 1:5000 dilution of goat anti-mouse IgG (H+L), peroxidase conjugated is recommended. Incubate the membrane in 2.5 mL of diluted secondary antibody solution for 1 hour at room temperature.
- Wash the membrane 6 times for 5 minutes each.
- Transfer the system to the Dedon Lab (500 Tech Sq) for imaging. Be sure to bring the luminol and enhancer solution, a Falcon tube, aluminum foil, and clear sheet protector in a chilled Styrofoam box.
- Combine .5 mL of the luminol solution with .5 mL of the enhancing solution.
- Incubate the membrane in the mixed luminol-enhancer solution for 5 minutes while covered. Shake at room temperature.
- Remove the membrane and put in between two slices of a cut sheet protector. Place on top of a clear Petri dish. Remove as many air bubbles as possible with a Kim wipe.

## IMAGING

- Place the sheet protector-blot sandwich into the Alpha Innotech FluorChem 8900.
- Make sure the iris is fully open, and zoom all the way in on a subject. Adjust the focus. Zoom out to see the whole membrane.
- Close the bottom door of the FluorChem 8900, but leave the top door open. Leave at position 1 (no filter).
- Open up the FluorChem 8900 software. Choose the highest resolution and chemidisplay. Pick the appropriate exposure time (1, 3, 10 minutes). Put the warning sign on the bottom door so that no one will open it while the camera is operating.
- Perform image processing as needed. Make sure all images that are meant to be compared are taken at the same exposure time with the same black, white, and gamma properties.

## **A.16 Semiquantification of Immunoblot Bands**

### **SOFTWARE**

- AlphaEase FC
  - Microsoft Excel
- 

### **PROCEDURE**

- Open image to be analyzed in AlphaEase FC software. Go to Toolbox window and click on Analysis Tools tab. Then click on Spot denso.
- Using the rectangle tool under object, draw a border around the protein bands of interest. Do not draw too large or too small of a band; some background should be included.
- Click on auto bkgd. This calculates the average of the 10 lowest pixel values in the rectangle and subtracts it from each pixel value in the integrated density value (IDV) to be calculated.
- Output the area, IDV, avg (IDV/area), and bkgd data to a txt file. Open up this file in Excel and compile for all segment samples.
  - In this study, the avg statistic was used to compare relative protein concentration.

## **A.17 Direct Immunofluorescence Measurement of Protein in Formalin Fixed, Paraffin-Embedded Tissue**

adapted from P. Castellazzi, E. Ueda (2008), A. Alexander

### **SUPPLIES**

- Xylene (Histoprep)
- Ethyl alcohol, 200 proof (Histoprep)
- Antigen Unmasking Solution (Cat. No. H-3300, Vector)
- Antibody Diluent (Cat. No. S0809, Dako)
- PAP pen (Cat. No. Z377821, Sigma)
- Phosphate Buffered Saline (PBS) (Cat. No. P3813, Sigma)
- Fluorophore-conjugated primary antibody
  - Monoclonal  $\alpha$ SMA-Cy3 (Cat. No. C6198, Sigma)
- 4',6-diamidino-2-phenylindole (DAPI), dihydrochloride (Cat. No. D1306, Invitrogen)
- Shandon Immu-Mount (Cat. No. 9990402, Fisher Scientific)
- Wheaton Glass Staining Dish (Cat. No. 08-811, Fisher Scientific)
- 10 (20 back-to-back) glass slide rack

### **SOLUTIONS**

- Ethanol 80%, 95%
- Antigen retrieval buffer: 2 mL antigen unmasking solution, 212 mL distilled water
  - Store unused buffer at 4°C

### **EQUIPMENT**

- Microwave
- Centrifuge
- Humid chamber: Tupperware container lined inside with wet paper towels, filled with as many upside down empty pipette containers that can fit inside the container (for slides to rest on), and covered with a lid. Wrap the outside of the container (if clear) with aluminum foil to protect slides from light.

---

## **PROCEDURE**

### **PREPARATION**

- For slides to be stained, let bake on slide dryer for at least an additional hour before deparaffinizing.

### **IMMUNOFLUORESCENT LABELING**

- Deparaffinize and rehydrate paraffin-embedded sections:
  - Xylene (or substitute) 2 x 5 min
  - 100% alcohol 2 x 3 min
  - 95% alcohol 2 x 2 min
  - 80% alcohol 1 min
  - Wash in running tap water 5 min

- Heat Induced Epitope Retrieval:
  - Pour ~150 mL antigen retrieval buffer in staining dish. Put in glass slide rack and cover with glass lid. Pre-heat the setup for 1 minute in the microwave on power setting 1.
  - Uncover the staining dish. Place slides into rack immersed in warmed antigen retrieval buffer. Return glass lid on dish and microwave setup for 10 minutes on power setting 1.
  - Let cool, uncovered, at room temperature for 20 minutes.
- Wash slides with PBS for 3 × 5 min at room temperature.
- Remove the slides from the PBS but pipet a small but sufficient amount (10-20 μL) of PBS onto the samples as to keep them from drying. Use the hydrophobic PAP pen to draw circles around each sample to reduce the amount of reagent needed.
- Whenever handling fluorophore-conjugated antibody, work in a dim setting. Dilute α SMA-Cy3 antibody 1:100 in antibody diluent. Centrifuge for 2 minutes at 10000 min<sup>-1</sup>. Pipet ~20 μL of the diluted antibody onto each sample and let incubate overnight at 4°C in a humid chamber.
- Wash slides with PBS for 3 × 5 min at room temperature.
- Pipet 200 ng/ml DAPI diluted in distilled water (~30 μL) onto each sample for 10 min at room temperature.
- Wash slides with PBS at room temperature for 3 × 5 min.
- Cover the samples with Immu-Mount and coverslip.
- Let dry for an hour before handling.

## IMAGING

- Bring slides to Olympus BX60 microscope (VA Medical Center, R1-118). Turn on the computer, monitor, and mercury lamp.
- Locate the tissue with the lowest magnification objective by using the UV filter to find and focus on the DAPI-stained nuclei. If the section is intact (no missing pieces, not cracked, not folded onto itself) and clean (no air bubbles from mounting medium, no debris), continue with protocol. Else pan around the slide for the duplicate or triplicate section.
- Turn on the appropriate filter for the fluorophore used (e.g. Rhodamine filter for Cy3).
- Open the DP Controller program on the computer. Pull out the knob on the microscope eyepiece to allow light only to be passed through to the camera. Adjust the focus so that it looks correct on the computer screen.
- With the settings of ISO800 and image size 680x512, capture the image under 333 ms exposure with 10X objective or 100 ms exposure with 20X objective. This step is particular to the amount of protein present in the sample, the antibody concentrations, incubation conditions, and the properties of the fluorophore. Repeat until entire region of interest is captured.
  - If cell information is important, repeat image capture using 25 ms (10X objective) or 10 ms (20X objective) with UV filter set.

## SLIDE STORAGE

- Keep slides lying flat in a microscope slide folder at 4°C. If necessary, cover the slide folder in aluminum foil to protect slides from light.

## **A.18 Determining Immunoblot Correction Factor for $\alpha$ SMA Using Immunofluorescence Data**

### **SOFTWARE**

- Adobe Photoshop
  - ImageJ
  - Microsoft Excel
- 

### **PROCEDURE**

This procedure was used for a correction factor in the  $\alpha$  SMA immunoblot data, which due to the limitations of sampling collagen tube treated segments, included expression from external scar on the outside surface of the collagen tube. Silicone treated segments were removed from the tube prior to tissue digestion, and so  $\alpha$  SMA correction was not used.

Note: one should be careful in using scaling factors for  $\alpha$  SMA and cellular content determined by immunofluorescence sections (2D) for immunoblot samples (3D), especially if the scaling factors are a function of location within the nerve. The most accurate scaling factor should be developed by repeating this procedure from as many locations within the nerve as possible.

### **PHOTO STITCHING**

- Open 10X images for  $\alpha$  SMA-cy3 fluorescent nerve in Adobe Photoshop. Align and merge images until nerve cross section is complete. Clean up any debris that exists outside of the cross section using the black paintbrush tool.
- Repeat steps using 10X images for DAPI fluorescence.

### **$\alpha$ SMA CORRECTION FACTOR**

- Open image of  $\alpha$  SMA fluorescent, complete nerve cross section in Image J. Set the scale under Analyze>Set Scale...
  - With the image capture settings of 680x512 using the Olympus BX60 microscope (VA Medical Center, R1-118), the scale is defined at 156 px = 200  $\mu$ m
  - Make this setting global if continuing to work with multiple nerve cross section images
- Add an additional measurement by going to Analyze>Set Measurements... and click on Integrated Density.
- Go to Edit>Invert and Image>Type>8-bit to convert the image for analysis.
- Under Image>Adjust>Threshold, determine a threshold that defines positive staining.
- Select the positively stained areas by going to Edit>Selection>Create Selection.
- Run Analyze>Measure to determine the area and integrated density of the entire fluorescence in the image.
- Using the polygon selections tool, define a border around the internal nerve regenerate (you may have to remove the threshold first, draw the border, and then restore the threshold). Run Analyze>Measure to determine the area and integrated density of the fluorescence coming internally.
- Open Excel and compile the area and integrated density measurements contributed by the total nerve cross section and by the internal regenerate. Determine the percent expression

from the regenerate by dividing the integrated density of the internal over the integrated density of the total section (percent integrated density is more accurate than percent area). It may be useful to determine the percent expression external to the regenerate (1-percent expression from internal)

- Arrange data according to location of cross section along the length of the explant.
- Per each location, generate mean percent expression from regenerate  $\pm$  SEM data. If statistically okay to combine all measurements regardless of location in explant, then do so as a first order approximation.
- Use mean percent as a coefficient in  $\alpha$  SMA immunoblot data.

#### **CELLULAR CONTENT CORRECTION FACTOR**

- Open image of DAPI stained, complete nerve cross section in Image J.
- Go to Edit>Invert and Image>Type>8-bit to convert the image for analysis.
- Under Image>Adjust>Threshold, determine a threshold that defines positive staining.
- Run Analyze>Analyze Particles. In the summary locate the number of particles analyzed, which should be the total number of nuclei in the entire cross section.
- Using the polygon selections tool, define a border around the internal nerve regenerate (you may have to remove the threshold first, draw the border, and then restore the threshold). Run Analyze>Analyze Particles to determine the number of nuclei from the regenerate.
- Open Excel and compile number of particle measurements contributed by the total nerve cross section and by the internal regenerate. Determine the cellular percent from the regenerate by dividing the number of particles from the internal region of interest over the number of particles from the total section.
- Arrange data according to location of cross section along the length of the explant.
- Per each location, generate mean cellular percent from regenerate  $\pm$  SEM data. If statistically okay to combine all measurements regardless of location in explant, then do so as a first order approximation.
- Use mean cellular percent as a coefficient in  $\alpha$  Tubulin immunoblot data.

## A.19 Quantifying $\alpha$ SMA Fluorescence Intensity Using Concentric Shell Sampling Specified by Radial Distance from Edge

### SOFTWARE

- ImageJ
  - Microsoft Excel
- 

### PROCEDURE

- Open image to be analyzed in ImageJ. Go to Plugins>Macros>Run and select EdgeIntensity.txt (code to follow). If running this macro repeatedly, you may find it convenient to make Edge Intensity a shortcut by editing the Plugins>Macros>About Startup Macros... file.
- A window should appear asking for the scale measurements (as determined by the microscope-camera capture settings), sampling information (how many pixels apart should each sample be, and for how many pixels away from the edge should the program run), and sample orientation (whole nerve cross section, or top left, top right, bottom left, or bottom right portion of the nerve cross section). Enter the information specific to the picture being analyzed.
  - Note the code currently works for whole nerve cross sections and bottom right sections. Cross sections of the other orientations are flipped until they seem like bottom right cross sections.
- Once the information has been entered, a region of interest (ROI) must be determined by the user. This region is the part of the image from where the program will sample the intensity. Select the region of interest with a selection tool or just use the whole image by selecting all (Ctrl A). Go to Edit>Selection>Create Mask. At this point the program will generate a series of images with the Red, Green, and Blue channel intensities from your original image.
- At this point, an edge must be defined. In collagen treated nerve cross sections, the edge is the boundary between the collagen tube and the nerve regenerate. In silicone treated nerve cross sections, the edge is between the negative space (black) and the nerve regenerate.
  - If using a portion rather than the whole nerve cross section, be careful to define the leftmost and topmost edges at the leftmost and topmost boundary of the image.
  - If the edge is difficult to see, open up the corresponding DAPI image (and if necessary, flip the image to seem as bottom right orientation of nerve tube). Select the edge using the polygons selection tool, save the selection as a ROI (Ctrl T, then save in the ROI Manager), and close the DAPI image. Return to the RGB image and click on the ROI generated in the manager. Create a mask by going to Edit>Selection>Create Mask.
- The program will run on its own, sampling the image as user specified. When finished, the results window will contain the average intensities for the Red (Channel 0), Green (Channel 1), and Blue (Channel 2) channels as a function of distance away from the edge. Copy and paste this information in Excel.



- In Excel, delete the intensities corresponding to Channel 1 and Channel 2. Only the Red channel is of interest due to the emission spectrum of cy3. Plot the intensities as a function of distance from the edge.
- As a statistic for comparing intensities between different cross sections, sum the average red intensity from the edge to a certain distance away.

## ASSOCIATED CODE

### Code contained inside EdgeIntensity.txt

```
// Modified from "EdgeRatio" code by Liang Cai
// Adapted by Kathy Miu
//
// Analysis of immunofluorescent staining
// as a function as distance from edge
// (whole nerve or portions of cross section)
//
// For RGB tif file
//
// measure R G B channel presented by 0 1 2
// ratio Blue to Green, presented by 4
// ratio Blue to Red, presented by 5
// ratio Green to Red, presented by 6
//

macro "MeasureEdge-RGB" {
    requires("1.34m");
    run("Clear Results");

    title = getTitle();

// inputs for the macro
    steppix = 5; // expand or shrink per px during the measure
    distance = 100; // total +/- distance from the edge, in px
    orientation = 0; // default picture contains whole nerve

// scaling: how many pixels per  $\mu\text{m}$ ?
// default px/ $\mu\text{m}$  using 10X mag and Olympus BX60 setup (VA Med Ctr, R1-118)
    pxscale = 156;
    umscale = 200;

    Dialog.create("How to measure the edge");
    Dialog.addMessage("To measure the edge of a cell:");
    Dialog.addMessage(" 1. select the region you want to analyze and create
a mask");
    Dialog.addMessage(" 2. use threshold and wand tool to outline the cell
and create another mask");
    Dialog.addMessage(" 3. use the excel to graph the result");

    Dialog.addMessage("How many pixels per  $\mu\text{m}$ ?");
    Dialog.addNumber("Number of pixels:", pxscale);
    Dialog.addNumber("per how many  $\mu\text{m}$ :", umscale);

    Dialog.addMessage("Configure the program:");
    Dialog.addNumber("Number of px per step:", steppix);
    Dialog.addNumber("Distance to measure in px:", distance);
}
```

```

Dialog.addNumber("Nerve section (0=whole,1=top left,2=top
right,3=bottom left,4=bottom right):", orientation);
Dialog.show();
pxscale = Dialog.getNumber();
umscale = Dialog.getNumber();
steppix = Dialog.getNumber();
distance = Dialog.getNumber();
orientation = Dialog.getNumber();

if ((distance % steppix) > 0) {
    exit("Remainder must be 0!");
}

if (orientation == 0) {}
else if (orientation == 1) {
    run("Flip Horizontally");
    run("Flip Vertically");}
else if (orientation == 2) {
    run("Flip Vertically"); }
else if (orientation == 3) {
    run("Flip Horizontally");}
else if (orientation == 4) {}
else {
    exit("Wrong input for nerve section type");
}

// initiate array
realpair = distance / steppix;
// counts = realpair * 2 + 1;
counts = realpair + 1;
// realpair + 1 + 4 + one more
RealCount = minOf((realpair + 7), counts);

selectWindow(title);
RGB = newArray("red", "green", "blue");
yMin = newArray(255,255,255);
yMax = newArray(0,0,0);

// create data from shrunked/expanded mask, smaller to bigger, do 3 times for
RGB
// run("Create Mask"); use other way to get Mask!!

selectWindow(title);
run("RGB Split");
rename("blue");
wait(140);
run("Put Behind [tab]");
rename("green");
wait(140);
run("Put Behind [tab]");
rename("red");
wait(140);
run("Put Behind [tab]");

run("RGB Merge...", "red=red green=green blue=blue keep");
run("Enhance Contrast", "saturated=0.5");

```

```

setTool(2);

stepone = 0;
while (isOpen("Mask")!=true && stepone == 0) {
    wait(1000);
    showStatus("Please Make Mask for ROI First");
}
selectWindow("Mask");
rename("ROI-red");
run("Duplicate...", "title=ROI-green");
run("Duplicate...", "title=ROI-blue");
stepone = 1;

selectWindow("RGB");
run("8-bit");
run("Enhance Contrast", "saturated=0.5 normalize");

setTool(8);

while (isOpen("Mask")!=true && stepone == 1) {
    wait(1000);
    showStatus("Please Make Mask First");
}

selectWindow("RGB");
close();

i = 0;
while (i < RealCount) {
    selectWindow("Mask");
    run("Duplicate...", "title=MaskRun");
    if ((i - realpair) > 0) {
        selectWindow("MaskRun");
        run("Maximum...", "radius="+((i - realpair) * steppix));
        selectWindow("MaskRun");
        run("Duplicate...", "title=MaskErase");
        selectWindow("MaskRun");
        run("Outline");
    }
    else if ((i - realpair) == 0) {
        selectWindow("MaskRun");
        run("Duplicate...", "title=MaskErase");
        selectWindow("MaskRun");
        run("Outline");
    }
    else {
        selectWindow("MaskRun");
        run("Minimum...", "radius="+((realpair - i) * steppix));
        selectWindow("MaskRun");
        run("Duplicate...", "title=MaskErase");
        selectWindow("MaskRun");
        run("Outline");
    }
}

if (orientation != 0){

```

```

        selectWindow("MaskErase");
        run("Translate...", "x=-2 y=-2");
        imageCalculator("Subtract", "MaskRun", "MaskErase");
        selectWindow("MaskRun");
    }

    rename("MaskRun-red");
    run("Duplicate...", "title=MaskRun-green");
    run("Duplicate...", "title=MaskRun-blue");
    selectWindow("MaskErase");
    close();

    for(rgbcycle=0; rgbcycle<3; rgbcycle++) {
        run("Image Calculator...", "image1=MaskRun-
"+RGB[rgbcycle]+" operation=AND image2="+RGB[rgbcycle]);
        run("Image Calculator...", "image1=MaskRun-
"+RGB[rgbcycle]+" operation=AND image2=ROI-"+RGB[rgbcycle]);
        setThreshold(1, 255);
        run("Set Measurements...", "area standard mean limit
redirect=None decimal=2");
        selectWindow("MaskRun-"+RGB[rgbcycle]);
        run("Measure");

        callSD = getResult("StdDev", (nResults - 1));
        callN = getResult("Area", (nResults - 1));
        SEM = callSD / sqrt(callN);

        xValues = ((i - realpair) * steppix) * umscale / pxscale;
        yValues = getResult("Mean", (nResults - 1));

        yMin[rgbcycle] = minOf(yMin[rgbcycle], yValues);
        yMax[rgbcycle] = maxOf(yMax[rgbcycle], yValues);

        setResult("RGB-channel", (nResults - 1), rgbcycle);
        setResult("Distance", (nResults - 1), xValues);
        setResult("Intensity", (nResults - 1), yValues);
        setResult("SemOfInt", (nResults - 1), SEM);

        close();
    }

    i ++;
    updateResults();
}

selectWindow("Mask");
close();
selectWindow("ROI-red");
close();
selectWindow("ROI-green");
close();
selectWindow("ROI-blue");
close();

run("RGB Merge...", "red=red green=green blue=blue");

// ratio Blue to Green, presented by 4

```

```

// ratio Blue to Red, presented by 5
// ratio Green to Red, presented by 6

    i = 0;
    while (i < RealCount) {
        for(j=0; j<3; j++) {
            setResult("PercInt", (i*3+j), ((getResult("Mean", (i*3+j))
- yMin[j]) / (yMax[j] - yMin[j])) );
            setResult("PercSEM", (i*3+j), (getResult("SemOfInt",
(i*3+j)) / (yMax[j] - yMin[j])) );
            setResult("b2g-Ratio", (i*3+j), (getResult("Mean", (i*3 +
2)) / getResult("Mean", (i*3 + 1)))) );
            setResult("b2r-Ratio", (i*3+j), (getResult("Mean", (i*3 +
2)) / getResult("Mean", (i*3)))) );
            setResult("g2r-Ratio", (i*3+j), (getResult("Mean", (i*3 +
1)) / getResult("Mean", (i*3)))) );
        }
        i ++;
    }
    updateResults();

    selectWindow("RGB");
    close();
}

```